In Sync

In Sync:

Neural Oscillations and their Relation to Visual Perception and Learning

Maryam Karimian

DOCTORAL THESIS, MAASTRICHT UNIVERSITY

Cover design: Maryam Karimian, Zahed Allahyari
Layout: Maryam Karimian
Production: Ipskamp Printing | www.ipskampprinting.nl

ISBN: 978-94-6421-895-4

First release, October 2022

In Sync:

Neural Oscillations and their Relation to Visual Perception and Learning

Dissertation

To obtain the degree of Doctor at Maastricht University, on the authority of the Rector Magnificus, Prof.dr. Rianne M. Letschert, In accordance with the decision of the board of Deans, to be defended in public on Monday the 31st of October 2022, at 16:00 hours

by

Maryam Karimian

The work in this thesis was supported by the Dutch province of Limburg.

Promotor

Prof. dr. Peter De Weerd

Co-promotors

Dr. Mario Senden
Dr. Ronald Westra

Assessment Committee

Prof. dr. Alexander Sack (chair)
Maastricht University

Prof. dr. Gustavo Deco
Pompeu Fabra University

Prof. dr. Pascal Fries
Ernst Strungmann Institute (ESI)

Dr. Vincent van de Ven
Maastricht University

Table of Contents

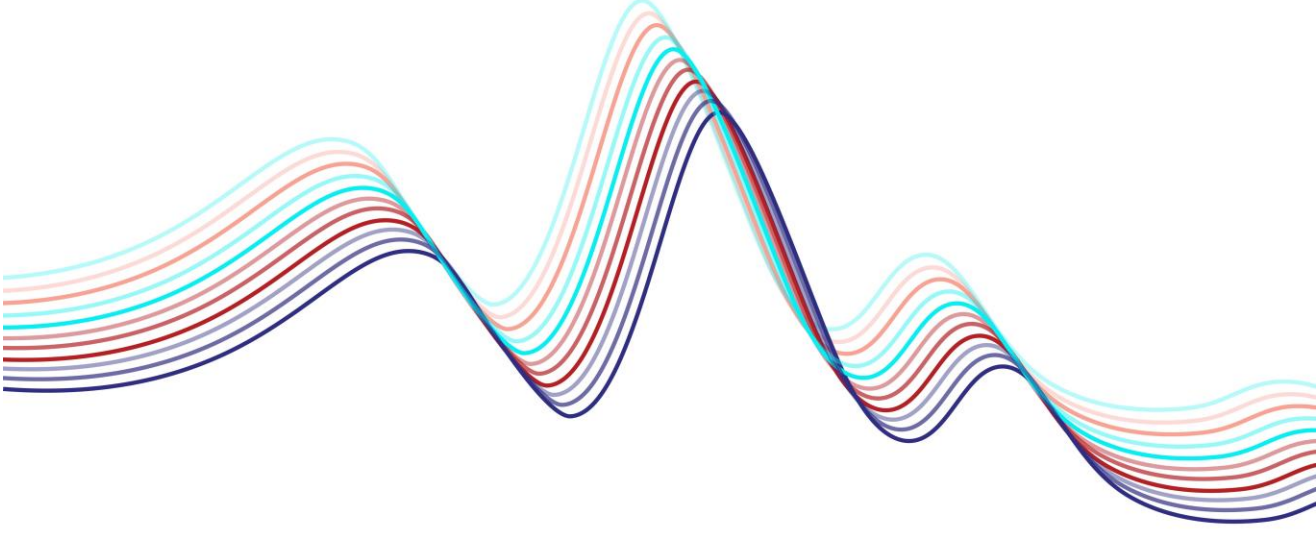

Chapter 1

General Introduction

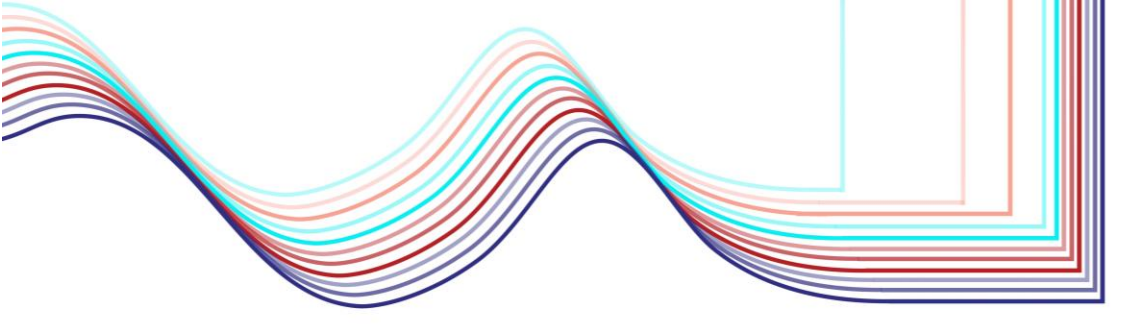

1-1. Brain Oscillations and Their Role in the Brain

Brain oscillations refer to the periodic neural activity that characterizes the central nervous system (Bauer, Wilson, & MacNamara, 2022). Brain oscillations occur in a wide range of frequency bands (György Buzsáki, 2009; von Stein & Sarnthein, 2000). Oscillations can arise in individual neurons due to intrinsic electrochemical fluctuations (Izhikevich, 2004a), but they more commonly result from interactions among interconnected neuronal populations. High-frequency oscillations in the gamma range (above 25 Hz) are created locally through interactions within microcircuits (von Stein & Sarnthein, 2000; M. A. Whittington, Traub, Kopell, Ermentrout, & Buhl, 2000). For oscillations in intermediate and low-frequency bands such as alpha (8-12 Hz), theta (4-8 Hz) and delta (1-4 Hz), it is assumed that interactions over larger distances such as among cortical areas (Sarnthein, Petsche, Rappelsberger, Shaw, & von Stein, 1998; Schack, Vath, Petsche, Geissler, & Möller, 2002; von Stein & Sarnthein, 2000) or even between cortical and subcortical structures play a role (Gould, Rushworth, & Nobre, 2011; Lopes Da Silva & Storm Van Leeuwen, 1977; von Stein & Sarnthein, 2000). For example, the thalamus is thought to be intrinsically involved in generating alpha oscillations (Hughes & Crunelli, 2005), and the septum has been shown to be instrumental in generating theta oscillations in the hippocampus when animals are in an active (encoding) state (Chee, Menard, & Dringenberg, 2015). For some specific high-frequency oscillations, the origin can also be subcortical, as is the case for hippocampal ripples (Bragin, Engel, Wilson, Fried, & Buzsáki, 1999), which play a role in memory consolidation (G. Buzsáki, 1996). Oscillations in different frequency bands may coexist or become rhythmically synchronized or nested into each other. In this way, a highly structured and coordinated collaboration of different frequency bands involving different areas, cortical layers, and subcortical structures emerges that could play a fundamental role in cognitive function and behaviour (Başar et al., 2000; Kahana, 2006).

The exact mechanisms explaining how networks give rise to oscillations in different frequency ranges are still a topic of debate. Nevertheless, there is ample evidence for the crucial role of coordinated inhibitory and excitatory neural interactions in the generation of networkoscillations (Buzśaki & Wang, 2012; Fries, 2015; Wang & Buzsáki, 1996). These interactions are best understood for gamma oscillations. Two main models exist for cortical gamma (P. Tiesinga & Sejnowski, 2009). According to the first model (the Pyramidal Interneuron Network Gamma model, or PING model), (sensory) input to excitatory pyramidal cells followed by inhibitory feedback drives the gamma rhythm (Hansel & Mato, 2003; M. A.

Whittington et al., 2000; Wilson & Cowan, 1972). In particular, in conditions of high excitatory drive of pyramidal cells, a feedback loop is activated in which fast-spiking (FS) basket cells become depolarized and send inhibitory feedback to the pyramidal cells. In these pyramidal cells, a competition arises between the ongoing excitatory drive and the decaying Gamma-aminobutyric acid (GABA) inhibition. Once the excitation overcomes the inhibition, the pyramidal neuron can spike again and the cycle repeats. Hence, important factors determining the frequency of gamma are the level of excitatory input impinging on the pyramidal cells and the time constant of inhibitory decay (P. H. Tiesinga, Fellous, Salinas, José, & Sejnowski, 2004; M. A. Whittington et al., 2000). Gap junctions among inhibitory interneurons may play an additional role in the rapid spatial spread and synchronization of gamma rhythms in a stimulated network (Fukuda, Kosaka, Singer, & Galuske, 2006).

Whereas in the PING model, pyramidal cells drive the gamma rhythm, in the Interneuron network Gamma (ING) model, the periodic activity of FS basket cells entrains the activity of pyramidal cells and induces periodic activity in the entire network through rhythmic inhibition (Cardin et al., 2009; Fellous & Sejnowski, 2003; Hasenstaub et al., 2005; Lytton & Sejnowski, 1991; P. Tiesinga & Sejnowski, 2009; M Vinck, Womelsdorf, & Fries, 2013). Specifically, according to the ING model, the synchronized activity of basket cells that results from their mutual inhibition, entrains the activity of pyramidal cells (Bartos, Vida, & Jonas, 2007; Wang & Buzsáki, 1996; Miles A. Whittington, Traub, & Jefferys, 1995). In this case, the timing of pyramidal cells depends on the rhythmic inhibition of basket cells, which itself depends on the decay time course of GABA (Miles A. Whittington et al., 1995).

Gamma is ubiquitous in the visual cortex when presenting a stimulus and hence is important in bottom-up processing (Bastos et al., 2015; Herrmann, Munk, & Engel, 2004). Many experiments have additionally shown that the bottom-up gamma response is modulated by cognitive factors such as expectation, attention, working memory and other factors (Bastos et al., 2015; Engel, Fries, & Singer, 2001; P. Fries, Reynolds, Rorie, & Desimone, 2001). Cognitive demands generally increase gamma power and frequency (Fitzgibbon, Pope, MacKenzie, Clark, & Willoughby, 2004)while simultaneously reducing alpha and beta frequencies (Engel et al., 2001). Alpha oscillations tend to suppress the activity of neural groups encoding non-attended stimuli, with higher power signifying more suppression (Gould et al., 2011; Haegens, Nácher, Luna, Romo, & Jensen, 2011; von Stein & Sarnthein, 2000). Beta oscillations generate feedback in the visual system (Bastos et al., 2015) and reinforce the activity of neural groups encoding attended stimuli (Bastos et al., 2015). Hence, there are intrinsic interactions among oscillations in different frequency bands that

orchestrate the interplay between feedforward (FF) and feedback (FB) processing that enables cognition (Colgin & Moser, 2010; Fries, 2015).

The intrinsic mechanisms of oscillations are embedded in the structure of the network and its nodes, and are not easily modifiable. At the same time, oscillations provide a means for flexibility in neural communication that may be essential in allowing the flexibility of cognitive functioning (Christoph von der Malsburg, 1995; Milanese, 1994; Pavlaslk, 1998; Treisman, 1996). Communication or information exchange presupposes interactions between at least two networks (oscillators) operating in a common (or sufficiently similar) frequency band. Figure 1.1 schematically depicts the conditions for information exchange according to the communication through coherence hypothesis (CTC). In Figure 1.1A, the excitatory phases of the two networks are closely matched in time, so that spikes emitted by one network arrive within the excitatory phase of the other, and hence can influence the state and output of the receiving network. In Figure 1.1B, the two networks show oscillations in opposite phases, so that spikes from the sending network are received during the inhibitory phase of the receiving network, rendering mutual communication difficult. Figure 1.1C illustrates cross-frequency interactions. Note that the emphasis on in-phase synchronization is a strict interpretation of CTC. According to this interpretation, interactions between neurons (or neuronal groups) can only occur when their phases are perfectly aligned (after taking potential transmission delays into account). However, most neurons (and neuronal groups) advance or delay their phase in response to incoming perturbations that precede or follow their excitatory peak, respectively (Gutkin, Ermentrout, & Reyes, 2005; Stiefel, Gutkin, & Sejnowski, 2008). The direction and magnitude of these phase adjustments are captured by phase response curves (Gutkin et al., 2005), which are typically sufficiently broad to allow neurons (and neuronal) groups to synchronize to spike trains that differ somewhat in phase (and even frequency) (Crook, Ermentrout, & Bower, 1998; Gutkin et al., 2005). In the present thesis, we consider this less strict interpretation of CTC.

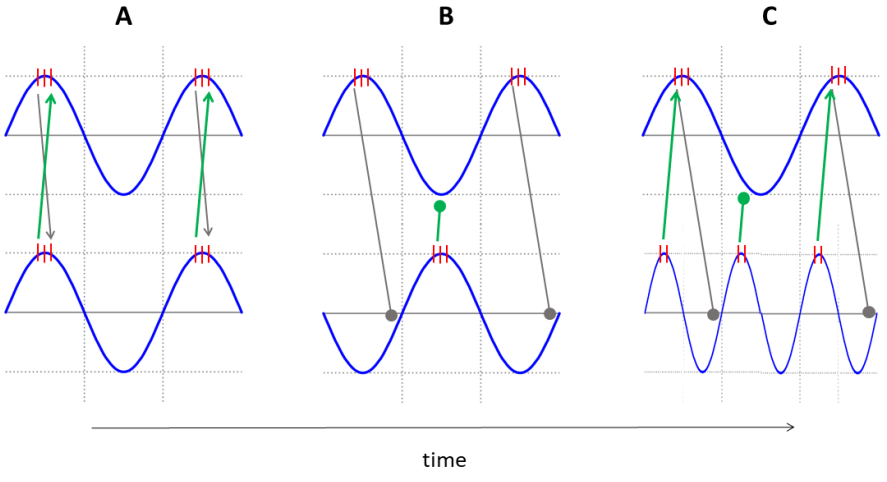

Figure 1.1: A schematic view reflecting the importance of phase relations according to the communication through coherence hypothesis. **A**, simultaneous excitation peaks (in-phase synchronization) for two neural oscillators provide a common communication window. This leads to the on-time arrival of input from the presynaptic to the peak excitability of the postsynaptic neuron (shown by pointed arrows), allowing for effective communication between the two neurons. **B**, anti-phase synchronization of two neural oscillators prevents effective communication, as in this case, inputs from the presynaptic neuron always miss the peak excitability of the postsynaptic neuron (shown by round arrowheads). **C**, partial coherence (p:q phase-locking (Izhikevich, 2004c)) between the excitation peaks that at some points may lead to a certain level of communication.

Regardless of the specific interpretation of CTC, and of the potential additional relevance of oscillations in lower frequency ranges (Schroeder & Lakatos, 2009), CTC emphasizes the role of gamma in selective long-range communication and assumes that the flexibility in long-range communication depends on dynamic patterns of coherence in the gamma range (Fries, 2005, 2015). Part of the work in the present thesis focuses on the interplay between modifiable delays and modifiable coupling strength in a network of oscillators and permits interpretations in the context of long-range communication. Another part of the thesis focuses primarily on a putative role of intra-regional gamma oscillations as a mechanism for local information processing. Specifically, we investigated the extent to which synchronization patterns within a low-level visual area can contribute to the segregation of figure from ground in textured stimuli. The underlying idea is that retinotopically organized cortical microcircuits oscillating in the gamma range are stimulated by visual patterns and segregate into regions differentiated by levels of synchronization, thereby distinguishing figure from ground (Hummel, 2010; Sporns, Tononi, & Edelman, 1991; Christoph von der Malsburg & Buhmann, 1992). These

functional networks are flexibly reconstituted with every new stimulus and hence provide an additional illustration of how gamma oscillations contribute to the flexibility of cognition. These ideas can be related to Gestalt laws in perception (Wagemans et al., 2012), where synchronization could be considered as the mechanism that groups similar elements in an image and segregates different groups from each other. The way in which we use the concept of synchronization to study visual figure-ground segregation can also be linked with the larger concept of 'binding' (Gray, König, Engel, & Singer, 1989a; C. von der Malsburg, 1999). Binding refers to brain-wide interactions that link different aspects of an object processed in different parts of the brain into a coherent whole, similar to the long-range interactions hypothesized in CTC. However, in our study of visual figure-ground segregation in textures, we study the binding among elements (and their segregation from others) in a more local sense (within a visual area). If the mechanisms we study in the context of our figure-ground segregation experiments were to be compared to binding, we would qualify this comparison and refer to a 'local' form of binding.

1-2. Modelling Neural Oscillations using the Theory of Weakly Coupled Oscillators

In computational neuroscience, there are many mathematical formulations to model oscillations and their interactions at different spatial scales (Borisyuk, Borisyuk, Kazanovich, & Ivanitskii, 2002). For example, at the scale of individual neurons, several models capture interactions between activation and inactivation variables that give rise to repetitive firing (neuronal oscillations). The Hodgkin and Huxley model (Hodgkin, Huxley, & Katz, 1952; Nelson & Rinzel, 1998) is arguably the most prominent example of such models. When modelling neural populations, models typically capture interactions between neurons that give rise to oscillations at the network level. In such cases, it is common practice to refrain from modelling individual neurons and instead use more abstract descriptions like neural mass models and simple phase oscillators. This is legitimate because phase oscillator models may capture the oscillatory behaviour of neural networks equally well as models that simulate individual neurons. For instance, Bhowmik and Shanahan (2012) (Bhowmik & Shanahan, 2012a) replicated two studies on large-scale networks of oscillators whose population dynamics were modelled by the Kuramoto model (Jadbabaie, Motee, & Barahona, 2018; Kuramoto, 1984). The authors replicated a number of studies that used the Kuramoto model and replaced the model by (populations of) quadratic integrate-and-fire (QIF) neurons (Latham, Richmond,

Nelson, & Nirenberg, 2000) as well as Hodgkin-Huxley neurons (Hodgkin et al., 1952) and showed that these changes did not significantly affect the results of the original studies (Bhowmik & Shanahan, 2012b). Likewise, Lowet et al., (2015) compared synchronization behaviour of coupled Kuramoto oscillators with that of coupled PING models where individual neurons were of the Izhikevich type (Izhikevich, 2004b). Analytical results derived from the Kuramoto model matched well to simulations of the spiking neuron model for a wide range of coupling and detuning conditions that were inspired by experimental (neurophysiological) observations. Taken together, these findings indicate that phase oscillator models capture many of the essential characteristics of the neural oscillatory processes of interest in the present thesis.

In phase oscillator modelling approaches, the state of neural populations in the oscillatory activity is reduced to its phase. Specifically, the phase $\theta\,(t)$ of an oscillator evolves according to a linear or nonlinear function $f\,(\theta\,(t))$; i.e. $\dot{\theta}(t) = f\,(\theta\,(t))$, and exhibits periodicity t_0, $\theta(t + t_0) = \theta\,(t)$. The Kuramoto model is a popular choice in computational neuroscience for specifying $f\,(\theta\,(t))$ and has been successfully used to reveal under which conditions synchronization occurs among groups of oscillators (Acebr et al., 2005; Kuramoto, 1984; Kuramoto & Kuramoto Y., 1975). Kuramoto specified the phase dynamics of a group of n weakly coupled oscillators as

$$\dot{\theta}_i = \omega_i + \frac{k}{n}\sum_{j=1}^{n} \sin\big(\theta_j - \theta_i\big) \tag{1.1}$$

where ω_i is the intrinsic frequency of oscillator i and k is the coupling strength between oscillators. For small coupling strengths, each oscillator evolves according to its intrinsic frequency, whereas for large[1] coupling strengths the oscillators synchronize, rendering coupling strength an essential factor for predicting the state of synchronization in the network. The value of k at which a transition between asynchronous to synchronous behaviour occurs is commonly referred to as the critical coupling strength. Another important factor is the mismatch between oscillators‘ intrinsic frequencies (their frequency detuning). Indeed, Kuramoto has shown that $k \geq \frac{|\omega_\mathrm{i} - \omega_\mathrm{j}|}{2}$ is a necessary condition for synchronization (stable phase-relationship) between pairs of oscillators i and j and thus constitutes a lower bound

[1] Note that “large” only means that coupling strength exceeds the critical value. Coupling always needs to be sufficiently weak such that interactions among neuronal groups only affect each others’ phases.

for the critical coupling strength. As such, in a network of oscillators, weaker coupling among oscillators or a larger frequency mismatch will reduce the likelihood of synchronization. The interplay between these two factors can be visualized in the 'Arnold tongue' (Coombes & Bressloff, 1999; Pikovsky, Rosenblum, Self, & 2001, 2003; P. H. Tiesinga & Sejnowski, 2010), named after Vladimir Arnold (1937-2010) (Adjan et al., 1965). For the simplest case, which involves two identical oscillators with coupling strength k and detuning level $\Delta\omega$, the Arnold tongue is displayed in Figure 1.2. The two oscillators show synchronization only if their combination of k and $\Delta\omega$ falls inside a triangular region which traditionally is referred to as a 'tongue' (grey region).

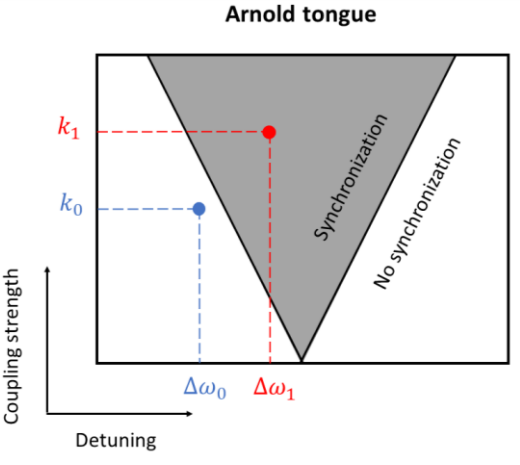

Figure 1.2: The Arnold tongue for a system of two identical oscillators with coupling strength k and detuning level $\Delta\omega$. $(\Delta\omega_0, k_0)$ fall outside the grey area (tongue) which means this combination does not fulfil the synchronization conditions. On the contrary, the system would end up with synchronous oscillations for any combination of $\Delta\omega$ and k that falls inside the tongue (like $(\Delta\omega_1, k_1)$).

1-3. Oscillations in the early visual system

Brain oscillations play a fundamental role in sensory functions involving the transmission and processing of neural signals that convey sensory information (Kandel, Schwartz, Jessell, & Siegelbaum, 2000a). In the human brain, vision is potentially the most complicated sensory function, as almost half of the cerebral cortex is dedicated to it (Longstaff & Ronczkowski, 2011). Human and non-human primate cortex contain on the order of 20-30 visual areas (David C. van Essen et al., 2001; David C. van Essen & Glasser, 2018), which form intricate networks that serve major processing goals, such as recognizing objects and determining their location

(Mishkin, Ungerleider, & Macko, 1983). However, all high-level processing goals derive from low-level processing at the level of early visual areas, such as the primary and secondary visual cortices (V1 and V2). Since two chapters of the thesis present research related to visual processing in the early visual cortex, an introduction to that processing level is provided below.

1-3-1. Anatomy and function of the early visual system

Low-level visual processing starts from the stimulation of retinal receptors in the back of the two eyes. The retinal circuitry affords ganglion cells with round, antagonistic centre-surround receptive fields. These receptive fields exist in two varieties, either with an ON centre and an OFF surround, or with an OFF centre and an ON surround. ON sub-regions are best stimulated by light onset and OFF regions by light offset. The antagonistic nature of these sub-regions yields high sensitivity to contrast. Ganglion cell axons exit the eye in a bundle that forms the optic tract to the lateral geniculate nucleus (LGN), from where neurons project to the primary visual cortex. The projection of the retinal image to the cortex follows several principles. First, the temporal retinae project to the ipsilateral LGN and visual cortex, and the nasal retinae project to the contralateral LGN and visual cortex. As a result, a view of the left visual hemifield from both eyes projects to the right LGN and visual cortex and a view of the right visual hemifield from both eyes projects to the left LGN and visual cortex. Second, the input from the two eyes remains segregated in different layers in the LGN but then combines in V1 by projecting to the same neurons. Furthermore, for the entire visual field, the projection is retinotopic, which means that neighbouring points on the retina will project to neighbouring points in the LGN and to neighbouring points in V1 and V2 (Kandel, Schwartz, Jessell, & Siegelbaum, 2000b). In addition, because of the low convergence of retino-geniculo-cortical projections in central vision (where the density of photoreceptors is extremely high), and the high convergence of the retino-geniculo-cortical projections in peripheral vision, the amount of cortical surface per visual degree decreases sharply with the increase of the eccentricity (cortical magnification) (Kandel et al., 2000b).

One of the most remarkable transformations between LGN and area V1 is the change from center-surround receptive fields in LGN to Gabor-like receptive fields in V1 (referred to as ‘simple’ cells (Hubel & Wiesel, 1968)). These neurons, therefore, are sensitive to the orientation of luminance-defined lines and edges. Notably, neurons with the same preferred orientation are organized in so-called ‘orientation columns’ that span the thickness of the cortex from top to bottom (with

the exception of layer 4C). However, the antagonistic sub-regions composing the receptive fields of simple cells in V1 render them also highly sensitive to local contrast and to spatial frequency. This suggests that LGN and simple cells play a role both in the detection of boundaries and edges of objects, but also in the processing of fine textures and details that define the surfaces encompassed by their boundaries (Kandel et al., 2000b). Whereas the brief overview of the visual system provided here focused on the major feed-forward projections driving responses in the early visual cortex, additional circuitry exists that provides the basis for contextual interactions. In particular, V1 neurons are laterally connected over distances of up to 6 mm (C. D. Gilbert & Wiesel, 1983, 1989; Charles D. Gilbert & Wiesel, 1979; Levitt, Yoshioka, & Lund, 1994; Rockland & Lund, 1982; Yoshioka, Blasdel, Levitt, & Lund, 1996), providing a basis for interaction between local stimuli placed in neighbouring locations in the visual field (C. D. Gilbert & Wiesel, 1989; Lund, Angelucci, & Bressloff, 2003; Ts'o, Gilbert, & Wiesel, 1986). Similar lateral anatomical connectivity exists in V2 and other extrastriate visual cortical areas. Furthermore, the visual system contains feedback projections from higher-level to lower-level visual areas (D. C. van Essen, Felleman, DeYoe, Olavarria, & Knierim, 1990).

1-3-2. The debate about the functional role of gamma oscillations in the early visual system

Research into the contribution of gamma oscillations to visual processing started in the late 1980s when Grey and Singer (Gray, König, Engel, & Singer, 1989b) reported strong synchronization among V1 neurons in the gamma band in response to visual stimulation. Subsequently, further empirical studies in cat, monkey and human visual cortex (Chalk et al., 2010; Friedman-Hill, Maldonado, & Gray, 2000; Gieselmann & Thiele, 2008; Hoogenboom, Schoffelen, Oostenveld, Parkes, & Fries, 2006; Livingstone, Freeman, & Hubel, 1996; Ray & Maunsell, 2010; Rols, Tallon-Baudry, Girard, Bertrand, & Bullier, 2001; Martin Vinck et al., 2010; Womelsdorf & Fries, 2007; Yu & Ferster, 2010) confirmed this finding. Nevertheless, whether gamma oscillations play a role in vision, and generally, cognitive processes, remains a controversial topic. The power and frequency of gamma oscillations depend on stimulus features, including eccentricity, motion, and contrast (Buia & Tiesinga, 2006; Womelsdorf, Fries, Mitra, & Desimone, 2005). In recent years, the debate related to the usefulness of gamma has focused on the high contrast dependence of gamma frequency. Ray & Maunsell (2010) used dual-site recordings in conjunction with Gabor and grating stimuli to demonstrate contrast-dependent differences in

gamma frequency among different cortical locations encoding these stimuli. The authors argued that such spatial variance in gamma frequency across locations within an object runs counter the idea of binding, and therefore precludes a role of gamma in visual processing. Moreover, some studies have shown that gamma frequency and power may vary randomly (Burns, Xing, & Shapley, 2011; Xing et al., 2012) or in accordance with the idea of internal fluctuations (Gray & McCormick, 1996) even during constant exposure to static stimuli. If these temporal variations were independent across different visual areas, or across different locations within an area, then this would argue against gamma synchronization as a means of neural communication. Finally, variability in conduction delays may be problematic for a role of gamma in communication. Conduction delays have the potential to disrupt information transmission, because each cortical site receives many signals from many sources with highly distributed distances and the corresponding wide-range conduction delays might interfere with achieving gamma coherence and therefore communication (Ray & Maunsell, 2015).

Although the above arguments, at first sight, are appealing, they lack a coherent theoretical framework. When gamma is considered in light of the theory of weakly coupled oscillators (TWCO) (Izhikevich & Kuramoto, 2005), it becomes obvious that the observation of frequency differences cannot be seen as an argument against synchronization (phase-locking) without also considering coupling (anatomical connectivity). This is directly demonstrated in the Arnold tongue (Coombes & Bressloff, 1999; Pikovsky et al., 2003; P. H. Tiesinga & Sejnowski, 2010), which can be analytically derived from the Kuramoto model (Acebr et al., 2005). The Arnold tongue shows how synchronization results from appropriate combinations of frequency difference and coupling. To show that this theoretical model directly applies to neural communication in V1, Lowet et al. (2015, 2017) (Lowet et al., 2015; Lowet, Roberts, Peter, Gips, & de Weerd, 2017) translated the concepts of the Arnold tongue to the architecture and function of V1. Specifically, they considered that when assessing the synchronization of gamma between two nearby recorded V1 sites, the coupling parameter might be related to the strength of horizontal anatomical connections and hence distance between electrodes, and the detuning to the difference in gamma frequency imposed by stimulation with local stimuli at different contrasts. Following that idea, they manipulated the strength of coupling (anatomical connectivity) by changing the distance between recording sites, and the magnitude of detuning (gamma frequency difference) by changing the contrast difference between the two stimuli. Both modelling and neurophysiological results (Lowet et al., 2015, 2017) showed that the stimulus dependency of gamma oscillations does not hamper the (partial) synchronization of gamma oscillations as long as it is

matched by sufficiently strong coupling. Hence, frequency differences, rather than precluding a role of gamma in neural processing, are an inherent part of synchronization. Hence, the mere observation of frequency differences at cortical sites representing the same or different stimuli does not tell much about whether communication is going on between these sites. Instead, frequency differences are in fact part of how the visual cortex encodes information in visual images (Lowet et al., 2015).

A similar reasoning holds with respect to the observation of noise (Lowet et al., 2015, 2017). Noise is a natural phenomenon in neurophysiological data, and observing it at a single recording site is uninformative with respect to the question whether it would preclude a role of gamma synchronization in neural communication. If the noise were sufficiently correlated in different sites, it would not prevent gamma synchronization between these sites. Roberts et al. (2013) have shown robust gamma synchronization between V1 and V2 for different peaks in the gamma spectrum set by stimuli of different contrasts. Importantly, they also found large fluctuations over time of the spectral peaks for constant stimulation. However, these fluctuations correlated tightly between V1 and V2. This implies that communication between V1 and V2 through gamma synchronization is possible, which is also what they demonstrated.

Finally, there is the issue of conduction delays. Conduction delays will depend on various factors, including the length, diameter and state of myelination of the projecting neuron's axon, and can vary from a few milliseconds to several tens of milliseconds (Caminiti, Ghaziri, Galuske, Hof, & Innocenti, 2009; Stoelzel, Bereshpolova, Alonso, & Swadlow, 2017). Because the gamma cycle has a duration of about 20 ms, it could be argued that locking at an appropriate phase difference can overcome conduction delays between sites. For feedforward projections from one cortical area to the next, this strategy might be sufficient to preserve a role for gamma in long-range communication. For feedback connections, which may occasionally be extremely long-range, phase-shifting within the gamma cycle may be insufficient to permit communication, and communication may be more efficient in lower frequency bands. This reasoning fits to some extent with reports showing that gamma serves feedforward communication, and lower frequency ranges (alpha, beta) serve feedback (Bastos et al., 2015; Engel et al., 2001; P. Fries et al., 2001; Herrmann et al., 2004; von Stein & Sarnthein, 2000). Hence, although it is reasonable to state that not all conduction delays are compatible with communication in the gamma range, it is equally reasonable to maintain that for a subset of long-range communications, gamma is well-suited to play this role. Furthermore,

conduction delays are likely too short to noticeably affect synchronization in the gamma range within cortical areas.

An additional perspective on the effects of conduction delays on neural communication comes from recent insights into the complementary roles of grey and white matter plasticity (Zatorre, Fields, & Johansen-berg, 2012). Synchronization in the gamma band in response to long-term, repeated visual stimulation in fact plays an important role in eliciting both synaptic and white matter plasticity (Fregnac, Shulz, Thorpe, & Bienenstock, 1992; Galuske, Munk, & Singer, 2019; Jenkins, Merzenich, Ochs, Allard, & Guic-Robles, 1990; Kilgard & Merzenich, 1998; Recanzone, Merzenich, & Dinse, 1992; A. Schoups, Vogels, Qian, & Orban, 2001; Schuett, Bonhoeffer, & Hübener, 2001). The plastic changes in the neural networks are often the consequence of either changes in the synaptic strength (grey matter plasticity) or changes in the thickness or structure of the myelin sheath around the axons that in some way plays the role of an insulator (white matter plasticity). Both types of plasticity are activity-dependent and can increase the efficiency of signal transmission and information flow in neural networks. This is relevant for the issue of conduction delays, as an increase in myelination could be a tool to bring conduction delays within a range allowing the gamma band to contribute to neural communication. Therefore, activity-dependent myelination may be able to resolve the problem of variable long-range conduction delays in reaching gamma synchronization among distributed neural populations (Fields, 2015; Fields & Bukalo, 2020; Scholz, Klein, Behrens, & Johansen-Berg, 2009).

Taken together, the above brief review supports the idea that gamma oscillations are an important vehicle for communication in various cognitive tasks (Bosman et al., 2012; Brunet et al., 2015; Colgin & Moser, 2010; Engel, König, Kreiter, & Singer, 1991; Engel, Kreiter, König, & Singer, 1991; Gray et al., 1989b; Hermes, Miller, Wandell, & Winawer, 2015; Lowet et al., 2015; Uhlhaas, Pipa, Neuenschwander, Wibral, & Singer, 2011; Womelsdorf & Fries, 2007). In addition, TWCO is successful in bringing together disparate findings and views on the function of gamma oscillations. Accordingly, TWCO also constitutes the primary theoretical framework for hypothesis formation in the present thesis.

1-4. A paradigm for inducing visual plasticity – visual perceptual learning

Memory exists in declarative (explicit) and non-declarative (implicit) forms. Perceptual learning, a form of non-declarative memory formation, is defined as the experience-induced incremental process of changes in the detection and

discrimination of sensory attributes (Crist, Kapadia, Westheimer, & Gilbert, 1997). The sensory information may be visual, auditory, tactile or olfactory. In vision, a particularly important perceptual skill that can improve through perceptual learning is the ability to discriminate between a figure and its background.

Most of the studies investigating perceptual learning in the context of figure-ground distinction involve psychophysics experiments with stimuli in which the figure differs from its background with respect to simple visual features such as luminance (H. C. Nothdurft, 1990a; H.-C. Nothdurft, 2015) orientation (de Weerd, Sprague, Vandenbussche, & Orban, 1994; Hans Christoph Nothdurft, 2000; H. C. Nothdurft, 1985a), contrast (Hadjipapas, Lowet, Roberts, Peter, & de Weerd, 2015; H.-C. Nothdurft, 2015), spacing between the texture elements (H. C. Nothdurft, 1990c), or the size of elements with respect to their spacing (Gori & Spillmann, 2010; H. C. Nothdurft, 1985b, 1990b) as well as combinations of these features (Gori & Spillmann, 2010; Julesz & Bergen, 1983; Julesz & Papathomas, 1984; WILLIAMS & JULESZ, 1992).

The learning process of acquiring better skill in figure-ground segregation shows specific characteristics. In the process of daily training, progress is fast during the first few days but slows down as training becomes asymptotic and performance plateaus (Ahissar & Hochstein, 2004; Karni & Bertini, 1997; Lange, Lowet, Roberts, & Weerd, 2018). Many studies have shown that after extensive asymptotic training, the skill becomes specific to the stimulus and to its location in the visual field (Ahissar & Hochstein, 1996; Crist et al., 1997; Karni & Sagi, 1991; Lange et al., 2018; A. A. Schoups, Vogels, & Orban, 1995; A. Schoups et al., 2001). The specificity to location and stimulus characteristics is in line with a contribution of low-level visual areas to this form of learning (Ahissar & Hochstein, 1996; Crist et al., 1997; Karni & Sagi, 1991; Lange et al., 2018; A. A. Schoups et al., 1995; A. Schoups et al., 2001). There is a debate, however, regarding the mechanisms that lead to the specificity of visual skills. One view, known as the 'lowest-level theory' (Karni & Bertini, 1997), suggests that learning initially requires higher-level areas to establish strategies for performing the task. However, during asymptotic learning, long-term and slow structural tuning changes would occur within lower-level areas (Ahissar & Hochstein, 2004; Karni & Bertini, 1997; Lange et al., 2018), which form the 'memory trace' for the skill. In other words, according to this view, plasticity in low-level sensory areas is a core mechanism in perceptual learning. The 'reverse hierarchy hypothesis' (Ahissar & Hochstein, 1997), on the other hand, suggests that perceptual learning increasingly fine-tunes the read-out from low-level sensory areas by high-level areas, rather than requiring plasticity within these low-level areas. According to this hypothesis, the skill may be embedded in a broader network that

enables the enhanced read-out (Ahissar & Hochstein, 1997, 2004; Hochstein & Ahissar, 2002; Liu & Weinshall, 2000; Rubin, Nakayama, & Shapley, 1997). There are also in-between views that propose the concurrent occurrence of both suggested processes (Crist et al., 1997; Dosher & Lu, 1998; Roelfsema, van Ooyen, & Watanabe, 2010).

In the present thesis, we will design a stimulus and a perceptual learning task for which it is reasonable to assume that neural activity in the gamma band is involved in the perception of the figure, and the training-induced enhancement of figure-ground segregation. This will then permit the formulation of hypotheses regarding figure-ground segregation as well as its enhancement by training based on TWCO.

1-5. Summary and thesis organization

In this thesis, we investigated mechanisms by which neural oscillators reach or lose synchronization, and implications for the role of gamma synchronization in cortical information processing. According to TWCO, the degree of heterogeneity in oscillators' intrinsic frequencies (frequency detuning), and the strength of their interactions (coupling strength) determine the success or failure of their synchronization (Pikovsky et al., 2003). There is evidence that variability in signal propagation delays, as well as in stimulus features, affects the heterogeneity of (gamma) frequencies (detuning) (Buia & Tiesinga, 2006; Fries, 2005). In this thesis, we investigated effects of detuning and coupling strength on model network synchronization and visual perception. Chapter 2 presents a study concerning the effect of activity-dependent (plastic) coupling changes on synchronization behaviour in a network of coupled phase oscillators. Coupling changes were considered not only in terms of synaptic plasticity but also in terms of plastic changes in conduction velocities (a proxy of white matter plasticity). We were interested in assessing to what extent experience-dependent changes in conduction velocities would interact with experience-dependent synaptic changes during the formation of synchronized clusters in a network of oscillators. Chapters 3 and 4 focused on the synchronization of gamma oscillations in V1 as a potential underlying mechanism of figure-ground segregation. In these two chapters, a phase oscillator network capturing relevant properties of V1 is exposed to texture stimuli, in which the figure is a group of texture elements showing a spatial distribution of contrast differing from that in the background. Through the manipulation of figure contrast heterogeneity and spacing between texture elements (grid coarseness), we aim to control, respectively, detuning and interaction strength among local V1 neural oscillators. Differences in V1 model synchronization between figure and background were used to predict human figure-

ground segregation in the same conditions as used with the V1 oscillator model. The fourth chapter investigates whether training-induced improvement in task performance is mediated by altered synchronization patterns in V1 that result from plasticity-induced changes in coupling. Finally, the last chapter includes a thorough discussion of the methodology, results and conclusions presented in this thesis.

References

Acebr, J. A., Gradenigo, V., Matematica, D., Acebrón, J. A., Bonilla, L. L., Vicente, C. J. P., … Spigler, R. (2005). The Kuramoto model: A simple paradigm for synchronization phenomena. *Reviews of Modern Physics*, 77 (January), 137–185.

Adjan, S., Arnol′d, V. I., Demuškin, S. P., Gurevic, Ju. S., Kemhadze, S. S., Klimov, N. I., … Tašbaev, V. (1965). *Eleven papers on number theory, algebra and functions of a complex variable*. American Mathematical Society.

Ahissar, M., & Hochstein, S. (1996). Learning Pop-out Detection: Specificities to Stimulus Characteristics. *Vision Research*, 36 (21), 3487–3500.

Ahissar, M., & Hochstein, S. (1997). Task difficulty and the specificity of perceptual learning. *Nature 1997 387:6631*, 387 (6631), 401–406.

Ahissar, M., & Hochstein, S. (2004). The reverse hierarchy theory of visual perceptual learning. *Trends in Cognitive Sciences*, 8 (10), 457–464.

Bartos, M., Vida, I., & Jonas, P. (2007). Synaptic mechanisms of synchronized gamma oscillations in inhibitory interneuron networks. *Nature Reviews Neuroscience 2007 8:1*, 8 (1), 45–56.

Başar, E., Başar-Eroglu, C., Karakaş, S., Schürmann, M., Basar, E., Basar-Eroglu, C., … Schürmann, M. (2000). Brain oscillations in perception and memory. *International Journal of Psychophysiology : Official Journal of the International Organization of Psychophysiology*, 35 (2–3), 95–124.

Bastos, A. M., Vezoli, J., Bosman, C. A., Schoffelen, J. M., Oostenveld, R., Dowdall, J. R., … Fries, P. (2015). Visual Areas Exert Feedforward and Feedback Influences through Distinct Frequency Channels. *Neuron*, 85 (2), 390–401.

Bauer, E. A., Wilson, K. A., & MacNamara, A. (2022). Cognitive and Affective Psychophysiology. *Comprehensive Clinical Psychology*, 49–61.

Bhowmik, D., & Shanahan, M. (2012a). How well do oscillator models capture the behaviour of biological neurons? *Proceedings of the International Joint Conference on Neural Networks*.

Bhowmik, D., & Shanahan, M. (2012b). How well do oscillator models capture the behaviour of biological neurons? *Proceedings of the International Joint Conference on Neural Networks*.

Borisyuk, G. N., Borisyuk, R. M., Kazanovich, Y. B., & Ivanitskii, G. R. (2002). Models of neural dynamics in brain information processing — the developments of “the decade.” *Physics-Uspekhi*, 45 (10), 1073–1095.

Bosman, C. A., Schoffelen, J. M., Brunet, N., Oostenveld, R., Bastos, A. M., Womelsdorf, T., … Fries, P. (2012). Attentional Stimulus Selection through Selective Synchronization between Monkey Visual Areas. *Neuron*, 75 (5), 875–888.

Bragin, A., Engel, J., Wilson, C. L., Fried, I., & Buzsáki, G. (1999). High-Frequency Oscillations in Human Brain. *Hippocampus*, 9, 137–142.

Brunet, N., Bosman, C. A., Roberts, M., Oostenveld, R., Womelsdorf, T., de Weerd, P., & Fries, P. (2015). Visual Cortical Gamma-Band Activity During Free Viewing of Natural Images. *Cerebral Cortex*, 25 (4), 918–926.

Buia, C., & Tiesinga, P. (2006). Attentional modulation of firing rate and synchrony in a model cortical network. *Journal of Computational Neuroscience*, 20 (3), 247–264.

Burns, S. P., Xing, D., & Shapley, R. M. (2011). Is Gamma-Band Activity in the Local Field Potential of V1 Cortex a "Clock" or Filtered Noise? *Journal of Neuroscience*, 31 (26), 9658–9664.

Buzsáki, G. (1996). The Hippocampo-Neocortical Dialogue. *Cerebral Cortex*, 6 (2), 81–92.

Buzśaki, G., & Wang, X. J. (2012, June 20). Mechanisms of gamma oscillations. *Annual Review of Neuroscience*. Annual Reviews.

Buzsáki, György. (2009). *Rhythms of the Brain*. *Rhythms of the Brain*. Oxford University Press.

Caminiti, R., Ghaziri, H., Galuske, R., Hof, P. R., & Innocenti, G. M. (2009). Evolution amplified processing with temporally dispersed slow neuronal connectivity in primates. *Proceedings of the National Academy of Sciences*, 106 (46), 19551–19556.

Cardin, J. A., Carlén, M., Meletis, K., Knoblich, U., Zhang, F., Deisseroth, K., … Moore, C. I. (2009). Driving fast-spiking cells induces gamma rhythm and controls sensory responses. *Nature*, 459 (7247), 663–667.

Chalk, M., Herrero, J. L., Gieselmann, M. A., Delicato, L. S., Gotthardt, S., & Thiele, A. (2010). Attention Reduces Stimulus-Driven Gamma Frequency Oscillations and Spike Field Coherence in V1. *Neuron*, 66 (1), 114–125.

Chee, S. S. A., Menard, J. L., & Dringenberg, H. C. (2015). The lateral septum as a regulator of hippocampal theta oscillations and defensive behavior in rats. *Journal of Neurophysiology*, 113 (6), 1831–1841.

Colgin, L. L., & Moser, E. I. (2010). Gamma Oscillations in thenHippocampus. *Physiology*, 25 (5), 319–329.

Coombes, S., & Bressloff, P. C. (1999). Mode locking and Arnold tongues in integrate-and-fire neural oscillators. *Physical Review E*, 60 (2), 2086.

Crist, R. E., Kapadia, M. K., Westheimer, G., & Gilbert, C. D. (1997). Perceptual learning of spatial localization: Specificity for orientation, position, and context. *Journal of Neurophysiology*, 78 (6), 2889–2894.

Crook, S. M., Ermentrout, G. B., & Bower, J. M. (1998). Spike Frequency Adaptation Affects the Synchronization Properties of Networks of Cortical Oscillators. *Neural Computation*, 10 (4), 837–854.

de Weerd, P., Sprague, J. M., Vandenbussche, E., & Orban, G. A. (1994). Two stages in visual texture segregation: a lesion study in the cat. *Journal of Neuroscience*, 14 (3), 929–948.

Dosher, B. A., & Lu, Z. L. (1998). Perceptual learning reflects external noise filtering and internal noise reduction through channel reweighting. *Proceedings of the National Academy of Sciences of the United States of America*, 95 (23), 13988–13993.

Engel, A. K., Fries, P., & Singer, W. (2001). Dynamic predictions: Oscillations and synchrony in top–down processing. *Nature Reviews Neuroscience 2001 2:10*, 2 (10), 704–716.

Engel, A. K., König, P., Kreiter, A. K., & Singer, W. (1991). Interhemispheric Synchronization of Oscillatory Neuronal Responses in Cat Visual Cortex. *Science*, 252 (5009), 1177–1179.

Engel, A. K., Kreiter, A. K., König, P., & Singer, W. (1991). Synchronization of oscillatory neuronal responses between striate and extrastriate visual cortical areas of the cat. *Proceedings of the National Academy of Sciences of the United States of America*, 88 (14), 6048–6052.

Fellous, J. M., & Sejnowski, T. J. (2003). Regulation of Persistent Activity by Background Inhibition in an In Vitro Model of a Cortical Microcircuit. *Cerebral Cortex*, 13 (11), 1232–1241.

Fields, R. D. (2015). A new mechanism of nervous system plasticity: activity-dependent myelination. *Nature Reviews Neuroscience*, 16 (12), 756–767.

Fields, R. D., & Bukalo, O. (2020). Myelin makes memories. *Nature Neuroscience*, 23 (4), 469–470.

Fitzgibbon, S. P., Pope, K. J., MacKenzie, L., Clark, C. R., & Willoughby, J. O. (2004). Cognitive tasks augment gamma EEG power. *Clinical Neurophysiology*, 115 (8), 1802–1809.

Fregnac, Y., Shulz, D., Thorpe, S., & Bienenstock, E. (1992). Cellular analogs of visual cortical epigenesis. I. Plasticity of orientation selectivity. *Journal of Neuroscience*, 12 (4), 1280–1300.

Friedman-Hill, S., Maldonado, P. E., & Gray, C. M. (2000). Dynamics of Striate Cortical Activity in the Alert Macaque: I. Incidence and Stimulus-dependence of Gamma-band Neuronal Oscillations. *Cerebral Cortex*, 10 (11), 1105–1116.

Fries, P. (2005). A mechanism for cognitive dynamics: neuronal communication through neuronal coherence. *Trends in Cognitive Sciences*, 9 (10), 474–480.

Fries, P. (2015). Rhythms for Cognition: Communication through Coherence. *Neuron*, 88 (1), 220–35.

Fries, P., Reynolds, J. H., Rorie, A. E., & Desimone, R. (2001). Modulation of oscillatory neuronal synchronization by selective visual attention. *Science*, 291 (5508), 1560–1563.

Fukuda, T., Kosaka, T., Singer, W., & Galuske, R. A. W. (2006). Gap Junctions among Dendrites of Cortical GABAergic Neurons Establish a Dense and Widespread Intercolumnar Network. *Journal of Neuroscience*, 26 (13), 3434–3443.

Galuske, R. A. W., Munk, M. H. J., & Singer, W. (2019). Relation between gamma oscillations and neuronal plasticity in the visual cortex. *Proceedings of the National Academy of Sciences of the United States of America*, 116 (46), 23317–23325.

Gieselmann, M. A., & Thiele, A. (2008). Comparison of spatial integration and surround suppression characteristics in spiking activity and the local field potential in macaque V1. *European Journal of Neuroscience*, 28 (3), 447–459.

Gilbert, C. D., & Wiesel, T. N. (1983). Clustered intrinsic connections in cat visual cortex. *Journal of Neuroscience*, 3 (5), 1116–1133.

Gilbert, C. D., & Wiesel, T. N. (1989). Columnar specificity of intrinsic horizontal and corticocortical connections in cat visual cortex. *Journal of Neuroscience*, 9 (7), 2432–2422.

Gilbert, Charles D., & Wiesel, T. N. (1979). Morphology and intracortical projections of functionally characterised neurones in the cat visual cortex. *Nature 1979 280:5718*, 280 (5718), 120–125.

Gori, S., & Spillmann, L. (2010). Detection vs. grouping thresholds for elements differing in spacing, size and luminance. An alternative approach towards the psychophysics of Gestalten. *Vision Research*, 50 (12), 1194–1202.

Gould, I. C., Rushworth, M. F., & Nobre, A. C. (2011). Indexing the graded allocation of visuospatial attention using anticipatory alpha oscillations. *Journal of Neurophysiology*, 105 (3), 1318–1326.

Gray, C. M., König, P., Engel, A. K., & Singer, W. (1989a). Oscillatory responses in cat visual cortex exhibit inter-columnar synchronization which reflects global stimulus properties. *Nature*, 338 (6213), 334–337.

Gray, C. M., König, P., Engel, A. K., & Singer, W. (1989b). Oscillatory responses in cat visual cortex exhibit inter-columnar synchronization which reflects global stimulus properties. *Nature 1989 338:6213*, 338 (6213), 334–337.

Gray, C. M., & McCormick, D. A. (1996). Chattering Cells: Superficial Pyramidal Neurons Contributing to the Generation of Synchronous Oscillations in the Visual Cortex. *Science*, 274 (5284), 109–113.

Gutkin, B. S., Ermentrout, G. B., & Reyes, A. D. (2005). Phase-response curves give the responses of neurons to transient inputs. *Journal of Neurophysiology*, 94 (2), 1623–1635.

Hadjipapas, A., Lowet, E., Roberts, M. J., Peter, A., & de Weerd, P. (2015). Parametric variation of gamma frequency and power with luminance contrast: A comparative study of human MEG and monkey LFP and spike responses. *NeuroImage*, 112, 327–340.

Haegens, S., Nácher, V., Luna, R., Romo, R., & Jensen, O. (2011). α-Oscillations in the monkey sensorimotor network influence discrimination performance by rhythmical inhibition of neuronal spiking. *Proceedings of the National Academy of Sciences of the United States of America*, 108 (48), 19377–19382.

Hansel, D., & Mato, G. (2003). Asynchronous States and the Emergence of Synchrony in Large Networks of Interacting Excitatory and Inhibitory Neurons. *Neural Computation*, 15 (1), 1–56.

Hasenstaub, A., Shu, Y., Haider, B., Kraushaar, U., Duque, A., & McCormick, D. A. (2005). Inhibitory Postsynaptic Potentials Carry Synchronized Frequency Information in Active Cortical Networks. *Neuron*, 47 (3), 423–435.

Hermes, D., Miller, K. J., Wandell, B. A., & Winawer, J. (2015). Stimulus dependence of gamma oscillations in human visual cortex. *Cerebral Cortex*, 25 (9), 2951–2959.

Herrmann, C. S., Munk, M. H. J., & Engel, A. K. (2004). Cognitive functions of gamma-band activity: memory match and utilization. *Trends in Cognitive Sciences*, 8 (8), 347–355.

Hochstein, S., & Ahissar, M. (2002). View from the Top: Hierarchies and Reverse Hierarchies in the Visual System. *Neuron*, 36 (5), 791–804.

Hodgkin, A. L., Huxley, A. F., & Katz, B. (1952). Measurement of current-voltage relations in the membrane of the giant axon of Loligo. *The Journal of Physiology*, 116 (4), 424–448.

Hoogenboom, N., Schoffelen, J. M., Oostenveld, R., Parkes, L. M., & Fries, P. (2006). Localizing human visual gamma-band activity in frequency, time and space. *NeuroImage*, 29 (3), 764–773.

Hubel, D. H., & Wiesel, T. N. (1968). Receptive fields and functional architecture of monkey striate cortex. *The Journal of Physiology*, 195 (1), 215–243.

Hughes, S. W., & Crunelli, V. (2005). Thalamic mechanisms of EEG alpha rhythms and their pathological implications. *Neuroscientist*, 11 (4), 357–372.

Hummel, J. E. (2010). Complementary solutions to the binding problem in vision: Implications for shape perception and object recognition. *Visual Cognition*, 8 (3–5), 489–517.

Izhikevich, E. M. (2004a). *Dynamical Systems in Neuroscience*. *Dynamical Systems in Neuroscience: The Geometry of Excitability and Bursting*. San Diego, California: Springer-Verlag.

Izhikevich, E. M. (2004b). Simple Models. In *Dynamical Systems in Neuroscience: The Geometry of Excitability and Bursting* (pp. 357–396). San Diego, California: Springer-Verlag.

Izhikevich, E. M. (2004c). Synchronization. In *Dynamical Systems in Neuroscience: The Geometry of Excitability and Bursting* (pp. 301–351). San Diego, California: Springer-Verlag.

Izhikevich, E. M., & Kuramoto, Y. (2005). Weakly Coupled Oscillators. *Encyclopedia of Mathematical Physics*.

Jadbabaie, A., Motee, N., & Barahona, M. (2018). On the stability of the Kuramoto model of coupled nonlinear oscillators. *Proceedings of the 2004 American Control Conference*, 5, 4296–4301.

Jenkins, W. M., Merzenich, M. M., Ochs, M. T., Allard, T., & Guic-Robles, E. (1990). Functional reorganization of primary somatosensory cortex in adult owl monkeys after behaviorally controlled tactile stimulation. *Journal of Neurophysiology*, 63 (1), 82–104.

Julesz, B., & Bergen, J. R. (1983). Human Factors and Behavioral Science: Textons, The Fundamental Elements in Preattentive Vision and Perception of Textures. *Bell System Technical Journal*, 62 (6), 1619–1645.

Julesz, B., & Papathomas, T. v. (1984). On spatial-frequency channels and attention. *Perception & Psychophysics*, 36 (4), 398–399.

Kahana, M. J. (2006). The Cognitive Correlates of Human Brain Oscillations. *Journal of Neuroscience*, 26 (6), 1669–1672.

Kandel, E., Schwartz, J., Jessell, T., & Siegelbaum, S. (2000a). *Principles of neural science* (Vol. 4). New York: McGraw-hill.

Kandel, E., Schwartz, J., Jessell, T., & Siegelbaum, S. (2000b). The Constructive Nature of Visual Processing. In *priciples of Neural Science* (pp. 556–576). New York: McGraw-hill.

Karni, A., & Bertini, G. (1997). Learning perceptual skills: behavioral probes into adult cortical plasticity. *Current Opinion in Neurobiology*, 7 (4), 530–535.

Karni, A., & Sagi, D. (1991). Where practice makes perfect in texture discrimination: evidence for primary visual cortex plasticity. *Proceedings of the National Academy of Sciences*, 88 (11), 4966–4970.

Kilgard, M. P., & Merzenich, M. M. (1998). Cortical map reorganization enabled by nucleus basalis activity. *Science*, 279 (5357), 1714–1718.

Kuramoto, Y. (1984). *Chemical Oscillations, Waves, and Turbulence*. *Turbulence* (Vol. 19). Berlin, Heidelberg: Springer Berlin Heidelberg.

Kuramoto, Y., & Kuramoto Y. (1975). Self-entrainment of a population of coupled non-linear oscillators. In *Araki H. (eds) International Symposium on Mathematical Problems in Theoretical Physics* (p. Lecture Notes in Physics, vol 39). Berlin, Heidelberg: Springer.

Lange, G., Lowet, E., Roberts, M. J., & Weerd, P. de. (2018). Within-quadrant position and orientation specificity after extensive orientation discrimination learning is related to performance gains during late learning. *PLOS ONE*, 13 (9), e0201520.

Latham, P. E., Richmond, B. J., Nelson, P. G., & Nirenberg, S. (2000). Intrinsic dynamics in neuronal networks. I. Theory. *Journal of Neurophysiology*, 83 (2), 808–827.

Levitt, J. B., Yoshioka, T., & Lund, J. S. (1994). Intrinsic cortical connections in macaque visual area V2: Evidence for interaction between different functional streams. *Journal of Comparative Neurology*, 342 (4), 551–570.

Liu, Z., & Weinshall, D. (2000). Mechanisms of generalization in perceptual learning. *Vision Research*, 40 (1), 97–109.

Livingstone, M. S., Freeman, D. C., & Hubel, D. H. (1996). Visual Responses in V1 of Freely Viewing Monkeys. *Cold Spring Harbor Symposia on Quantitative Biology*, 61, 27–37.

Longstaff, A., & Ronczkowski, M. R. (2011). *BIOS Instant Notes in Neuroscience*. *BIOS Instant Notes in Neuroscience*. Taylor & Francis.

Lopes Da Silva, F. H., & Storm Van Leeuwen, W. (1977). The cortical source of the alpha rhythm. *Neuroscience Letters*, 6 (2–3), 237–241.

Lowet, E., Roberts, M., Hadjipapas, A., Peter, A., van der Eerden, J., & de Weerd, P. (2015). Input-Dependent Frequency Modulation of Cortical Gamma Oscillations Shapes Spatial Synchronization and Enables Phase Coding. *PLoS Computational Biology*.

Lowet, E., Roberts, M. J., Peter, A., Gips, B., & de Weerd, P. (2017). A quantitative theory of gamma synchronization in macaque V1. *ELife*, 6.

Lund, J. S., Angelucci, A., & Bressloff, C. P. (2003). Anatomical Substrates for Functional Columns in Macaque Monkey Primary Visual Cortex. *Cerebral Cortex*, 13 (1), 15–24.

Lytton, W. W., & Sejnowski, T. J. (1991). Simulations of cortical pyramidal neurons synchronized by inhibitory interneurons. *Journal of Neurophysiology*, 66 (3), 1059–1079.

Malsburg, Christoph von der. (1995). Binding in models of perception and brain function. *Current Opinion in Neurobiology*, 5 (4), 520–526.

Milanese, R. (1994). *Feature Binding through Synchronized Neuronal Oscillations: A Preliminary Study*. International Computer Science Institute.

Mishkin, M., Ungerleider, L. G., & Macko, K. A. (1983). Object vision and spatial vision: two cortical pathways. *Trends in Neurosciences*, 6 (C), 414–417.

Nelson, M., & Rinzel, J. (1998). *The Hodgkin—Huxley Model*. *The Book of GENESIS*. Springer, New York, NY.

Nothdurft, Hans Christoph. (2000). Salience from feature contrast: additivity across dimensions. *Vision Research*, 40 (10–12), 1183–1201.

Nothdurft, H. C. (1985a). Orientation sensitivity and texture segmentation in patterns with different line orientation. *Vision Research*, 25 (4), 551–560.

Nothdurft, H. C. (1985b). Sensitivity for structure gradient in texture discrimination tasks. *Vision Research*, 25 (12), 1957–1968.

Nothdurft, H. C. (1990a). Texton segregation by associated differences in global and local luminance distribution. *Proceedings of the Royal Society of London. B. Biological Sciences*, 239 (1296), 295–320.

Nothdurft, H. C. (1990b). Texton segregation by associated differences in global and local luminance distribution. *Proceedings of the Royal Society of London. B. Biological Sciences*, 239 (1296), 295–320.

Nothdurft, H. C. (1990c). Texture discrimination by cells in the cat lateral geniculate nucleus. *Experimental Brain Research 1990 82:1*, 82 (1), 48–66.

Nothdurft, H.-C. (2015). Feature contrast in salience and grouping: luminance and disparity The full paper can be downloaded from www.vpl-reports.de/3/ View publication stats View publication stats. *Visual Perception Laboratory (VPL)*, 3, 1–32.

Pavlaslk, I. (1998). The Binding Problem in Population Neurodynamics: A Network Model for Stimulus-Specific Coherent Oscillations. *I, Gen Phvsiol Biophys*, 17, 323–340.

Pikovsky, A., Rosenblum, M., Self, J. K.-, & 2001, undefined. (2003). A universal concept in nonlinear sciences. *Researchgate.Net*.

Ray, S., & Maunsell, J. H. R. (2015). Do gamma oscillations play a role in cerebral cortex? *Trends in Cognitive Sciences*, 19 (2), 78–85.

Ray, S., & Maunsell, J. H. R. (2010). Differences in Gamma Frequencies across Visual Cortex Restrict Their Possible Use in Computation | Elsevier Enhanced Reader. *Neuron*, 67, 885–896.

Recanzone, G. H., Merzenich, M. M., & Dinse, H. R. (1992). Expansion of the Cortical Representation of a Specific Skin Field in Primary Somatosensory Cortex by Intracortical Microstimulation. *Cerebral Cortex*, 2 (3), 181–196.

Roberts, M. J., Lowet, E., Brunet, N. M., TerWal, M., Tiesinga, P., Fries, P., & de Weerd, P. (2013). Robust gamma coherence between macaque V1 and V2 by dynamic frequency matching. *Neuron*.

Rockland, K. S., & Lund, J. S. (1982). Widespread periodic intrinsic connections in the tree shrew visual cortex. *Science (New York, N.Y.)*, 215 (4539), 1532–1534.

Roelfsema, P. R., van Ooyen, A., & Watanabe, T. (2010). Perceptual learning rules based on reinforcers and attention. *Trends in Cognitive Sciences*, 14 (2), 64–71.

Rols, G., Tallon-Baudry, C., Girard, P., Bertrand, O., & Bullier, J. (2001). Cortical mapping of gamma oscillations in areas V1 and V4 of the macaque monkey. *Visual Neuroscience*, 18 (4), 527–540.

Rubin, N., Nakayama, K., & Shapley, R. (1997). Abrupt learning and retinal size specificity in illusory-contour perception. *Current Biology*, 7 (7), 461–467.

Sarnthein, J., Petsche, H., Rappelsberger, P., Shaw, G. L., & von Stein, A. (1998). Synchronization between prefrontal and posterior association cortex during human working memory. *Proceedings of the National Academy of Sciences of the United States of America*, 95 (12), 7092–7096.

Schack, B., Vath, N., Petsche, H., Geissler, H. G., & Möller, E. (2002). Phase-coupling of theta–gamma EEG rhythms during short-term memory processing. *International Journal of Psychophysiology*, 44 (2), 143–163.

Scholz, J., Klein, M. C., Behrens, T. E. J. J., & Johansen-Berg, H. (2009). Training induces changes in white-matter architecture. *Nature Neuroscience*, 12 (11), 1370–1371.

Schoups, A. A., Vogels, R., & Orban, G. A. (1995). Human perceptual learning in identifying the oblique orientation: retinotopy, orientation specificity and monocularity. *The Journal of Physiology*, 483 (3), 797–810.

Schoups, A., Vogels, R., Qian, N., & Orban, G. (2001). Practising orientation identification improves orientation coding in V1 neurons. *Nature 2001 412:6846*, 412 (6846), 549–553.

Schroeder, C. E., & Lakatos, P. (2009). The gamma oscillation: Master or slave? *Brain Topography*, 22 (1), 24–26.

Schuett, S., Bonhoeffer, T., & Hübener, M. (2001). Pairing-Induced Changes of Orientation Maps in Cat Visual Cortex. *Neuron*, 32 (2), 325–337.

Sporns, O., Tononi, G., & Edelman, G. M. (1991). Modeling perceptual grouping and figure-ground segregation by means of active reentrant connections. *Proceedings of the National Academy of Sciences*, 88 (1), 129–133.

Stiefel, K. M., Gutkin, B. S., & Sejnowski, T. J. (2008). Cholinergic Neuromodulation Changes Phase Response Curve Shape and Type in Cortical Pyramidal Neurons. *PLOS ONE*, 3 (12), e3947.

Stoelzel, C. R., Bereshpolova, Y., Alonso, J. M., & Swadlow, H. A. (2017). Axonal Conduction Delays, Brain State, and Corticogeniculate Communication. *The Journal of Neuroscience : The Official Journal of the Society for Neuroscience*, 37 (26), 6342–6358.

Tiesinga, P. H., Fellous, J. M., Salinas, E., José, J. v., & Sejnowski, T. J. (2004). Inhibitory synchrony as a mechanism for attentional gain modulation. *Journal of Physiology-Paris*, 98 (4–6), 296–314.

Tiesinga, P. H., & Sejnowski, T. J. (2010). Mechanisms for phase shifting in cortical networks and their role in communication through coherence. *Frontiers in Human Neuroscience*, 4, 196.

Tiesinga, P., & Sejnowski, T. J. (2009). Cortical Enlightenment: Are Attentional Gamma Oscillations Driven by ING or PING? *Neuron*, 63 (6), 727–732.

Treisman, A. (1996). The binding problem. *Current Opinion in Neurobiology*, 6 (2), 171–178.

Ts'o, D. Y., Gilbert, C. D., & Wiesel, T. N. (1986). Relationships between horizontal interactions and functional architecture in cat striate cortex as revealed by cross-correlation analysis. *Journal of Neuroscience*, 6 (4), 1160–1170.

Uhlhaas, P. J., Pipa, G., Neuenschwander, S., Wibral, M., & Singer, W. (2011). A new look at gamma? High- (>60 Hz) γ-band activity in cortical networks: Function, mechanisms and impairment. *Progress in Biophysics and Molecular Biology*, 105 (1–2), 14–28.

van Essen, David C., & Glasser, M. F. (2018). Parcellating Cerebral Cortex: How Invasive Animal Studies Inform Noninvasive Mapmaking in Humans. *Neuron*, 99 (4), 640–663.

van Essen, David C., Lewis, J. W., Drury, H. A., Hadjikhani, N., Tootell, R. B. H., Bakircioglu, M., & Miller, M. I. (2001). Mapping visual cortex in monkeys and humans using surface-based atlases. *Vision Research*, 41 (10–11), 1359–1378.

van Essen, D. C., Felleman, D. J., DeYoe, E. A., Olavarria, J., & Knierim, J. (1990). Modular and Hierarchical Organization of Extrastriate Visual Cortex in the Macaque Monkey. *Cold Spring Harbor Symposia on Quantitative Biology*, 55, 679–696.

Vinck, Martin, Lima, B., Womelsdorf, T., Oostenveld, R., Singer, W., Neuenschwander, S., & Fries, P. (2010). Gamma-Phase Shifting in Awake Monkey Visual Cortex. *Journal of Neuroscience*, 30 (4), 1250–1257.

Vinck, M, Womelsdorf, T., & Fries, P. (2013). Gamma-band synchronization and information transmission. *Principles of Neural Coding*, 449–469.

von der Malsburg, C. (1999). The What and Why of Binding: The Modeler's Perspective. *Neuron*, 24 (1), 95–104.

von der Malsburg, Christoph, & Buhmann, J. (1992). Sensory segmentation with coupled neural oscillators. *Biological Cybernetics 1992 67:3*, 67 (3), 233–242.

von Stein, A., & Sarnthein, J. (2000). Different frequencies for different scales of cortical integration: from local gamma to long range alpha/theta synchronization. *International Journal of Psychophysiology*, 38 (3), 301–313.

Wagemans, J., Elder, J. H., Kubovy, M., Palmer, S. E., Peterson, M. A., Singh, M., & von der Heydt, R. (2012). A century of Gestalt psychology in visual perception: I. Perceptual grouping and figure-ground organization. *Psychological Bulletin*, 138 (6), 1172–1217.

Wang, X. J., & Buzsáki, G. (1996). Gamma Oscillation by Synaptic Inhibition in a Hippocampal Interneuronal Network Model. *Journal of Neuroscience*, 16 (20), 6402–6413.

Whittington, M. A., Traub, R. D., Kopell, N., Ermentrout, B., & Buhl, E. H. (2000). Inhibition-based rhythms: experimental and mathematical observations on network dynamics. *International Journal of Psychophysiology*, 38 (3), 315–336.

Whittington, Miles A., Traub, R. D., & Jefferys, J. G. R. (1995). Synchronized oscillations in interneuron networks driven by metabotropic glutamate receptor activation. *Nature 1995 373:6515*, 373 (6515), 612–615.

WILLIAMS, D., & JULESZ, B. (1992). Filters Versus Textons in Human and Machine Texture Discrimination. *Neural Networks for Perception*, 145–175.

Wilson, H. R., & Cowan, J. D. (1972). Excitatory and Inhibitory Interactions in Localized Populations of Model Neurons. *Biophysical Journal*, 12 (1), 1–24.

Womelsdorf, T., & Fries, P. (2007). The role of neuronal synchronization in selective attention. *Current Opinion in Neurobiology*, 17 (2), 154–160.

Womelsdorf, T., Fries, P., Mitra, P. P., & Desimone, R. (2005). Gamma-band synchronization in visual cortex predicts speed of change detection. *Nature 2006 439:7077*, 439 (7077), 733–736.

Xing, D., Shen, Y., Burns, S., Yeh, C. I., Shapley, R., & Li, W. (2012). Stochastic Generation of Gamma-Band Activity in Primary Visual Cortex of Awake and Anesthetized Monkeys. *Journal of Neuroscience*, 32 (40), 13873–13880a.

Yoshioka, T., Blasdel, G. G., Levitt, J. B., & Lund, J. S. (1996). Relation between patterns of intrinsic lateral connectivity, ocular dominance, and cytochrome oxidase-reactive regions in macaque monkey striate cortex. *Cerebral Cortex (New York, N.Y. : 1991)*, 6 (2), 297–310.

Yu, J., & Ferster, D. (2010). Membrane Potential Synchrony in Primary Visual Cortex during Sensory Stimulation. *Neuron*, 68 (6), 1187–1201.

Zatorre, R. J., Fields, R. D., & Johansen-berg, H. (2012). Plasticity in gray and white: Neuroimaging changes in brain structure during learning. *Nature Neuroscience*, 15 (4), 528–536.

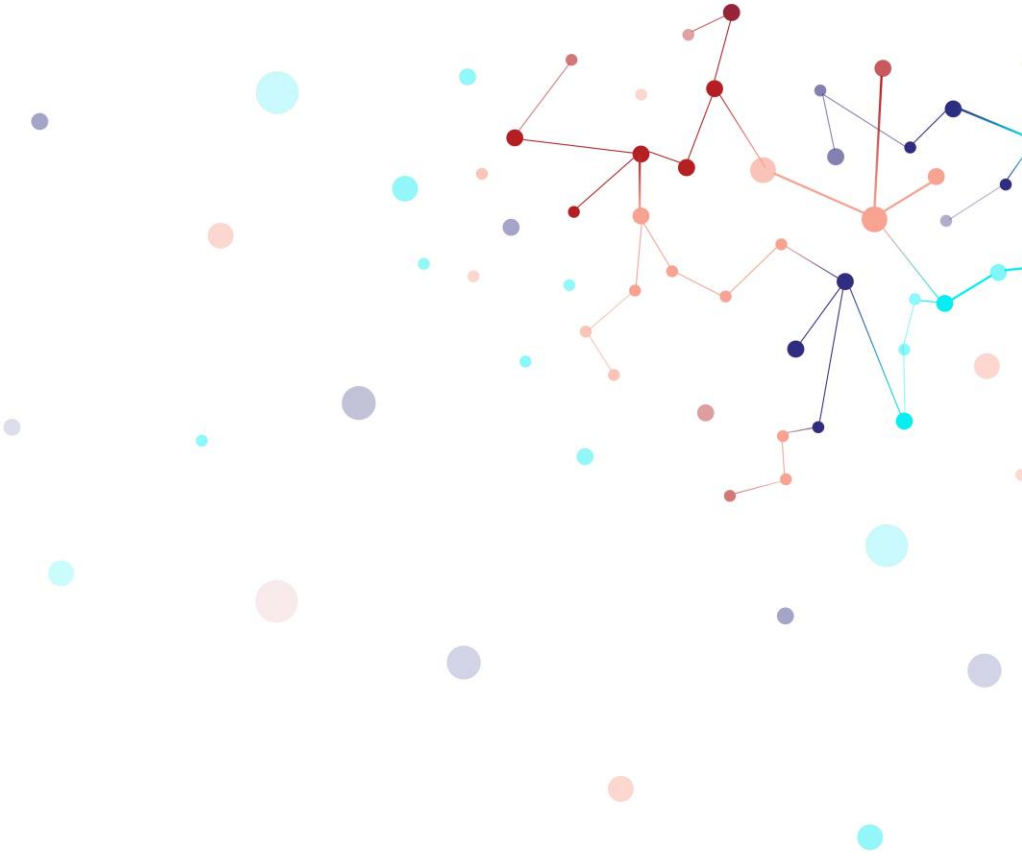

Karimian, M., Dibenedetto, D., Moerel, M., Burwick, T., Westra, R. L., De Weerd, P., & Senden, M., Chaos: An Interdisciplinary Journal Of Nonlinear Science 29. 8, 083122 (2019)

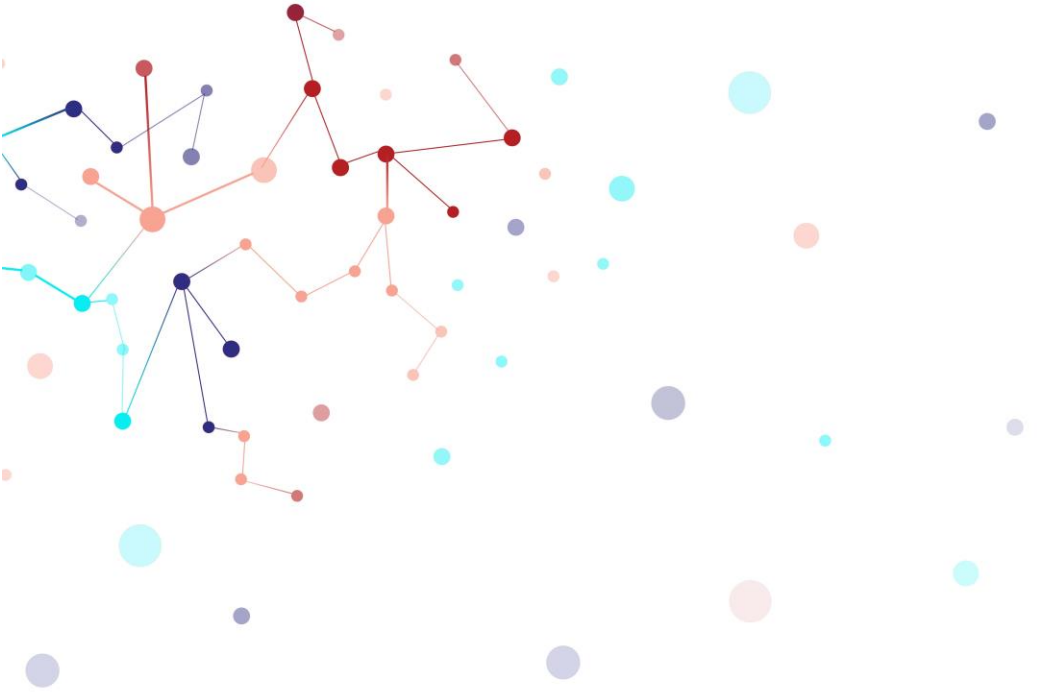

Chapter 2

Effects of Synaptic and Myelin Plasticity on Learning in a Network of Kuramoto Phase Oscillators

Abstract

Models of learning typically focus on synaptic plasticity. However, learning is the result of both synaptic and myelin plasticity. Specifically, synaptic changes often co-occur and interact with myelin changes, leading to complex dynamic interactions between these processes. Here, we investigate the implications of these interactions for the coupling behaviour of a system of Kuramoto oscillators. To that end, we construct a fully connected, one-dimensional ring network of phase oscillators whose coupling strength (reflecting synaptic strength), as well as conduction velocity (reflecting myelination), are each regulated by a Hebbian learning rule. We evaluate the behaviour of the system in terms of structural (pairwise connection strength and conduction velocity) and functional connectivity (local and global synchronization behaviour).

We find that adaptive myelination is able to both functionally de-couple structurally connected oscillators as well as to functionally couple structurally disconnected oscillators. With regard to the latter, we find that for conditions in which a system limited to synaptic plasticity develops two distinct clusters both structurally and functionally, additional adaptive myelination allows for functional communication across these structural clusters. These results confirm that network states following learning may be different when myelin plasticity is considered in addition to synaptic plasticity, pointing towards the relevance of integrating both factors in computational models of learning.

Synaptic and myelin plasticity are two crucial mechanisms underlying learning in the brain. Synaptic plasticity, which refers to activity-dependent changes of synaptic coupling, has been modelled intensely in recent decades. However, myelin plasticity, which refers to activity-dependent changes in the structure and thickness of myelin sheaths, has been largely absent from computational models of learning. These two plasticity mechanisms are likely to exhibit complex interactions. In this work, we suggest a simple mathematical framework as a first attempt to understand these interactions. Our results may pave the way for the development of new models of learning incorporating both synaptic and myelin plasticity.

2-1. Introduction

Synchronization, the mutual adjustment of rhythms among interacting oscillators (Haken, 2002; Pikovsky, Rosenblum, Self, & 2001, 2003), is a ubiquitous phenomenon in physics, biology, and neuroscience (El-Nashar, Zhang, Cerdeira, & Ibiyinka A., 2003; Gonze, Bernard, Waltermann, Kramer, & Herzel, 2005; Kumar, Verma, & P.Parmananda, 2017; Mörtl, Lorenz, & Hirche, 2014). In the latter, this phenomenon has been linked to various cognitive functions including perception (Hipp, Engel, & Siegel, 2011; Krause, Pörn, Lang, & Laine, 1997; Melloni et al., 2007), attention (Burylko, Kazanovich, & Borisyuk, 2018; Doesburg, Roggeveen, Kitajo, & Ward, 2008; Fell, Klaver, Elger, & Fries, 2003; Kazanovich & Borisyuk, 2017; Womelsdorf & Fries, 2007), and learning (Niyogi & English, 2009; Nowotny, Zhigulin, Selverston, Abarbanel, & Rabinovich, 2003; Pfister & Gerstner, 2006; Quiroga, Arnhold, & Grassberger, 2000; Seliger, Young, & Tsimring, 2002; Singer, 1993; Siri, Quoy, Delord, Cessac, & Berry, 2007; Song, Miller, & Abbott, 2000; Timms & English, 2014; Traubab et al., 1998; Zouridakis, Baluch, Stevenson, Diaz, & Subramanian, 2007). Learning involves the dynamic adjustment of connections among neuronal populations in the form of synaptic plasticity (D. O. Hebb, 1949). Mutual interactions between synaptic plasticity and synchronization have been of particular interest in neuroscience (H. Markram, L. H. R. Lübke, M. Frotscher, & B. Sakmann, 1997; Kasatkin, Yanchuk, Schöll, & Nekorkin, 2017; Maistrenko, Lysyansky, Hauptmann, Burylko, & Tass, 2007; Niyogi & English, 2009; Nowotny et al., 2003; Popovych, Yanchuk, & Tass, 2013; Seliger et al., 2002; Siri et al., 2007; Song et al., 2000; Timms & English, 2014; Traubab et al., 1998). However, synaptic plasticity is not the only factor being affected by as well as affecting synchronized activity in oscillating neuronal populations. Myelination is also activity-dependent (Chang, Redmond, & Chan, 2016; Fields, 2015; McKenzie et al., 2014; Nickel & Gu, 2018; Purger, Gibson, & Monje, 2016; R. D. Fields, 2014; Scholz, Klein, Behrens, & Johansen-Berg, 2009; Yeung & Strogatz, 1999) and since it influences the conduction velocity of neuronal signals, it is an additional dynamic factor potentially affecting synchronization behaviour. Myelination is integral to the unimpaired functioning of the brain as it ensures that signals originating from presynaptic sources at various locations nevertheless arrive within short succession of each other at a postsynaptic target (Pajevic, Basser, & Fields, 2014). The effect of myelination on signal transduction is quite profound with even slight changes in its thickness possessing the ability to bring about significant differences in the number of signals received by a specific neuron within a given time interval (Dutta et al., 2018; Pajevic et al., 2014). This, in turn, might strongly affect local and global

synchrony among neural groups. Therefore, it might be beneficial for the brain to dispose of the ability to dynamically adjust signal conduction among remote areas depending on the frequency with which they interact (engage in functional connectivity). Indeed, abundant biological evidence supports the idea of continued adaptive changes in myelination throughout the whole lifespan (Barrera et al., 2013; Fields, 2010; McKenzie et al., 2014; Nickel & Gu, 2018; Purger et al., 2016; Zatorre, Fields, & Johansen-berg, 2012). The fact that adaptive myelination constitutes a second dynamic factor in addition to synaptic plasticity, both of which depend on the temporal statistics of neural activations in pre- and post-synaptic neuronal populations (Pajevic et al., 2014), inspired us to systematically investigate their interactions in a system of weakly coupled oscillators. We employ a neural mass model to capture the phase evolution of weakly coupled neural groups as their connections undergo activity-dependent changes in coupling strength and conduction velocity.

Specifically, we consider a system of Kuramoto oscillators (Acebr et al., 2005) with distance-dependent delays previously established to study the effect of synaptic plasticity (Timms & English, 2014). We extend this model by dynamically adjusting conduction velocity (and hence transmission delays) in addition to synaptic weights. Changes in both synaptic weight and conduction depend on a Hebbian learning rule (D. O. Hebb, 1949), which is based on the frequency of the coactivations among pairs of network oscillators. That is, both connection weights and conduction velocity are time-dependent parameters influencing each other and the dynamics of the network as a whole.

2-2. Materials and Methods

2-2-1. Weakly-coupled oscillator model

In line with previous work (Timms & English, 2014), our network model consists of an ensemble of N phase oscillators arranged along a circle; i.e. a one-dimensional array with periodic boundary conditions. The network is fully connected with the exact coupling strengths between oscillators given by the real-valued directed connectivity matrix K. Local dynamics of each phase oscillator are governed by a Kuramoto model with transmission delays

$$\begin{cases} \dot{\varphi}_i(t) = \omega_i + \frac{1}{N}\sum_{j=1}^{N} K_{ij}\,(\mathrm{t})\, sin\left(\varphi_j\left(t - \boldsymbol{\tau_{ij}}\right) - \varphi_i(t)\right), & \tau_{ij} = \frac{d_{ij}}{v} \\ \dot{\varphi}_i(t) = \omega_i + \frac{1}{N}\sum_{j=1}^{N} K_{ij}\,(\mathrm{t})\, sin\left(\varphi_j\left(t - \boldsymbol{\tau_{ij}}\,(\boldsymbol{t})\right) - \varphi_i(t)\right), & \tau_{ij}\,(\mathrm{t}) = \frac{d_{ij}}{v_{ij}\,(t)} \end{cases} \quad (2.1)$$

where $\varphi_i(t) \in [0,2\pi)$ denotes the phase of oscillator i $(i = 1, \dots, N)$ at time t, ω_i is its intrinsic frequency and K_{ij} reflects the strength of the connection from the jth to the ith oscillator. The transmission delay from j to i is static (τ_{ij}) if conduction velocity is constant (v), or time-dependent $(\tau_{ij}\,(\mathrm{t}))$ if conduction velocity is dynamic $(v_{ij}\,(t)$, see Equation 2.4). Finally, d_{ij} is the distance between two oscillators. Due to periodic boundary conditions, this distance can be defined as

$$d_{ij} = \frac{L}{N}\min(|i-j|, N-|i-j|) \quad (2.2)$$

with L controlling the circumference of the circle. For the case of static delays, we define a coupling delay constant $T = \frac{L}{v}$ as the time needed for signals travelling at a velocity v to revolve once around the circle (Timms & English, 2014).

The coupling strength K_{ij} between oscillators i and j varies dynamically according to a form of Hebbian learning where the growth or decay of coupling strengths depend on the phase offset between oscillators (Bi & Poo, 1998; Wittenberg & Wang, 2006)

$$\begin{cases} \dot{K}_{ij}(t) = \varepsilon_s\left[\alpha_s\, cos\left(\varphi_i(t) - \varphi_j\left(t - \tau_{ij}\right)\right) - K_{ij}(t)\right], & \tau_{ij} = \frac{d_{ij}}{v} \\ \dot{K}_{ij}(t) = \varepsilon_s\left[\alpha_s\, cos\left(\varphi_i(t) - \varphi_j\left(t - \tau_{ij}\,(t)\right)\right) - K_{ij}(t)\right], & \tau_{ij}(\mathrm{t}) = \frac{d_{ij}}{v_{ij}(t)}. \end{cases} \quad (2.3)$$

In Equation 2.3, ε_s and α_s respectively control the learning rate and learning enhancement factor of the coupling strength. The learning enhancement factor α_s determines the maximum and minimum coupling strength (Niyogi & English, 2009) and ensures that these remain sufficiently weak.

For the case in which conduction velocities between pairs of oscillators vary dynamically, conduction velocity is no longer identical for all pairs of oscillators but varies according to a second Hebbian learning process

$$\dot{v}_{ij}(t) = \varepsilon_v \left[\alpha_v \cos\left(\varphi_i(t) - \varphi_j\left(t - \tau_{ij}(t)\right)\right) - v_{ij}(t)\right]. \qquad (2.4)$$

Here, ε_v and α_v are, respectively, the learning rate and learning enhancement factor of the conduction velocity. Note that conduction velocity was bounded from below because $v_{ij}(t)$ may otherwise grow too small leading to delays approaching infinity. We chose to bound $v_{ij}(t)$ at a value of 0.1 as this corresponds to $T = 10$ in the static case if all pairwise conduction velocities decay to this value.

2-2-2. Quantitative analyses

2-2-2-1. Global synchronization behaviour

In a network of globally coupled oscillators arranged along a ring with distance-dependent delays, the distribution of phases may show propagating structures, static phase increments from one oscillator to the next, referred to as coherent-wave modes (Timms & English, 2014; Zanette, 2000). Phase offsets with respect to a reference oscillator (e.g. the first) may exhibit periodicity at integer (or half-integer, see below) multiples of 2π. Frequency synchronization, identical frequencies but distributed phases, in such a system, can thus be characterized in terms of these multiples of 2π which are referred to as coherent-wave modes (denoted by m). However, for the system employed here, identification of coherent-wave mode values is complicated by the fact that either a single or two clusters of synchronized oscillators may form. We refer to the formation of a single cluster as single-cluster synchronization and to the formation of two (anti-phase) clusters as double-cluster synchronization. To overcome this problem, we measure both in-phase synchronization (r_1) and anti-phase synchronization (r_2). In-phase synchronization is characterized by the generalized order parameter (r_1) (Acebr et al., 2005; Dénes, Sándor, & Néda, 2019)

$$r_1 e^{i\psi(t)} = \frac{1}{N}\sum_{j=1}^{N} e^{i\varphi_j^*(t)} \qquad (2.5)$$

where $\psi(t)$ is the mean phase at time t (Acebr et al., 2005) and φ_j^* is the phase of oscillator j corrected for phase increments around the ring determined by the value of the mode m (Schröder, Timme, & Witthaut, 2017)

$$\varphi_j^*(t) = \varphi_j(t) \pm 2\pi m(j-1)/N\,. \qquad (2.6)$$

Anti-phase synchronization is given by (Niyogi & English, 2009; Timms & English, 2014)

$$r_2 = |r' - r_1|$$

where

$$r' e^{i\psi'(t)} = \frac{1}{N} \sum_{j=1}^{N} e^{2i\varphi_j^*(t)}. \tag{2.7}$$

The term r' measures in-phase and anti-phase synchronization by stretching the range from zero to π around the full circle. Hence, this measure needs to be adjusted for in-phase synchronization to obtain a measure of anti-phase synchronization (r_2). In accordance with previous work (Timms & English, 2014) we used a threshold on r_2 to determine the presence of a second cluster (here $r_2 \geq 0.15$). This implies that a second (smaller) cluster may exist even though $r_1 > r_2$.

To determine the mode of the system and whether it exhibits single- or double-cluster synchronization in any particular simulation, we compute both r_1 and r_2 for a range of candidate mode values ($m \in \{0,0.5,1,1.5,2\}$) and select the mode that maximizes the global phase-coherence [$\max(r_1, r_2)$]. Please note that for double-cluster synchronization m may take on half-integer values (Timms & English, 2014). This procedure, while able to detect double-clustered states when clusters are of unequal size, can only do so if the phase-offset between clusters equals π. This does not imply that two clusters may not exhibit smaller phase-offsets.

2-2-2-2. Pairwise connectivity

In addition to the global synchronization behaviour of the system, we also examine its local (i.e. pairwise) structural and functional connectivity. Structural connectivity is straightforwardly given by the coupling strength matrix K ranging from $-\alpha_s$ to α_s. To measure functional connectivity, we introduce a coherence matrix D whose elements are given by

$$D_{ij} = \frac{1}{\Delta t} \int_{t_r}^{t_r + \Delta t} \cos\big(\varphi_i(t) - \varphi_j(t)\big)\, dt. \tag{2.8}$$

Here, t_r marks a time-point after which the system no longer experiences major changes in coupling strength and/or conduction velocity. D_{ij} ranges from -1 to 1

with a value of 1 indicating that two nodes are in phase (over a time interval Δt) whereas a value of -1 indicates that two nodes are in anti-phase.

2-2-2-3. Numerical simulations

We analyze the system in terms of its global synchronization behaviour as well as in terms of pairwise structural and functional connectivity for three different cases: I) dynamic coupling strength and static conduction velocity; (c.f. (Timms & English, 2014)) II) static coupling strength and dynamic conduction velocity; and III) dynamic coupling strength and dynamic conduction velocity. For the first scenario, the system is evaluated for a range of combinations of parameters ε_s and T. For the latter two scenarios, ε_s is fixed at either 0 (no learning, scenario II) or 0.1 (fast learning, scenario III) and the behaviour is observed while the parameters ε_v and α_v are varied. The long-term behaviour of the system is characterized by its coherent-wave mode of synchronization and its cluster formation. For notational convenience, we denote each final state$\{m,c\}$, where *m* indicates the (half-)integer value of the coherent-wave mode and *c* indicates whether the network exhibits single (s) or double (d) cluster synchronization. For example, state$\{1,d\}$ describes a system exhibiting double cluster synchronization and a mode of 1.

For all simulations, intrinsic frequencies ω_i are drawn from a normal distribution $\aleph(1,0.01)$ and initial phases are drawn from a uniform distribution in the range $[0,2\pi)$. All simulations start from a network with coupling strengths fixed at their maximum value ($\alpha_s = 1$) which exceeds the critical coupling strength and supports interactions among oscillators. Furthermore, for those simulations for which velocity changes dynamically, conduction velocities are initialized as $v_{ij}\,(t=0) = 0.14$, which means that initial coupling delays correspond to the scenario where the delay constant (T) is ~7 for a ring length $L = 1$. Parameters characterizing the network are summarized in Table 1 while those characterizing the three simulated scenarios are summarized in Table 2.

Network parameter	**value**
N	100
L	1

Table 2.1: Network parameters

Scenario	parameter	value
Dynamic coupling strengths, static conduction velocities	α_s	1
	ε_v	0
	α_v	0
Static coupling strengths, dynamic conduction velocities	ε_s	0
	α_s	1
Dynamic coupling strengths and conduction velocities	ε_s	0.1
	α_s	1

Table 1.2: Simulation parameters

The model is implemented in MATLAB (R2016a) and integrated for 20000 time steps using the forward Euler method with a step size $dt = 0.01$ in arbitrary units of time. To accommodate for delays, we always first simulate 1000 time steps during which oscillators are non-interacting. Subsequently, the time delay interaction is switched on to simulate the 19000 time steps of interest.

We perform 50 simulations with different randomizations of initial conditions for each parameter combination in every scenario. We select the most frequently observed combination of coherent-wave mode of synchronization and cluster-formation (single vs double) as the characteristic final state of a given parameter combination. Whenever the characteristic state is observed in less than 70% of the simulations, we additionally identify a secondary state as the one occurring for at least 50% of the remaining simulations (i.e. of those not classified as the characteristic state). In this case, we regard the system as bistable. If no secondary state can be unambiguously identified and individual simulations yield different states, we regard the system as multistable. This procedure assumes that states are discernible for individual simulations; that is, they are indeed characterizable in terms of a unique combination of coherent-wave mode of synchronization and cluster-formation. This assumption may be violated if the system remains incoherent or by the formation of chimera-like states; i.e. different subsets of oscillators exhibit distinct 10 behaviours (Abrams & Strogatz, 2004; Breakspear, Heitmann, & Daffertshofer, 2010; Kotwal, Jiang, & Abrams, 2017; Laing, 2009; Yao, Huang, Lai, & Zheng, 2013). In this case, we regard the system as erratic.

2-3. Results

2-3-1. Scenario I: dynamic coupling strengths, static conduction velocities

We first examined learning in the context of static conduction velocity. For this purpose, we explored a parameter space defined by the delay constant T and the learning rate ε_s. Most parameter settings yield highly consistent results. However, some regions of parameter space exhibit diverse results. This is especially prevalent at borders between adjacent regions and likely reflects transitions in mode synchronization, cluster-formation, or both. At borders, the system may be multistable and the state observed for any given simulation depends on initial conditions. The two parameters affect the behaviour of the system in different, albeit interacting, ways. The learning rate mainly affects cluster-formation, with slow learning leading to the emergence of a single cluster while fast learning leads to the formation of two clusters (see Figure 2.1a). In the former case, changes in coupling strength between pairs of oscillators occur at a slower rate than synchronization. That is, the system synchronizes before large initial phase offsets can decrease coupling. In the latter case, changes in coupling strength between pairs of oscillators occur at a faster rate than synchronization. That is, initially large phase offsets between pairs of oscillators quickly drive their coupling strength to negative values, thus exacerbating their offset until they are separated by exactly π.

The delay constant interacts with learning rate as increasing delays allow for the formation of two clusters at progressively lower learning rates (Nakamura, Tominaga, & Munakata, 1994). However, it mainly affects mode synchronization with longer delays leading to larger m (see Figure 2.1). Specifically, for non-zero values, phases distribute around the circle such that the offset between each pair of neighbouring oscillators is $\frac{2\pi}{N}m$ (within a cluster) or $\frac{2\pi}{N}m + \pi$ (across clusters). Note that for the emergence of two clusters, half-integer values can be obtained (Figure 2.1d, f). This is in line with previous observations (Timms & English, 2014) that half-integer values are the result of the two clusters interconnecting. Oscillator pairs within a cluster "*see"* each other in phase when their phase offsets are matched by their delays. That is, due to delays, from the perspective of each oscillator in a cluster, the other oscillators within the same cluster appear in-phase whereas to an external observer they may appear out of phase. For the emergence of a single cluster, there is an exception to this observation for oscillator pairs with a phase offset around $\frac{\pi}{2}$. For these values, the trailing oscillator sees the leading oscillator in phase. However, the leading oscillator sees the trailing one in anti-phase. This asymmetry affects the

coupling strength such that the structural connection from the leading to the trailing oscillator is positive while that from the trailing to the leading is negative. The magnitude of their coupling strength is otherwise equal. This leads to one or two stripes of negative values in the structural connectivity matrix for modes $m = 1$ and $m = 2$, respectively (see Figure 2.2g,h). Interestingly, the structural connectivity matrices emerging for double-cluster formation also exhibit stripes for non-zero modes (Figure 2.2d-f). The number of these stripes in each case is twice its corresponding mode value m. According to the Hebbian learning rule (Equation 2.4), coupling strengths between every two oscillators i and j approach a stable value given by $K_{ij} = \alpha_s cos(\varphi_i - \varphi_j)$. For phase differences of $(2n-1)\frac{\pi}{2}$ this entails that the connection weights between the corresponding oscillators decay to zero. Since the mode determines the repetition of phase offsets equal to $(2n-1)\frac{\pi}{2}$ for each oscillator, it also determines the number of stripes in the structural connectivity matrices.

The emergence of stripes is also apparent in functional connectivity matrices (Figure 2.3). Here, stripes are symmetric, however, since functional connectivity is undirected. Therefore, twice as many stripes can be observed in functional connectivity matrices as compared to structural connectivity matrices. Furthermore, the exact location of stripes in the structural and functional connectivity matrices are different because temporal delays are not considered in the computation of pairwise correlations.

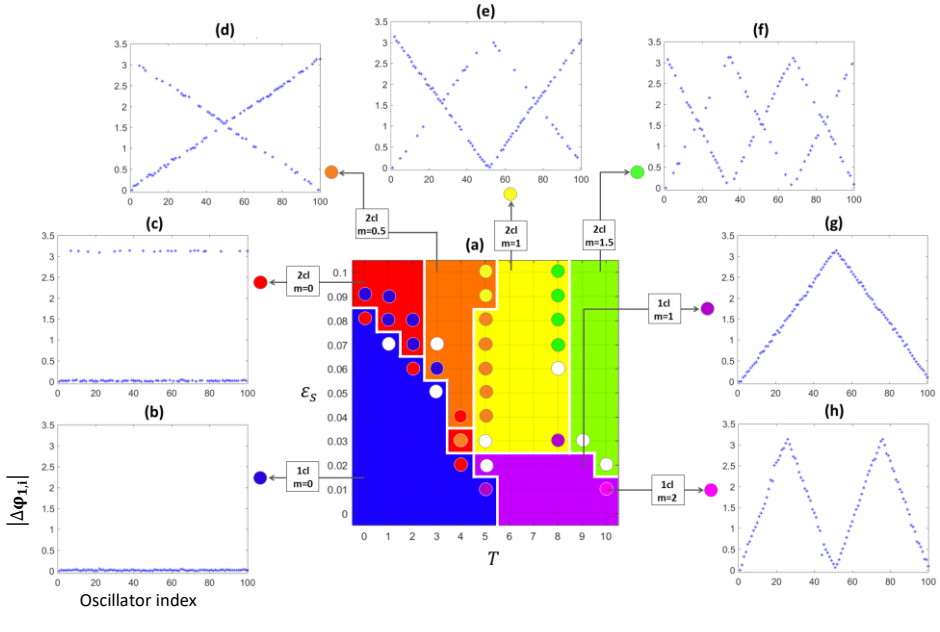

Figure 2.1: Arrangement of phase offsets with respect to the first oscillator when coupling strength is dynamic and conduction velocity is static. Panel a) shows the colour-coded state (coherent-wave mode of synchronization and cluster-formation) for each point in the parameter space defined by $\boldsymbol{T}$ and $\boldsymbol{\varepsilon_s}$. Colours indicate the characteristic states. Furthermore, coloured disks indicate secondary states (bistability). A white disk indicates multistability. **Panel b)** shows absolute phase offsets between every oscillator and the first $\left(\left|\Delta\boldsymbol{\varphi_{1,i}}\right|\right)$ for state{0,s}. All offsets are close to zero. **Panel c)** shows $\left|\Delta\boldsymbol{\varphi_{1,i}}\right|$ for the state{0,d}. Phase offsets are close to zero for oscillators falling into the same cluster as the first and close to π (half period) for those falling into the opposite cluster. **Panel d)** shows $\left|\Delta\boldsymbol{\varphi_{1,i}}\right|$ for the state{0.5,d}. Phase offsets exhibit one half-cycle; i.e. oscillators falling into the same cluster as the first increases with distance, whereas those in the opposite cluster decrease with distance. **Panel e)** shows $\left|\Delta\boldsymbol{\varphi_{1,i}}\right|$ for the state{1,d}. Phase offsets exhibit one full cycle with offsets for oscillators falling into the same cluster as the first mirroring those of oscillators in the opposite cluster. **Panel f)** shows $\left|\Delta\boldsymbol{\varphi_{1,i}}\right|$ for the state{1.5,d}. Phase offsets exhibit one and a half cycles with offsets for oscillators falling into the same cluster as the first mirroring those of oscillators in the opposite cluster. **Panel g)** shows $\left|\Delta\boldsymbol{\varphi_{1,i}}\right|$ for the state{1,s}. Phase offsets exhibit one full cycle. **Panel h)** shows $\left|\Delta\boldsymbol{\varphi_{1,i}}\right|$ for the state{2,s}. Phase offsets exhibit two full cycles passed by a single cluster. All phase offsets are averaged over the last 100 time steps. Phase offsets for each parameter combination are shown in supplementary Figure S2.1b.

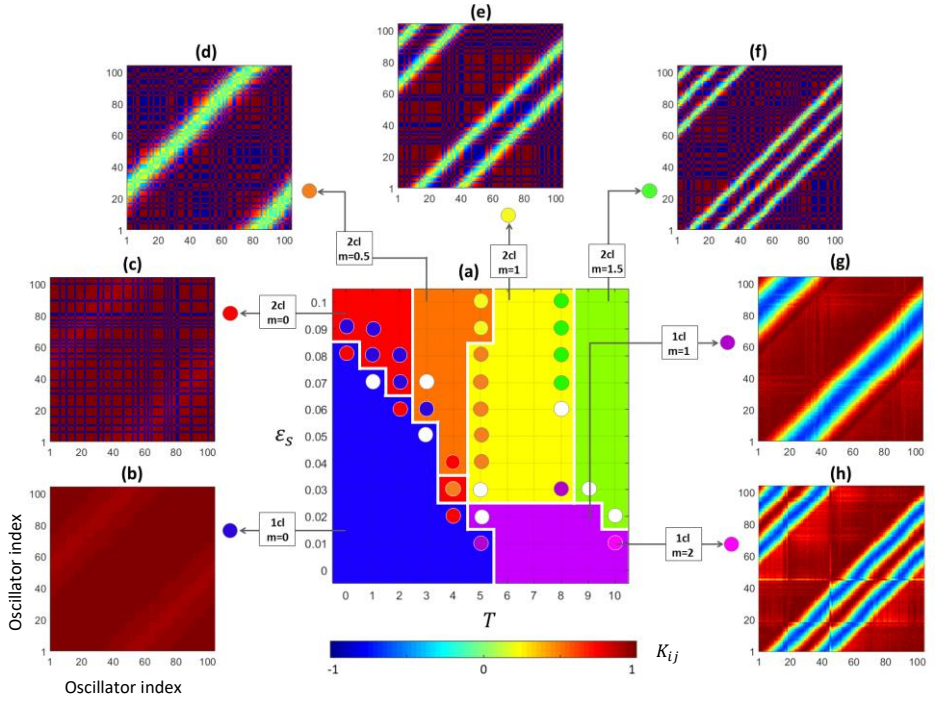

Figure 2.2: Pairwise structural connectivity emerging in the context of dynamic coupling and static conduction. Panel a) shows the colour-coded state of coherent-wave mode of synchronization

and cluster-formation observed at each point in the parameter space defined by $\boldsymbol{T}$ and $\boldsymbol{\varepsilon_s}$. As in Figure 2.1, the secondary state (bistability) is marked with coloured disks whereas white indicates multistability. **Panel b)** shows the structural connectivity matrix of the network for the state{0,s}. The network largely preserves the initial connectivity pattern. **Panel c)** shows structural connectivity of the network for the state{0,d}. Pairwise connection weights are close to $+\boldsymbol{\alpha_s}$ and $-\boldsymbol{\alpha_s}$ for oscillator pairs belonging to the same or distinct clusters, respectively. **Panels d-f)** show structural connectivity matrices of the network for the state{0.5,d} (panel d), state{1,d} (panel e), state{1.5,d} (panel f). As before, coupling weights have approached $+\boldsymbol{\alpha_s}$ for within cluster connections and $-\boldsymbol{\alpha_s}$ for between cluster connections. However, based on the mode synchronization, 1, 2 and 3 stripes of near-zero connection weights have formed in panels d, e and f, respectively. **Panel g)** shows the structural connectivity matrix of the network for the state{1,s}. All possible phase offsets ($(\boldsymbol{n-1})(\boldsymbol{2\pi/N})$) with respect to the first oscillator can be observed. **Panel h)** shows the structural connectivity matrix for a network given the state{2,s}. The same observations as for panel g can be made, with the difference that phase differences are repeated. The structural connectivity matrices are averaged over the last 100 time steps of the simulation. Structural connectivity matrices for each parameter combination are shown in supplementary Figure S2.1c.

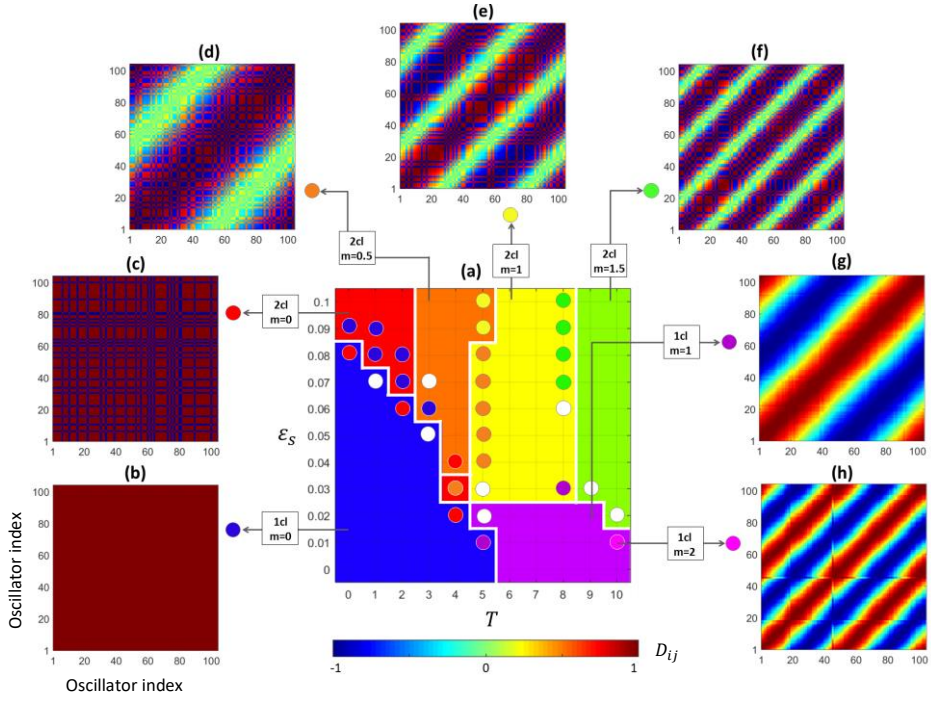

Figure 2.3: Pairwise functional connectivity among oscillators emerging when coupling strength is dynamic and conduction is static. Panel a) shows the colour-coded state of coherent-wave mode of synchronization and cluster-formation observed at each point in the parameter space defined by $\boldsymbol{T}$ and $\boldsymbol{\varepsilon_s}$. Colour coding is the same as in Figure 2.1. **Panel b)** shows the functional connectivity matrix of the network for the state{0,s}. The globally correlated functional connectivity matrix resembles the structural connectivity matrix. **Panel c)** shows the functional connectivity matrix of a network for the

state{0,d}. **Panels d-f)** show functional connectivity matrices of networks for the state{1.5,d} (panel d), state{1,d} (panel e), state{1.5,d} (panel f). The functional pairwise correlations are associated with the cluster-formation of oscillators as they are 1 or close to 1 for intra-cluster correlations and are -1 or close to -1 for between cluster correlations. Based on the mode of synchronization, 2, 4 and 6 stripes of zero or very weak correlations in panel d, e and f are formed, respectively. **Panel g)** shows the functional connectivity matrix of a network for the state{1,s}. Pairwise functional connectivity values are 1 for the neighbouring oscillators and decrease to -1 as a function of distance. **Panel h)** shows the functional connectivity matrix of the network for the state{2,s}. A similar pattern as for panel g manifests, but reflecting two complete revolutions of phase offsets around the circle. The elements of correlation matrices were computed over the last 100 time steps of the simulation. Functional connectivity matrices for each parameter combination are shown in supplementary Figure S2.1d.

2-3-2. Scenario II: static coupling strengths, dynamic conduction velocities

Next, we examine the effects of dynamic conduction velocity on a network with static connection weights to establish the unique effects of adaptive myelination on functional connectivity among phase oscillators. To that end, we vary the learning rate ε_v and enhancement factor α_v controlling dynamic changes in conduction velocity. Note that we no longer vary the coupling delay constant T since delays depend on conduction. Rather, we initialize conduction velocity among oscillator pairs such that $v_{ij}(t=0) = 0.14$, which means that the initial coupling delays correspond to the case where $T \cong 7$. These parameter settings correspond to a system exhibiting state$\{1,s\}$ in simulations where conduction remains static. For dynamic conduction velocity, state$\{1,s\}$ is still observed most frequently irrespective of which values have been chosen for ε_v and α_v. However, within a contiguous region of parameter space, the system exhibits state$\{2,d\}$ as its secondary state, which is indicative of bistability (Figure 2.4a). Furthermore, at the borders of this region, the system exhibits highly variable behaviour, indicative of multistability.

Figure 2.4 shows absolute phase offsets of all oscillators with respect to the first. Remarkably, for state$\{2,d\}$ phases cluster around 0 and π with sharp transitions between the two rather than smooth transitions. In fact, dynamic conduction velocity pushes phase offsets to either 0 or π which brings about a transformation from state$\{2,s\}$ to state$\{2,d\}$. This localized clustering leads to highly structured clusters, where an oscillator's affiliation with a cluster is determined by its location along the ring rather than by randomly distributed initial phase values. Interestingly, conduction matrices emerging for state$\{2,d\}$ suggest that the system exhibits four distinct clusters rather than two (see Figure 2.5d); one cluster for each peak and trough of the phase offsets (cf. Figure 2.4d). That is, signals are conducted fast among oscillators within a peak (trough) and slow among oscillators across peaks

(troughs). This is the result of initial conditions. With conduction velocity being equal, short distances among oscillators within a peak (trough) lead to short delays, whereas long distances across peaks (troughs) lead to long delays. In this case, the pressure to synchronize peaks (troughs) is most easily met when signals are transmitted instantaneously within a peak (trough) or with a delay matching exactly one period across peaks (troughs). Functionally, these four clusters are not discernible (see Figure 2.6d) since oscillators falling into both peaks (troughs) exhibit no phase-offset with respect to each other.

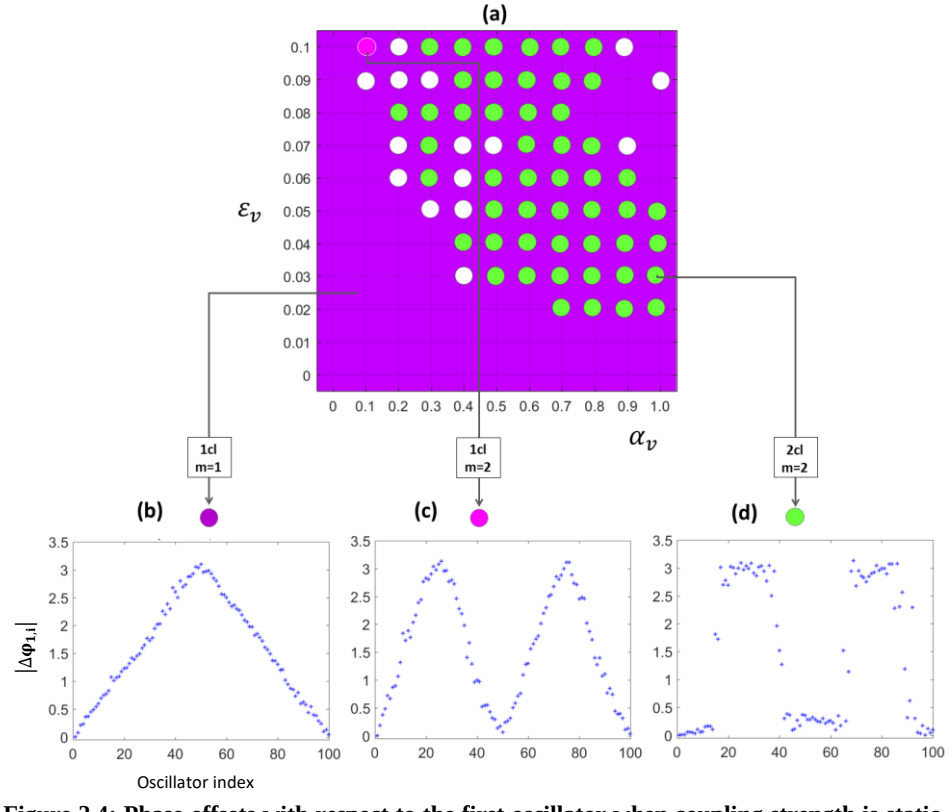

Figure 2.4: Phase offsets with respect to the first oscillator when coupling strength is static and conduction is dynamic. Panel a) shows the colour-coded state of coherent-wave mode of synchronization and cluster-formation observed at each point in the parameter space defined by $\boldsymbol{\varepsilon_v}$ and $\boldsymbol{\alpha_v}$. Colour coding is the same as in Figure 2.1. The entire parameter space is primarily characterized by state{1,s}. However, a wide region of parameter space exhibits a secondary state defined by a mode of 2 and the formation of two clusters. **Panel b)** shows $|\Delta\boldsymbol{\varphi_{1,i}}|$for state{1,s}. Phase offsets exhibit one full cycle. **Panel c)** shows $|\Delta\boldsymbol{\varphi_{1,i}}|$ for state{2,s}. Phase offsets exhibit two full cycles. **Panel d)** shows $|\Delta\boldsymbol{\varphi_{1,i}}|$for state{2,d}. Phase offsets are largely pushed to either $\mathbf{0}$ or $\boldsymbol{\pi}$, depending on cluster affiliation.

All phase offsets are averaged over the last 100 time steps. Phase offsets for each parameter combination are shown in supplementary Figure S2.2b.

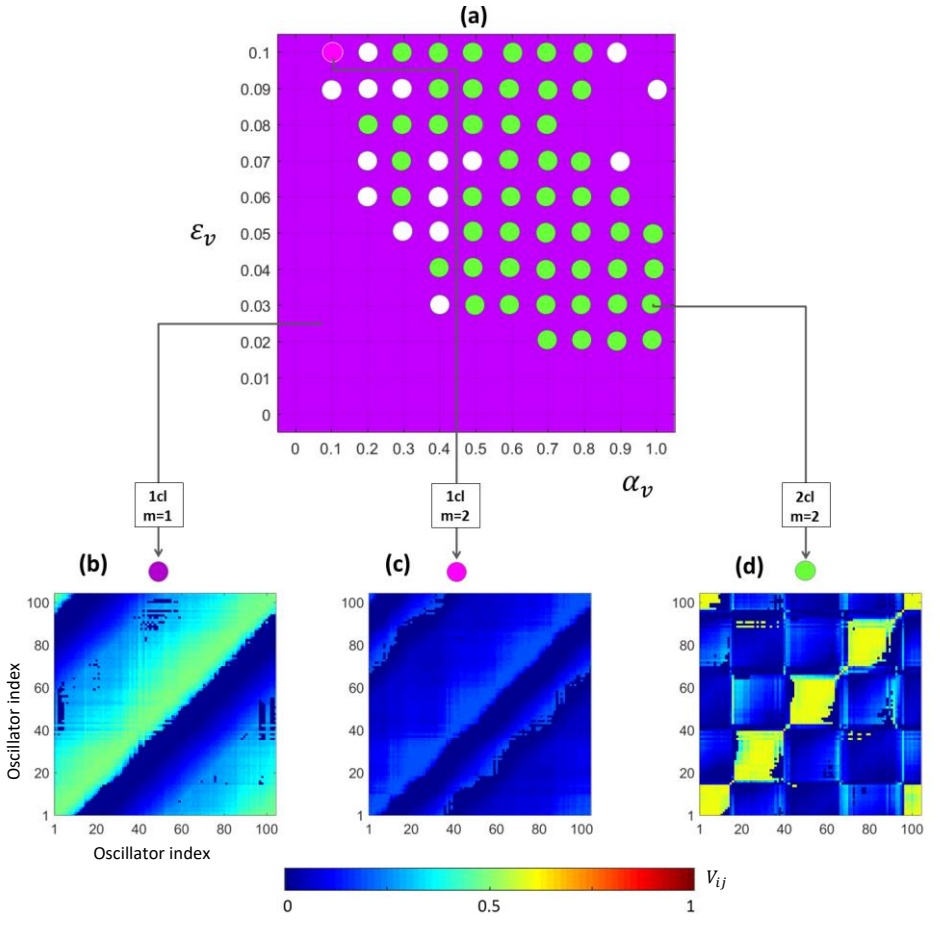

Figure 2.5: Conduction velocity matrices when coupling strength is static and conduction is dynamic. Panel a) shows the colour-coded state of coherent-wave mode of synchronization and cluster-formation observed at each point in the parameter space defined by $\boldsymbol{\varepsilon_v}$ and $\boldsymbol{\alpha_v}$. Colour coding is the same as in Figure 2.1. **Panels b and c)** show the pairwise conduction velocity matrices for state{1,s} (reflecting one full cycle of phase offsets), and state{2,s} (reflecting two full cycles of phase offsets), respectively. **Panel d)** shows the pairwise conduction velocity matrices for state{2,d}. Conduction velocities between the intra--cluster oscillators are noticeably higher than those between other pairs. The conduction velocity matrices are averaged over the last 100 time steps of the simulation. Conduction velocity matrices for each parameter combination are shown in supplementary Figure S2.2c.

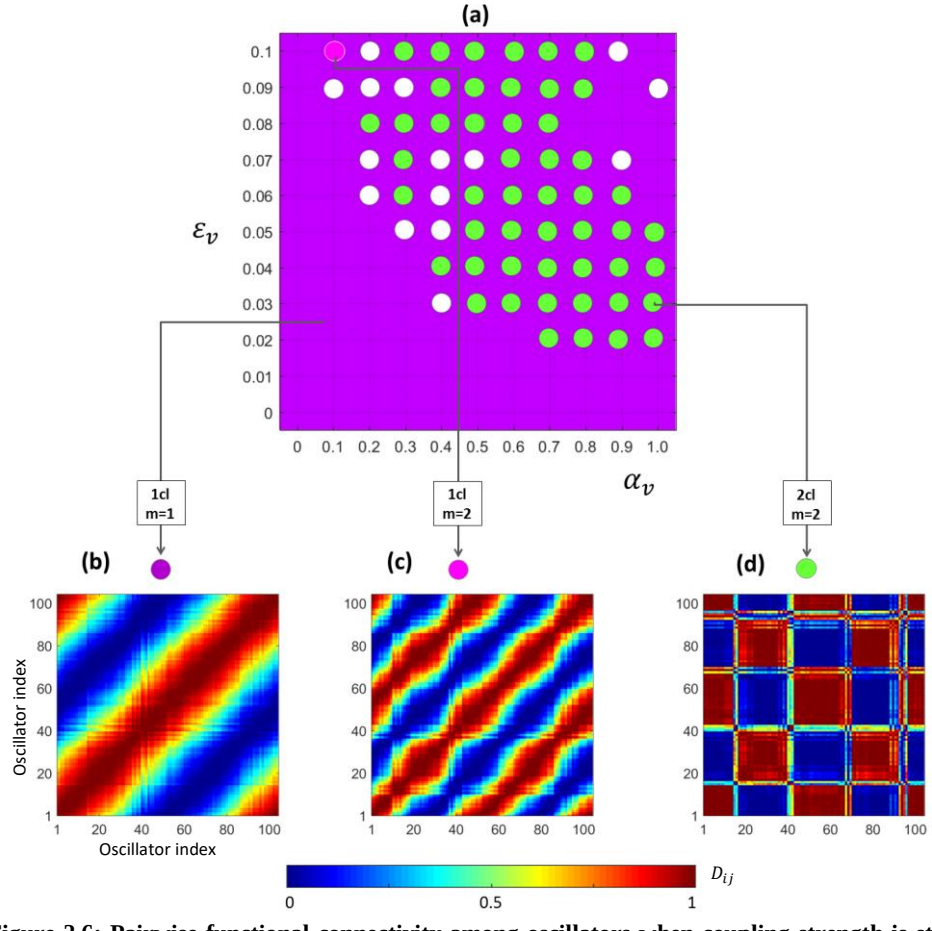

Figure 2.6: Pairwise functional connectivity among oscillators when coupling strength is static and conduction is dynamic. Panel a) shows the colour-coded state of coherent-wave mode of synchronization and cluster-formation observed at each point in the parameter space defined by $\boldsymbol{\varepsilon_v}$ and $\boldsymbol{\alpha_v}$. Colour coding is the same as in Figure 2.1. **Panel b)** shows a representative functional connectivity matrix of the network for state{1,s}. The matrix reflects a full cycle of phase offsets. **Panel c)** shows a functional connectivity matrix of the network for state{1,s}. Two complete revolutions of the relative phase offsets are exhibited. **Panel d)** shows a functional connectivity matrix of the network for state{2,d}. A vast majority of the pairwise correlations reflect either in-phase or anti-phase relations among oscillators. The correlation matrices were computed over the last 100 time steps of the simulation. Functional connectivity matrices for each parameter combination are shown in supplementary Figure S2.2d.

2-3-3. Scenario III: dynamic coupling strengths and conduction velocities

Having explored the effects of dynamic structural connectivity and dynamic conduction velocity in isolation, we next investigate their interaction. Dynamic changes in connection strength and conduction velocity constitute the most biologically relevant scenario. In this simulation, initial values of the conduction velocity matrix v were again chosen such that they resemble the condition where $T \cong 7$. Furthermore, the learning rate ε_s was fixed at 0.1 (fast learning). Recall that this configuration produces state$\{1,d\}$ for static conduction velocity (cf. Figure 2.1a). As for scenario II, we explore the parameter space defined by the enhancement factor α_v and the learning rate ε_v controlling dynamic conduction velocity. Figure 2.7a reveals that the behaviour of the system is mainly affected by the enhancement factor α_v, which determines the maximum conduction velocity. If the learning rate ε_v is small, conduction velocity changes too slowly to have any discernible influence on the behaviour of the system and state$\{1,d\}$ is preserved for all values of α_v. Once the conduction learning rate ε_v is sufficiently large, however, the behaviour of the system is entirely determined by α_v. Note that in this case, the rate of change in conduction velocity may be still a factor of 10 smaller than the learning rate controlling synaptic plasticity.

For values of $\alpha_v < 0.14$, conduction necessarily decays towards values lower than initialization. This produces a situation essentially equivalent to fast learning and very long delays ($T \geq 9$) in scenario I and leads to the emergence of state$\{1.5,d\}$ (cf. Figure 2.1f). For $\alpha_v \cong 0.14$, the system frequently exhibits erratic behaviour. To account for the system's behaviour as α_v increases, it is essential to consider the fact that both coupling strengths and conduction velocities evolve according to the same Hebbian learning rule with the sole difference that conduction velocities are bounded from below at 0.1. This implies that whenever the coupling strength between two oscillators tends towards $+\alpha_s$, conduction velocity between the two increases (towards α_v). In contrast, whenever the coupling strength between two oscillators tends towards $-\alpha_s$, coupling velocity between the two decreases (towards 0.1). This implies that coupling strength and conduction velocity act agonistically for oscillators within the same cluster; these oscillators are both positively coupled and exhibit fast conduction velocity (short delays). However, for oscillators in separate clusters, coupling strength and conduction velocity act antagonistically. Negative coupling is paired with slow conduction velocity (long delays). For intermediate values of α_v, oscillators in different clusters 'see' each other in anti-phase for phase offsets smaller than π. They thus form two clusters whose offset is less than half a

period (depending on the exact offset, our procedure may label them as single or double cluster; 'see' boundary between red and blue regions in Figure 2.7). For large values of α_v, oscillators in different clusters 'see' each other in anti-phase for phase offsets close to zero (Figure 2.7d). This allows them to form a single functional cluster (Figure 2.10d) even though they may be structurally segregated, both in terms of coupling strength (Figure 2.8d) and conduction velocity (Figure 2.9d). The system can thus exhibit a wide array of states not observed when considering dynamic coupling strength alone.

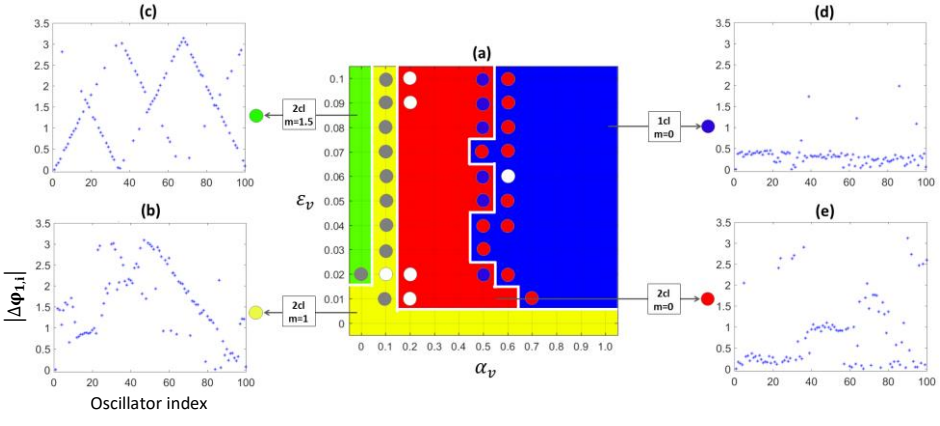

Figure 2.7: Phase offsets with respect to the first oscillator when coupling strength and conduction velocity are both dynamic. Panel a) shows the colour-coded state of coherent-wave mode of synchronization and cluster-formation observed at each point in the parameter space defined by $\boldsymbol{\varepsilon_v}$ and $\boldsymbol{\alpha_v}$. Colour coding is the same as in Figure 2.1. Grey circles mark erratic states. **Panel b)** shows $|\Delta\boldsymbol{\varphi_{1,i}}|$ for state{1,d}. **Panel c)** shows $|\Delta\boldsymbol{\varphi_{1,i}}|$ for state{1.5,d}. Phase offsets exhibit one and a half cycles **Panel d)** shows $|\Delta\boldsymbol{\varphi_{1,i}}|$ for state{0,s}. Aside from a few exceptions, offsets are generally close to zero. **Panel e)** shows $|\Delta\boldsymbol{\varphi_{1,i}}|$ for state{0,d}. While our procedure identified this example as 0-mode synchronization, visually it appears to not fit any state particularly well. Phase offsets were averaged over the last 100 time steps. Phase offsets for each parameter combination are shown in supplementary Figure S2.3b.

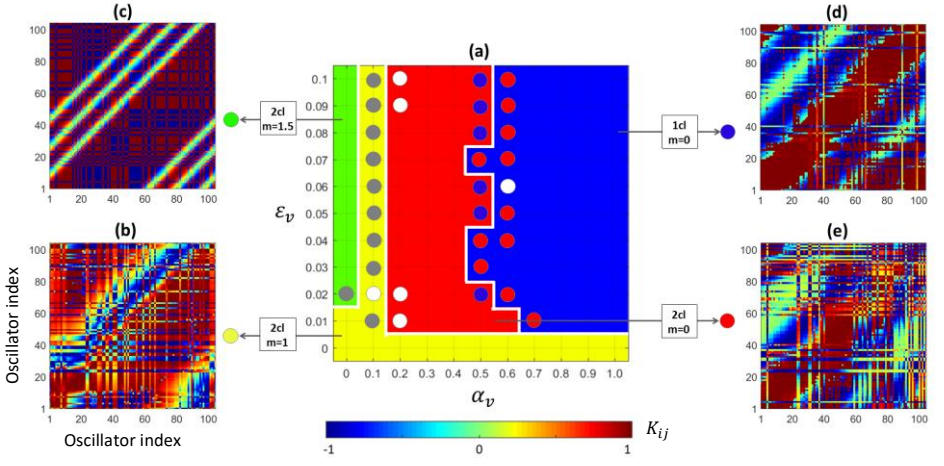

Figure 2.8: Pairwise structural connectivity emerging when coupling strength and conduction velocity are both dynamic. Panel a) shows the colour-coded state of coherent-wave mode of synchronization and cluster-formation observed at each point in the parameter space defined by $\boldsymbol{\varepsilon_v}$ and $\boldsymbol{\alpha_v}$. Colour coding is the same as in Figure 1 (grey disks as in Figure 2.7). **Panels b)** shows structural connectivity of the network for state{1,d}. **Panel c)** shows structural connectivity matrix of the network for state{1.5,d}. As for simulations with static conduction velocity, in this region, connectivity matrices exhibit 3 (2m) stripes reflecting weak connections. **Panel d)** shows structural connectivity of the network for state{0,s}. **Panel e)** shows structural connectivity of the network for state{0,d}. The structural connectivity matrices are averaged over the last 100 time steps of the simulation. Structural connectivity matrices for each parameter combination are shown in supplementary Figure S2.3c.

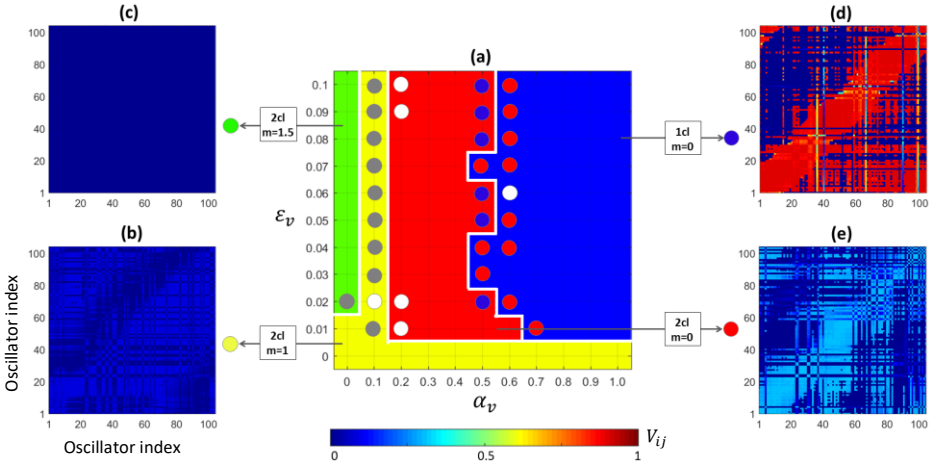

Figure 2.9: Pairwise conduction velocities among oscillators when coupling strength and conduction velocity are both dynamic. Panel a) shows the colour-coded state of coherent-wave mode of synchronization and cluster-formation observed at each point in the parameter space defined by $\boldsymbol{\varepsilon_v}$

and α_v. Colour coding is the same as in Figure 1 (grey disks as in Figure 2.7). **Panel b)** shows the pairwise conduction velocity of the network for state{1,d}. Conduction velocities only change slightly relative to their initial values. **Panel c)** shows pairwise conduction velocity of the network for state{1.5,d}. Conduction velocities have decayed to zero. **Panel d)** shows pairwise conduction velocity of the network for state{0,s}. **Panel e)** shows pairwise conduction velocity of the network for state{0,d}. The conduction velocity matrices are averaged over the last 100 time steps of the simulation. Conduction velocity matrices for each parameter combination are shown in supplementary Figure S2.3d.

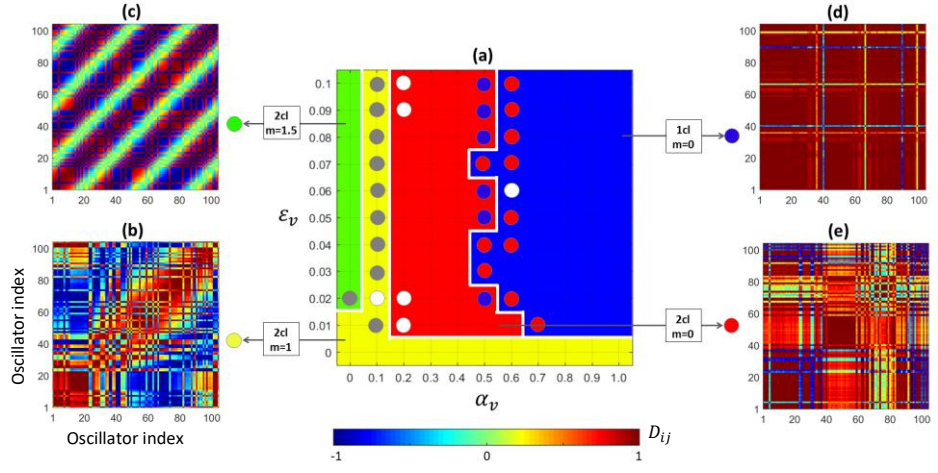

Figure 2.10: Pairwise functional connectivity among oscillators when coupling strength and conduction velocity are both dynamic. Panel a) shows the colour-coded state of coherent-wave mode of synchronization and cluster-formation observed at each point in the parameter space defined by ε_v and α_v. Colour coding is as in Figure 2.1 (grey disks as in Figure 2.7). **Panel b)** shows functional connectivity of the network for state{1,d}. **Panel c)** shows functional connectivity of the network for state{1.5,d}. The formation of 4m stripes of zero or very weak connection weights can be observed. **Panel d)** shows the functional connectivity matrix for a network of state{0,s}. **Panel e)** shows the functional connectivity matrix for a network of state{0,d}. Correlation matrix elements are averaged over the last 100 time steps of the simulation. Functional connectivity matrices for each parameter combination are shown in supplementary Figure S2.3e.

2-4. Discussion

In the present study we investigated the effects of dynamic coupling strength and dynamic conduction velocity on the synchronization behaviour of weakly coupled oscillators arranged on a circle. For dynamic coupling strength combined with static conduction velocity, we found that depending on the learning rate controlling changes in coupling strength, a single or two clusters can emerge. This is in line with previous studies on dynamic coupling in the Kuramoto model (Niyogi & English, 2009). Furthermore, depending on delay, phase offsets may exhibit periodicity

according to coherent-wave modes of synchronization (Niyogi & English, 2009; Timms & English, 2014). For non-zero modes, structural clusters become functionally apparent only after correcting for offsets.

For zero modes, a tight correspondence between structural and functional clusters is straightforwardly apparent. This is no longer the case once conduction velocity is allowed to vary. Already in the context of static coupling strength, we observed that dynamic conduction velocity dissociates structural from functional connectivity. In terms of coupling strength, the system may appear as a single cluster. However, in terms of conduction velocity, which is another structural aspect, a wide range of parameters leads to the formation of four distinct clusters with fast communication within clusters and slow communication across clusters. Interestingly, communication between neighbouring clusters is, while slower than within clusters, faster than between non-neighbouring clusters. This leads to the emergence of two functional clusters. Oscillator pairs with either very fast and very slow communication 'see' each other in phase since phase offsets are either close to zero or some integer multiple of 2π and hence form a single functional cluster. This cluster is spatially discontinuous and interleaved with oscillators belonging to a second cluster. Conduction velocity between oscillators in separate clusters is such that these oscillators 'see' each other in anti-phase. If conduction velocity is dynamic, it is thus

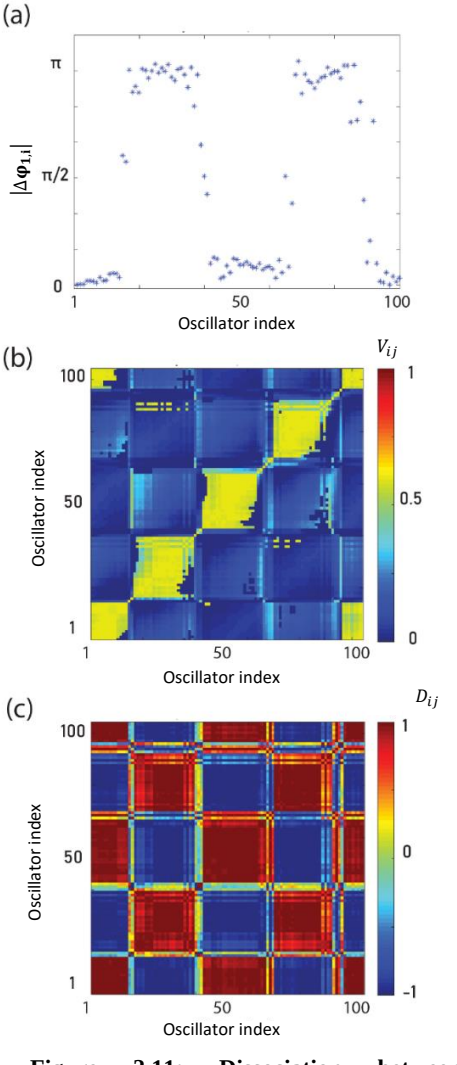

Figure 2.11: Dissociation between structural and functional clusters for state{2,d} observed in scenario 2. Panel a) phase offsets between every oscillator and the first ($|\Delta\varphi_{1,i}|$). Offsets reflect two anti-phase clusters. **Panel b)**, pairwise conduction velocity reflecting four structural clusters. **Panel c)**, pairwise functional connectivity reflecting two functional clusters.

possible that clusters are structurally connected in terms of coupling strength and yet functionally distinct because they are segregated by another structural factor (conduction velocity see Figure 2.11). If both coupling strength and conduction velocity are dynamic, we observed that for a sufficiently large enhancement factor, which determines maximum conduction velocity, a single functional cluster exhibiting zero-mode synchronization emerges. Yet, structural connectivity is characterized by positive values only for neighbouring oscillators and negative values between remote oscillators. Conduction velocity counteracts the repellent effects of negative coupling by producing delays of roughly half a period such that negatively coupled oscillator pairs 'see' each other in anti-phase when they are in fact in phase (see Figure 2.12). Dynamic conduction velocity thus appears to enable the system to resist the effects of coupling strength and allow for both functional integration of structurally segregated oscillators as well as functional segregation of structurally integrated clusters.

Figure 2.12: Dissociation between structural and functional clusters for state{0,s} observed in scenario 3. Panel a) phase offsets between every oscillator and the first ($|\Delta\varphi_{1,i}|$). Offsets reflect a

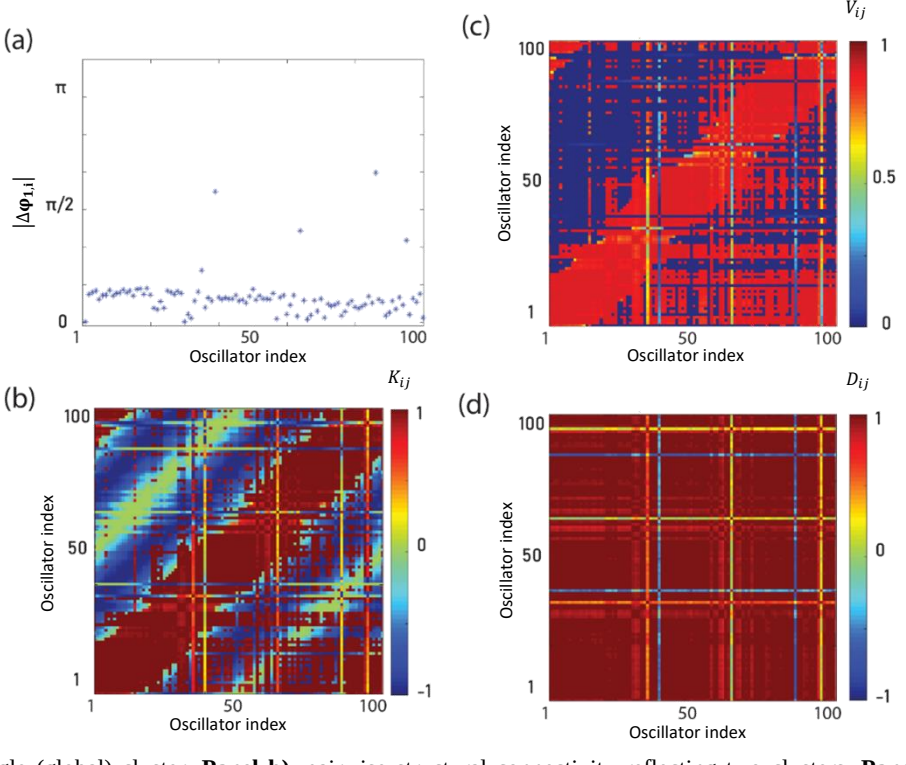

single (global) cluster. **Panel b)**, pairwise structural connectivity reflecting two clusters. **Panel c)**,

pairwise conduction velocity reflecting two clusters. **Panel d)**, pairwise functional connectivity reflecting a single cluster.

In line with previous work (Hauptmann, Omel'chenko, Popovych, Maistrenko, & Tass, 2007; Montbrió, Pazó, & Schmidt, 2006; Nakamura et al., 1994; Niebur, Schuster, & Kammen, 1991; Schuster & Wagner, 1989; Yeung & Strogatz, 1999), we observe bi- and multistability for non-zero delays, most prominently at boundaries in parameter space. Furthermore, regions of bi- / multistability appear to occur largely as a function of delay (cf. (Schuster & Wagner, 1989; Yeung & Strogatz, 1999)), either in the form of delay parameter T for scenario I or in the form of the enhancement factor α_v determining maximum delay for scenarios II and III. In contrast to previous studies which reported bistability of synchronous and incoherent states (Kotwal et al., 2017; Nickel & Gu, 2018; Yao et al., 2013), the circle topology of our network supports bi- / multistability between fully synchronous states which differ with respect to their coherent-wave mode of synchronization and single- vs double-cluster formation. At least as long as either coupling strength or conduction velocity are dynamic. When both coupling strength and conduction velocity are dynamic, we additionally observe bistability between states which can and those which cannot be characterized in terms of standing-wave mode and cluster formation. These latter states might simply reflect incoherence among oscillators. However, we cannot rule out that they reflect chimera states. This possibility is intriguing in light of previous studies showing that chimera states emerge from a pitchfork bifurcation as a function of coupling delay (Kotwal et al., 2017; Laing, 2009). The fact that this parameter is itself dynamic in our simulations may give rise to hitherto unobserved behaviour (such as chimera states characterized by mixtures of those states described here) and constitute an interesting avenue for further research.

In light of neuroscientific evidence that myelination continues to exhibit adaptive changes even in the adult brain (Gibson et al., 2014; Sampaio-Baptista et al., 2013; Scholz et al., 2009), our results highlight the importance of considering this factor in computational models of learning. For instance, our observation that dynamic conduction velocity provides the possibility for synchronization even in the context of fast learning highlights that adaptive myelination may have a useful dampening role to compensate for fast synaptic changes that might otherwise desynchronize neural groups. It may thus prevent networks in the brain from associating or dissociating too quickly under the influence of experiences. Interestingly, this compensation involves both increases and decreases in conduction velocity, highlighting that simply maximizing conduction speed is not necessarily

optimal (Fields, 2015). Furthermore, the compensatory effect of dynamic conduction velocity could be observed in our simulations even when its rate of change is a factor of 10 slower than that of synaptic strength. This suggests that our findings are relevant for the biologically plausible scenario where myelin related changes lag behind changes in synaptic efficacy, as it may take up to several weeks of daily stimulation of neuronal axons before changes in myelination can be detected (Demerens et al., 1996; Ishibashi et al., 2006). A role of slowly changing myelination in sharpening synchronization during neuronal communication would be in line with several theories in which rhythmic spike synchronization is thought to determine the efficiency of neural communication (Fries, 2005, 2015; Jensen & Lisman, 2000; Lowet et al., 2018). Our results call for an investigation of the neuro-computational mechanisms allowing for activity- and experience-dependent modulations of adaptive myelination. Based on observations that white matter structural changes resemble synaptic changes to the extent that they depend on the frequency of neural co-activation (Blumenfeld-Katzir, Pasternak, Dagan, & Assaf, 2011; Chang et al., 2016; Fields, 2015; McKenzie et al., 2014; Nickel & Gu, 2018; Purger et al., 2016; Sampaio-Baptista et al., 2013; Scholz et al., 2009), we implemented it as a Hebbian learning process. This is surely an over-simplification given that the control of myelination in adults, while incompletely understood, involves glia-neuronal interactions. We could not consider these here due to the simplicity of our model. Future work is thus needed to develop a more biologically appropriate learning mechanism and embed it in a model incorporating both types of cells. Nevertheless, our approach captures the most essential dynamical aspect of adaptive myelination, namely that conduction velocity of frequently used connections is strengthened while that of rarely used connections is weakened. Other simplifications of our work include the arrangement of oscillators along a circle, arbitrary units of space and time, and the lack of input. However, using these simplifications, we were able to decrease the complexity of computations and the number of parameters in order to plainly identify the influences of synaptic and myelin plasticity on collective behaviour of oscillators. Furthermore, since the system studied here is not intended to address any specific neural processes, our results are sufficiently general to be translated to several spatial and temporal scales. Future research will be necessary to investigate the contribution of realistic network topology as well as of functionally relevant external stimulation.

S2. Supplementary Material

See supplementary material for overall view of the changes in structural and functional characteristic behaviour of the network in relation to the learning parameters.

In the following, we present absolute phase offsets between every oscillator and the first, structural connectivity matrices (if coupling strengths are dynamic), functional connectivity matrices and conduction velocity matrices (if conduction velocities are dynamic) for every combination of learning parameters (i.e., T and ε_s for scenario I, and ε_v and α_v for scenarios II and III) obtained from a single example simulation for each scenario. The parameter space of each example case is depicted in panel (a) of each figure.

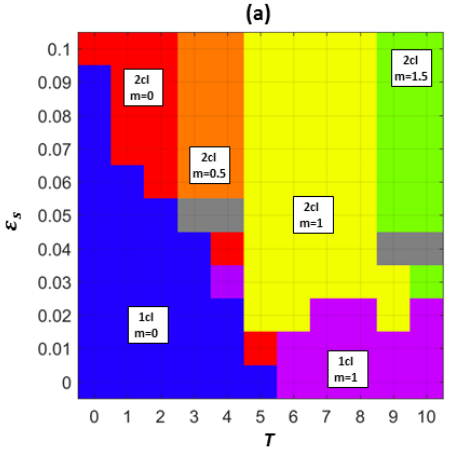

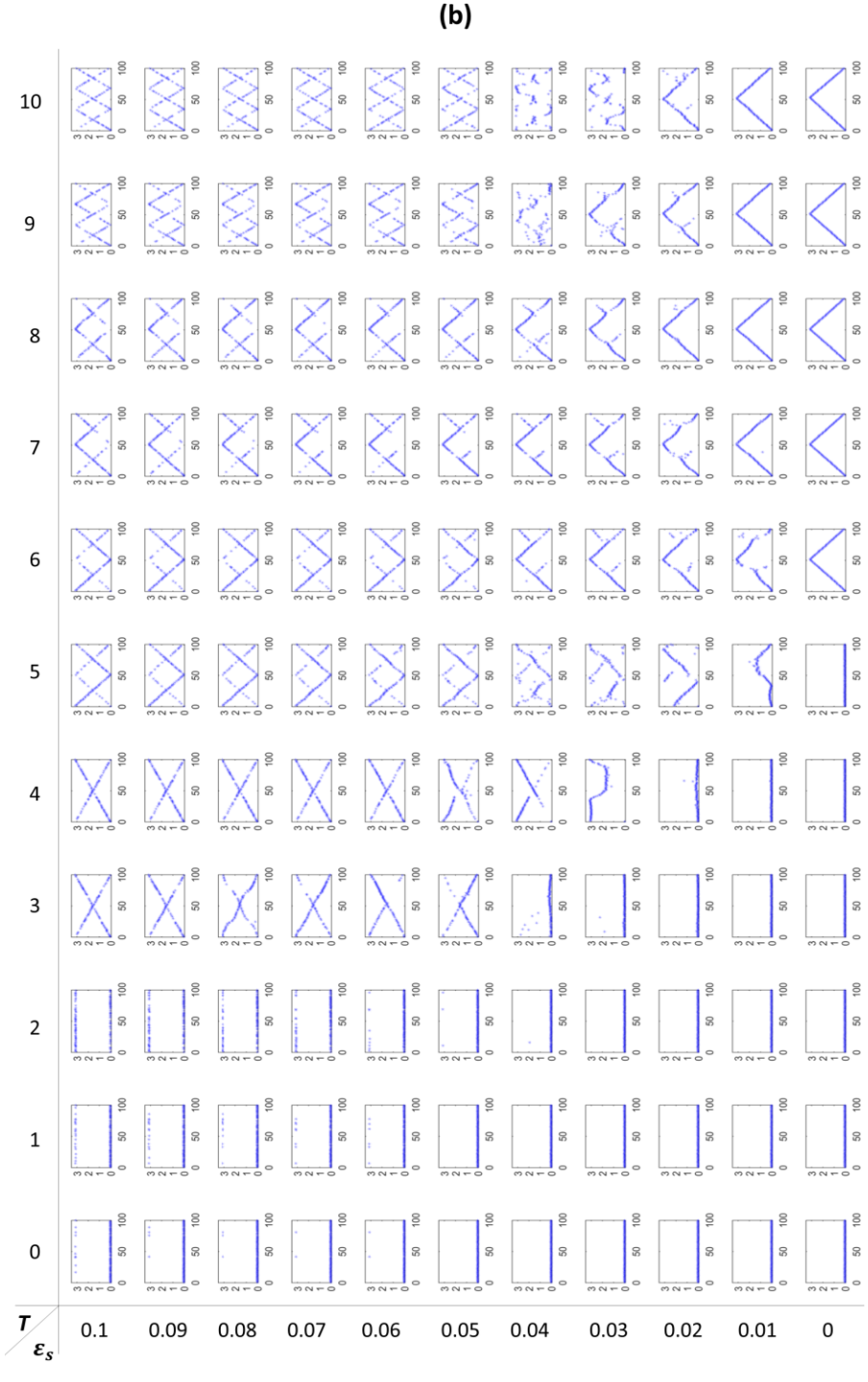
(b)
10
9
8
7
6
5
4
3
2
1
0
T
ε_s
0.1
0.09
0.08
0.07
0.06
0.05
0.04
0.03
0.02
0.01
0

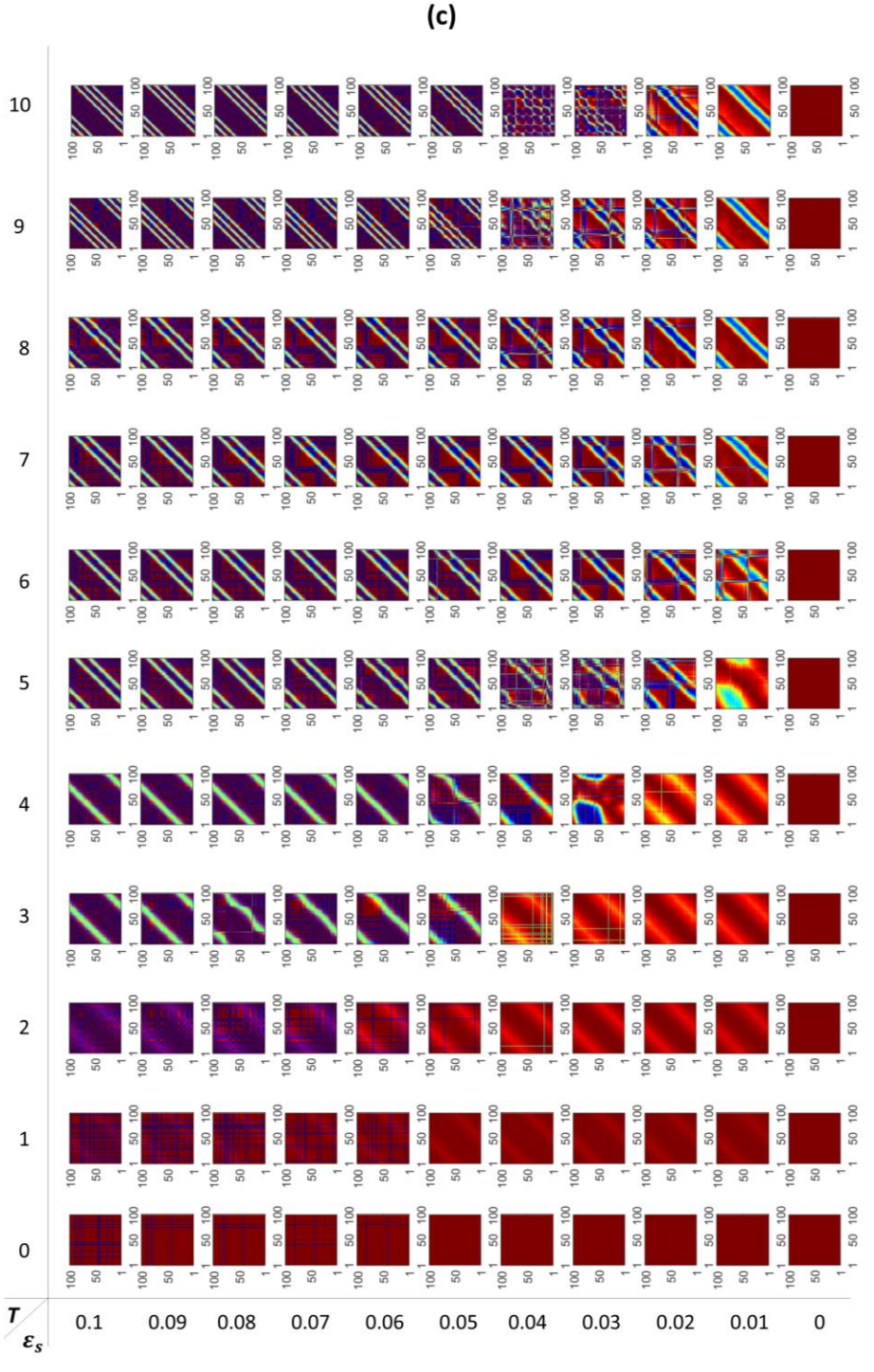
(c)
10
9
8
7
6
5
4
3
2
1
0
T
ε_s
0.1
0.09
0.08
0.07
0.06
0.05
0.04
0.03
0.02
0.01
0

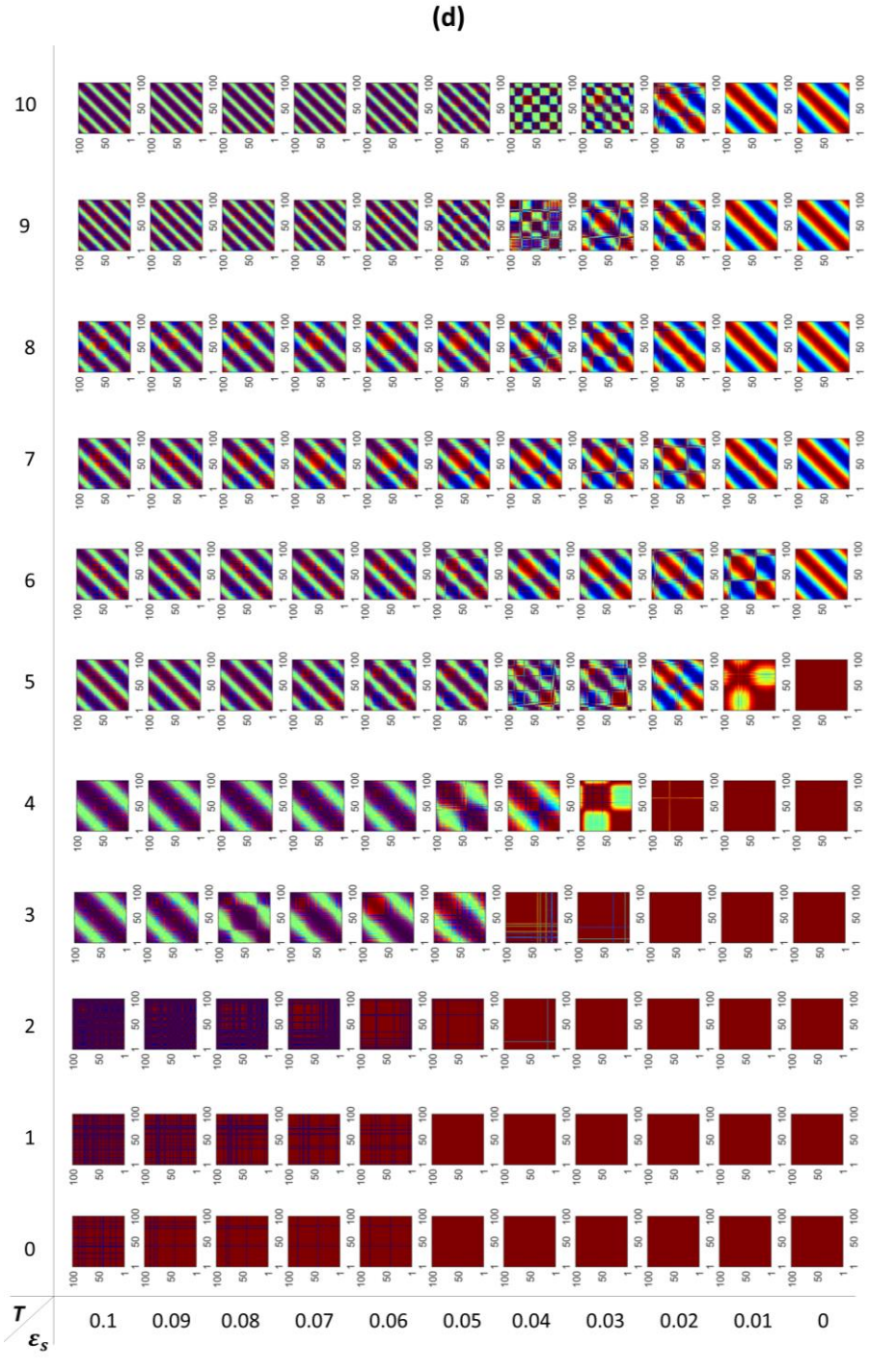
(d)
10
9
8
7
6
5
4
3
2
1
0
T
ε_s
0.1
0.09
0.08
0.07
0.06
0.05
0.04
0.03
0.02
0.01
0

Figure S2.1: Representation of structural and functional behaviour characteristics of scenario I for every point of the parameter space. Panel a) shows the colour-coded state of coherent-wave mode of synchronization and cluster-formation obtained from a single simulation. **Panel b)** shows the absolute phase offsets between every oscillator and the first ($|\Delta\varphi_{1,i}|$) for all combinations of ε_s and T. Phase offsets are averaged over the last 100 time steps of the simulation. **Panel c)** shows structural coupling matrices for all combinations of ε_s and T. **Panel d)** shows functional connectivity matrices for all combinations of ε_s and T. Matrix elements are averages over the last 100 time steps of the simulation in panels c and d. The learning enhancement factor α_s is fixed at 1 and all values of the connectivity matrix K were initialized to α_s.

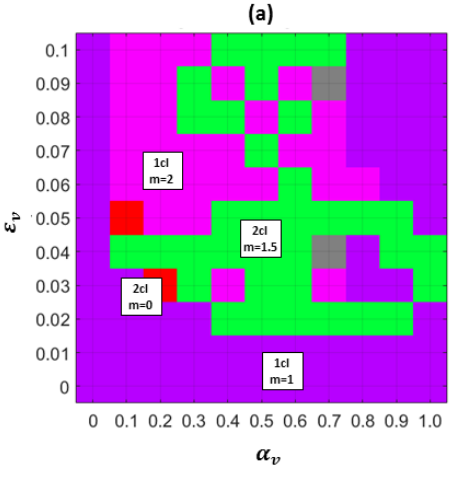

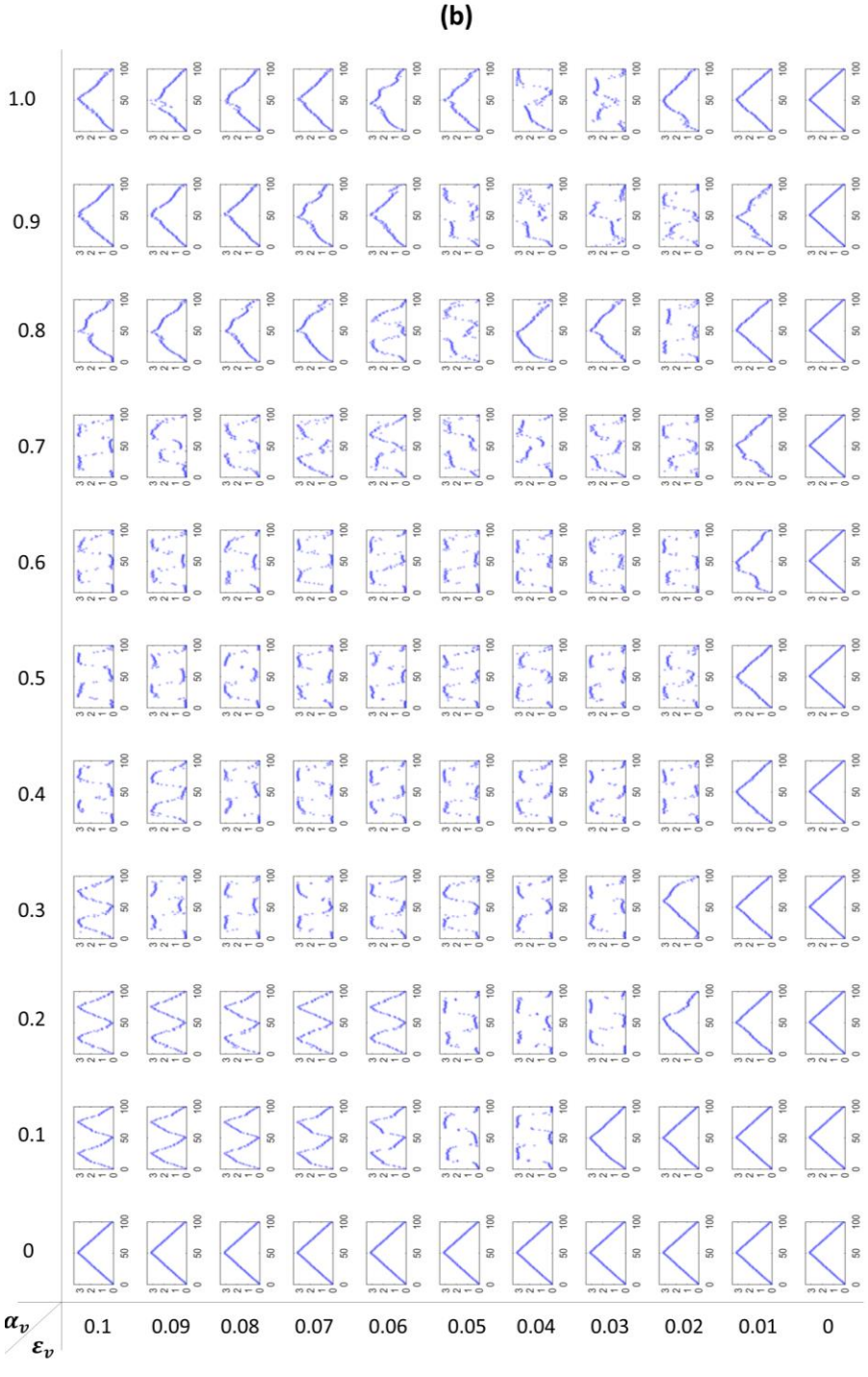
(b)
1.0
0.9
0.8
0.7
0.6
0.5
0.4
0.3
0.2
0.1
0
α_v
ε_v
0.1
0.09
0.08
0.07
0.06
0.05
0.04
0.03
0.02
0.01
0

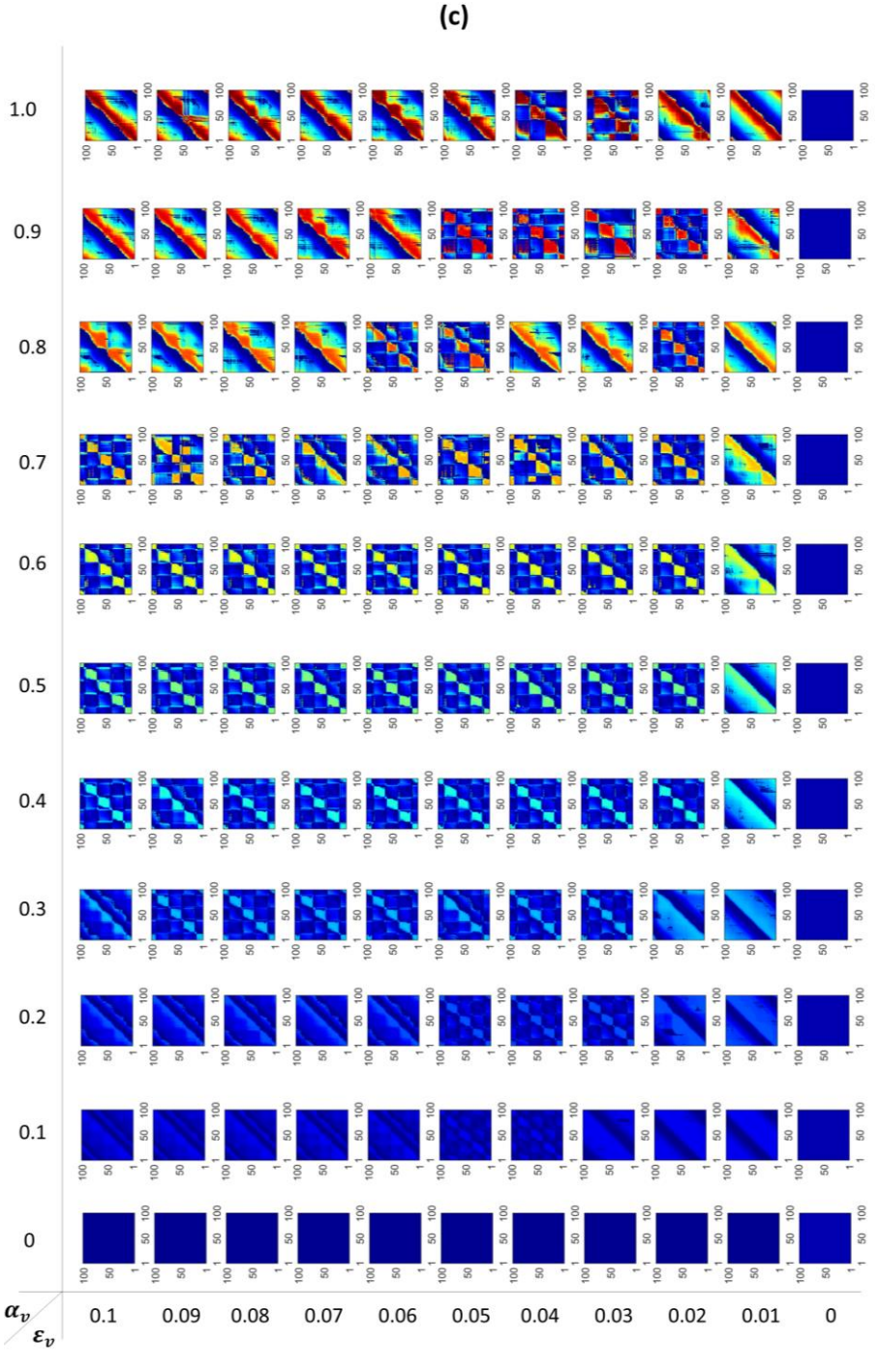
(c)
1.0
0.9
0.8
0.7
0.6
0.5
0.4
0.3
0.2
0.1
0
α_v
ε_v
0.1
0.09
0.08
0.07
0.06
0.05
0.04
0.03
0.02
0.01
0

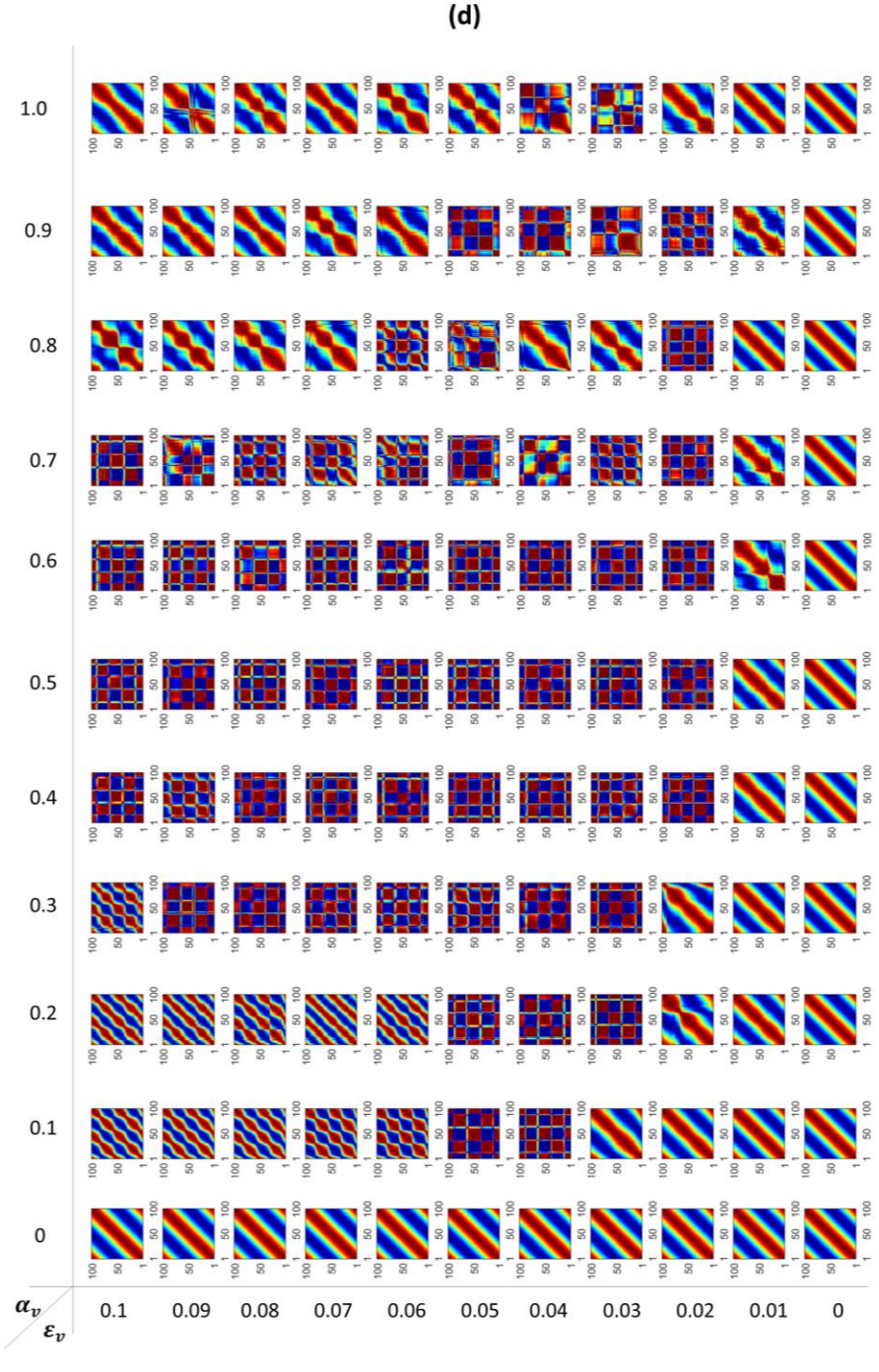
(d)
1.0
0.9
0.8
0.7
0.6
0.5
0.4
0.3
0.2
0.1
0
α_v
ε_v
0.1
0.09
0.08
0.07
0.06
0.05
0.04
0.03
0.02
0.01
0

Figure S2.2: Representation of structural and functional behaviour characteristic of scenario II for every point of the parameter space. Panel a) shows the colour-coded state of coherent-wave mode of synchronization and cluster-formation obtained from a single simulation. **Panel b)** shows absolute phase offsets between every oscillator and the first ($|\Delta\varphi_{1,i}|$) for all combinations of ε_v and α_v. Phase offsets are averaged over the last 100 time steps of the simulation. **Panel c)** shows conduction velocity matrices for all combinations of ε_v and α_v. **Panel d)** shows functional connectivity matrices for all combinations of ε_v and α_v. Matrix elements are averages over the last 100 time steps of the simulation in panels c and d.The connections' learning rate ε_s and the learning enhancement factor α_s are fixed at 0 and 1 respectively, and all values of the connectivity matrix K were fixed at α_s. The pairwise conduction velocities v_{ij} are initialized at 0.14, equivalent with the condition where $T \cong 7$.

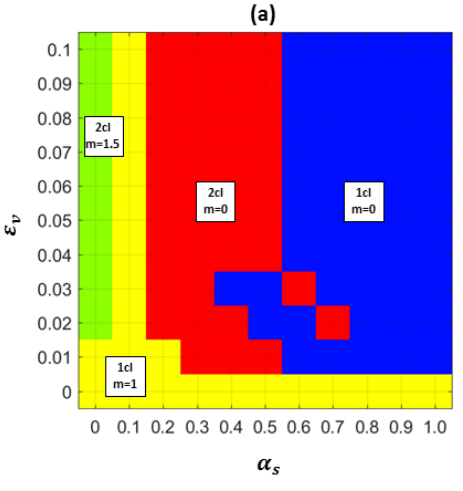

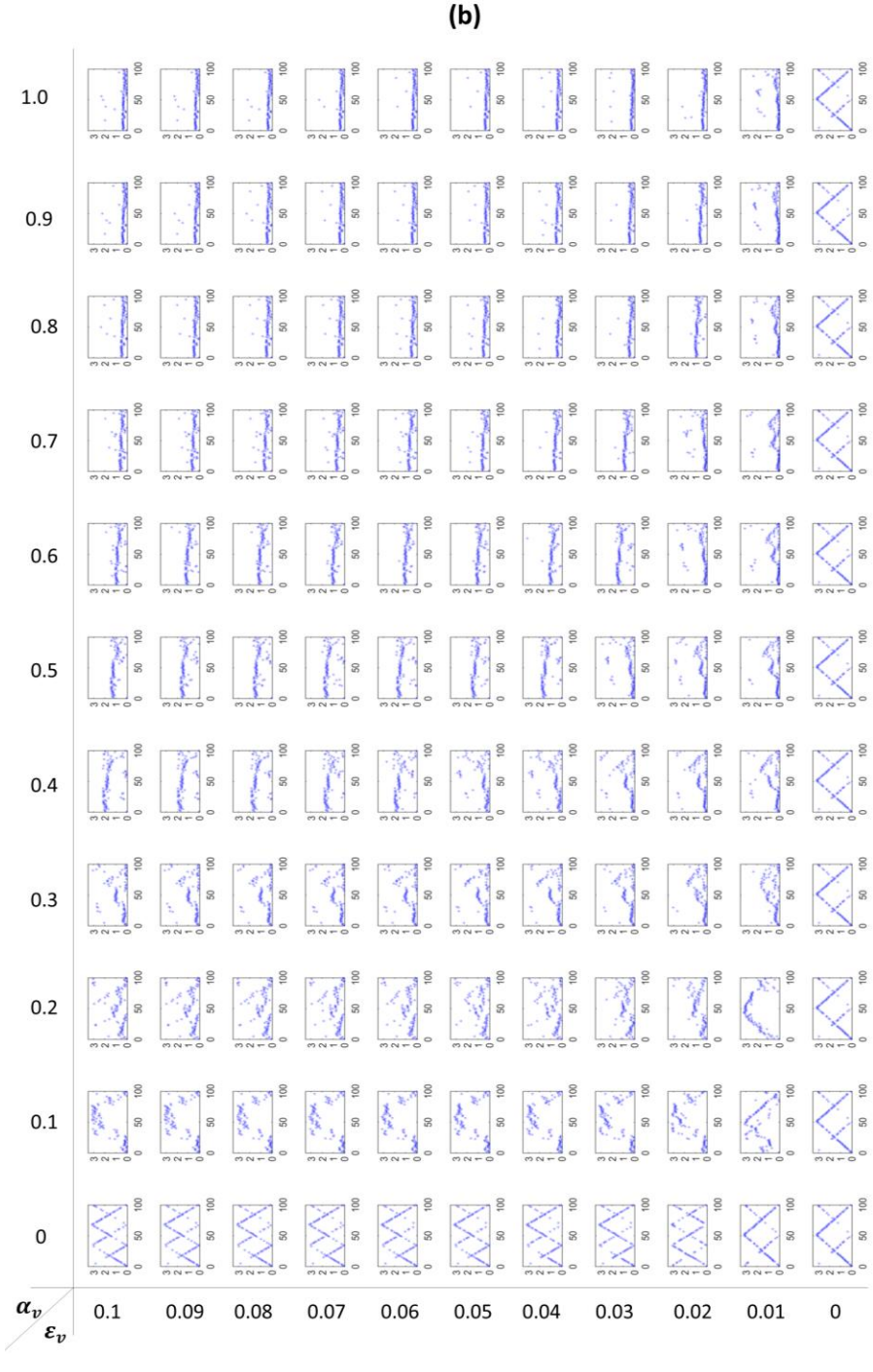
(b)
1.0
0.9
0.8
0.7
0.6
0.5
0.4
0.3
0.2
0.1
0
α_v
ε_v
0.1
0.09
0.08
0.07
0.06
0.05
0.04
0.03
0.02
0.01
0

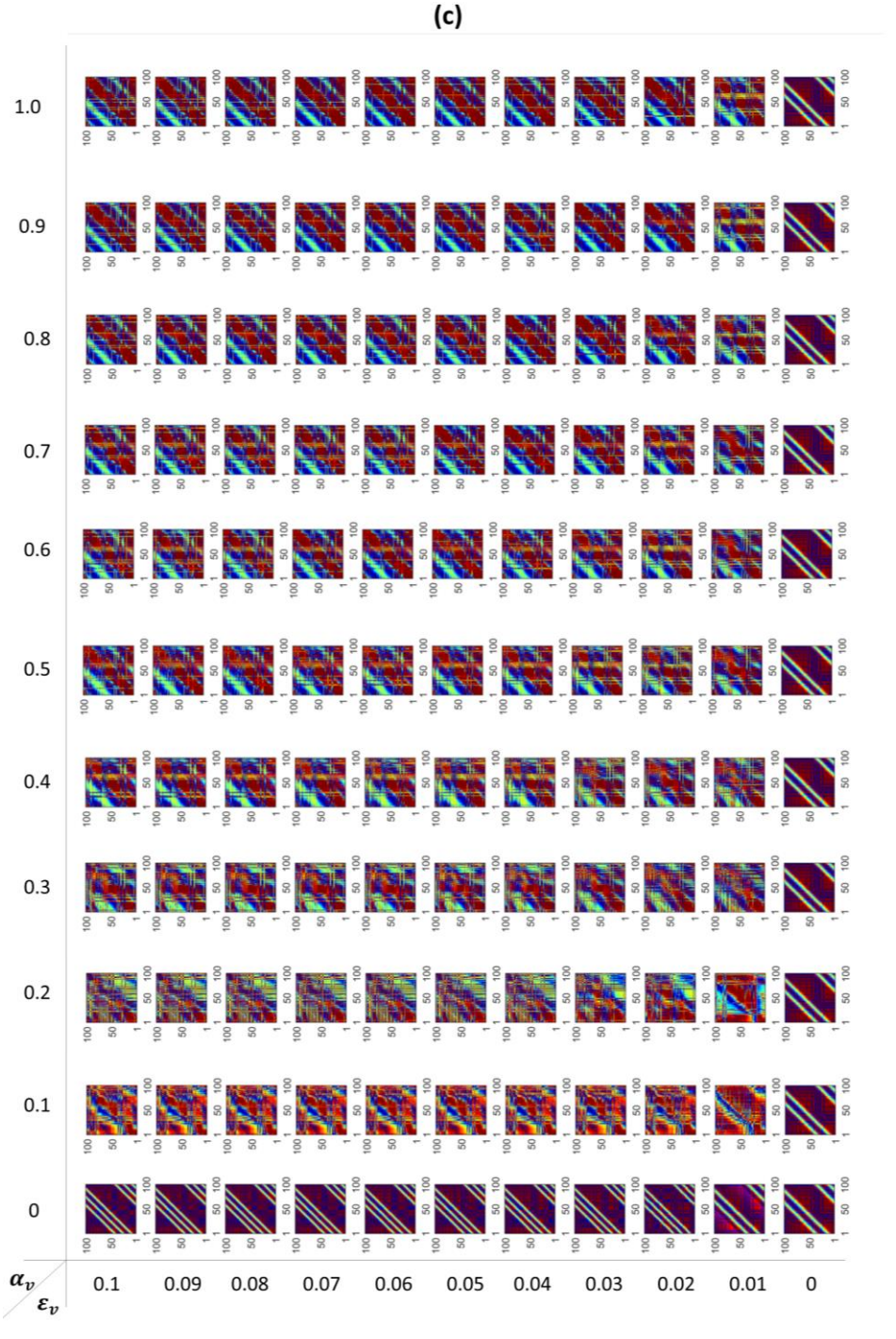
(c)
1.0
0.9
0.8
0.7
0.6
0.5
0.4
0.3
0.2
0.1
0
α_v
ε_v
0.1
0.09
0.08
0.07
0.06
0.05
0.04
0.03
0.02
0.01
0

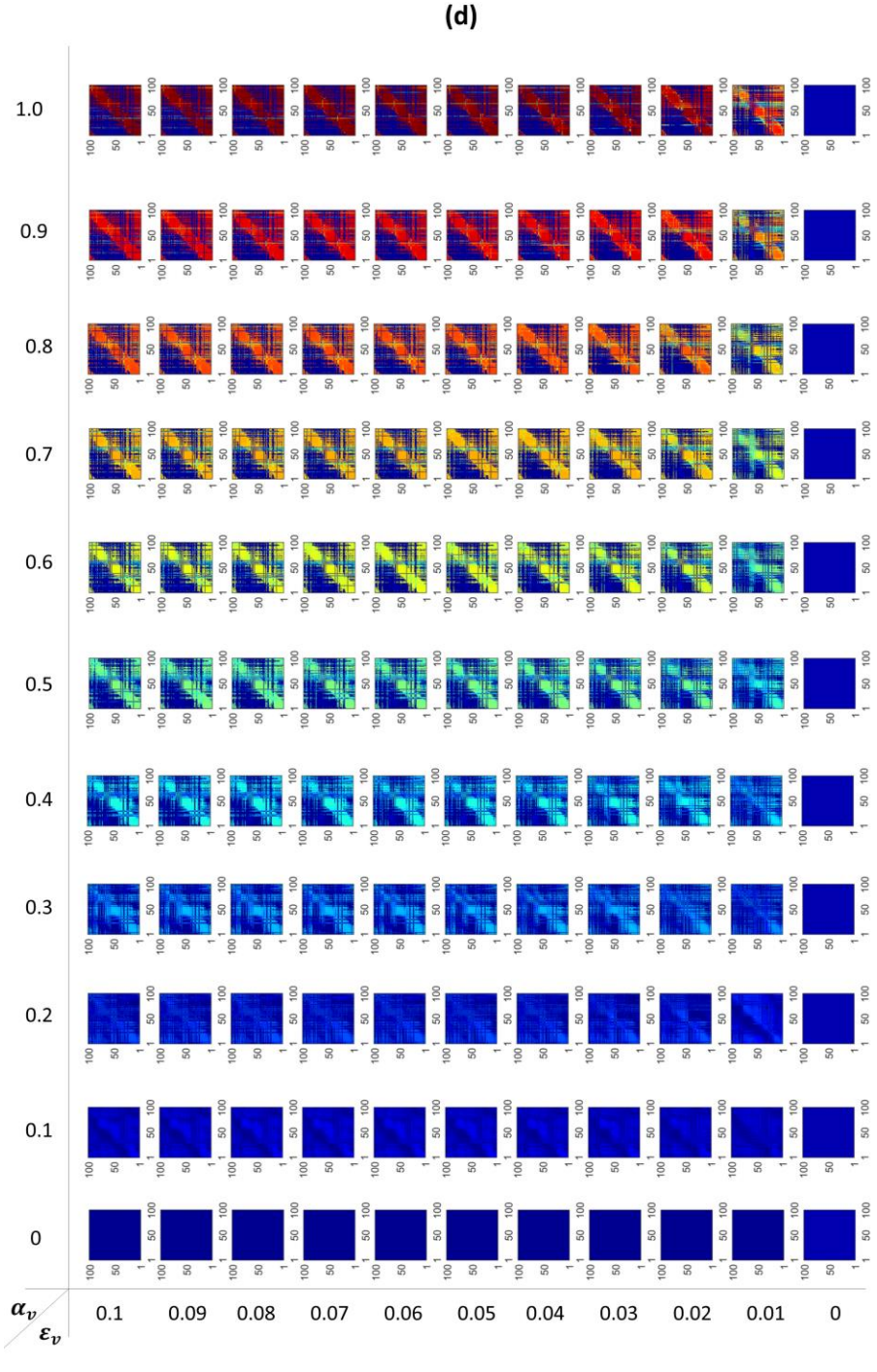
(d)
1.0
0.9
0.8
0.7
0.6
0.5
0.4
0.3
0.2
0.1
0
α_v
ε_v
0.1
0.09
0.08
0.07
0.06
0.05
0.04
0.03
0.02
0.01
0


(e)
1.0
0.9
0.8
0.7
0.6
0.5
0.4
0.3
0.2
0.1
0
α_v
ε_v
0.1
0.09
0.08
0.07
0.06
0.05
0.04
0.03
0.02
0.01
0

Figure S 2.3: Representation of structural and functional behaviour characteristic of scenario III for every point of the parameter space. Panel a) shows the colour-coded state of coherent-wave mode of synchronization and cluster-formation obtained from a single simulation. **Panel b)** shows absolute phase offsets between every oscillator and the first ($|\Delta\varphi_{1,i}|$) for all combinations of ε_v and α_v. Phase offsets are averaged over the last 100 time steps of the simulation. **Panel c)** shows structural coupling matrices for all combinations of ε_v and α_v. **Panel d)** shows conduction velocity matrices for all combinations of ε_v and α_v. **Panel e)** shows functional connectivity matrices for all combinations of ε_v and α_v. Matrix elements are averages over the last 100 time steps of the simulation in panels c, d and e. The connections' learning rate ε_s and the learning enhancement factor α_s are fixed at 0.1 and 1 respectively, and all values of the connectivity matrix K were fixed at α_s. The pairwise conduction velocities v_{ij} are initialized at 0.14, equivalent with the condition where $T \cong 7$.

Moreover, in Figure S 2.4, all Figures 2.7, 2.8, 2.9 and 2.10 are merged for an easier comparison between functional and structural characteristic behaviours.

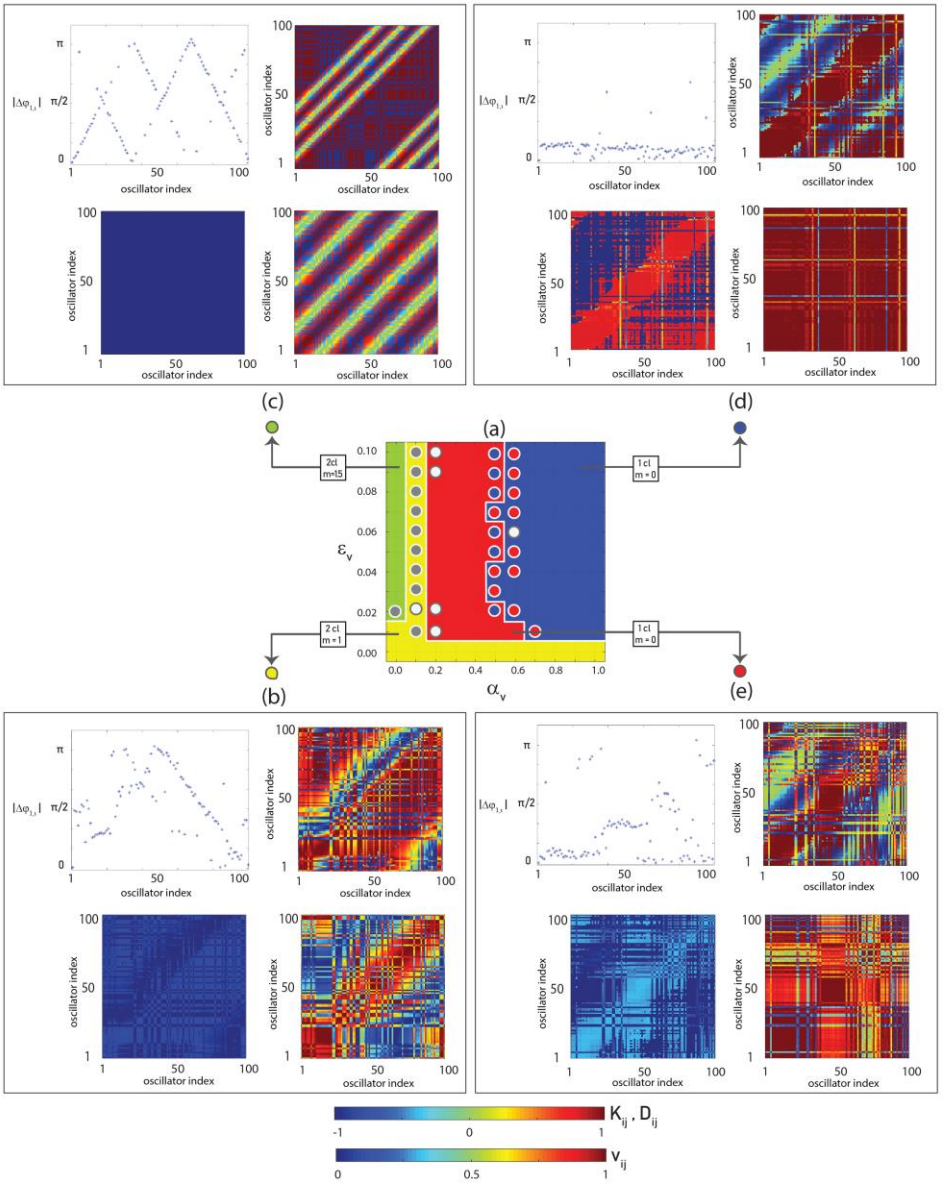

Figure S 2.4: Representation of structural and functional behaviour characteristic of scenario III. Panel a) shows the colour-coded state of coherent-wave mode of synchronization and cluster-formation obtained from a single simulation with respect to the changes of $\boldsymbol{\varepsilon_v}$ and $\boldsymbol{\alpha_v}$. **Panels b-e)** show $\left|\Delta\boldsymbol{\varphi}_{\boldsymbol{1,i}}\right|$ (top left of each panel), structural connectivity matrix (top right), conduction velocity matrix (bottom left) and functional connectivity matrix (bottom right) for state{1,d} in panel b, state{1.5,d} in panel c, state{0,s} in panel d and state{0,d} in panel e. Matrix elements are averages over the last 100 time steps of the simulation in panels c, d and e. The connections' learning rate $\boldsymbol{\varepsilon_s}$ and the learning enhancement

factor $\boldsymbol{\alpha_s}$ are fixed at 0.1 and 1 respectively, and all values of the connectivity matrix $\boldsymbol{K}$ were fixed at $\boldsymbol{\alpha_s}$. The pairwise conduction velocities $\boldsymbol{v_{ij}}$ are initialized at 0.14, equivalent with the condition where $\boldsymbol{T} \cong \boldsymbol{7}$.

Acknowledgements

Author PDW was supported by an NWO VICI grant (453.04.002). Author MS was funded by the European Union's Horizon 2020 Research and Innovation Program under Grant Agreement No. 785907 (HBP SGA2). Author MM was supported by an NWO VENI grant (451.15.012). This work was supported by the Dutch Province of Limburg.

References

Abrams, D. M., & Strogatz, S. H. (2004). Chimera States for Coupled Oscillators. *Physical Review Letters*, 93 (17), 174102.

Acebr, J. A., Gradenigo, V., Matematica, D., Acebrón, J. A., Bonilla, L. L., Vicente, C. J. P., … Spigler, R. (2005). The Kuramoto model: A simple paradigm for synchronization phenomena. *Reviews of Modern Physics*, 77 (January), 137–185.

Barrera, K., Chu, P., Abramowitz, J., Steger, R., Ramos, R. L., & Brumberg, J. C. (2013). Organization of myelin in the mouse somatosensory barrel cortex and the effects of sensory deprivation. *Developmental Neurobiology*, 73 (4), 297–314.

Bi, G. Q., & Poo, M. M. (1998). Synaptic modifications in cultured hippocampal neurons: dependence on spike timing, synaptic strength, and postsynaptic cell type. *The Journal of Neuroscience : The Official Journal of the Society for Neuroscience*, 18 (24), 10464–10472.

Blumenfeld-Katzir, T., Pasternak, O., Dagan, M., & Assaf, Y. (2011). Diffusion MRI of Structural Brain Plasticity Induced by a Learning and Memory Task, 6 (6), e20678.

Breakspear, M., Heitmann, S., & Daffertshofer, A. (2010). Generative Models of Cortical Oscillations: Neurobiological Implications of the Kuramoto Model. *Frontiers in Human Neuroscience*, 4 (November), 190.

Burylko, O., Kazanovich, Y., & Borisyuk, R. (2018). Winner-take-all in a phase oscillator system with adaptation. *Scientific Reports*, 8 (1), 416.

Chang, K.-J., Redmond, S. A., & Chan, J. R. (2016). Remodeling myelination: implications for mechanisms of neural plasticity. *Nature Neuroscience*, 19 (2), 190–197.

Demerens, C., Stankoff, B., Logak, M., Anglade, P., Allinquant, B., Couraud, F., … Lubetzki, C. (1996). Induction of myelination in the central nervous system by electrical activity. *Proceedings of the National Academy of Sciences of the United States of America*, 93 (18), 9887–92.

Dénes, K., Sándor, B., & Néda, Z. (2019). Pattern selection in a ring of Kuramoto oscillators. *Communications in Nonlinear Science and Numerical Simulation*.

Doesburg, S. M., Roggeveen, A. B., Kitajo, K., & Ward, L. M. (2008). Large-Scale Gamma-Band Phase Synchronization and Selective Attention. *Cerebral Cortex*, 18, 387.

D. O. Hebb. (1949). *The Organization of Behavior*.

Dutta, D. J., Ho Woo, D., Lee, P. R., Pajevic, S., Bukalo, O., Huffman, W. C., … Wake, H. (2018). Regulation of myelin structure and conduction velocity by perinodal astrocytes. *PNAS*, 115 (46), 11832–11837.

El-Nashar, H. F., Zhang, Y., Cerdeira, H. A., & Ibiyinka A., F. (2003). Synchronization in a chain of nearest neighbors coupled oscillators with fixed ends. *Chaos: An Interdisciplinary Journal of Nonlinear Science*, 13 (4), 1216–1225.

Fell, J., Klaver, P., Elger, C. E., & Fries, P. (2003). I s synchronized neuronal gamma activity relevant for selective attention ? *Brain Research Reviews*, 42, 265–272.

Fields, R. D. (2010). Change in the Brain's White Matter. *SCIENCE*, 330, 768–770.

Fields, R. D. (2015). A new mechanism of nervous system plasticity: activity-dependent myelination. *Nature Reviews Neuroscience*, 16 (12), 756–767.

Fries, P. (2005). A mechanism for cognitive dynamics: neuronal communication through neuronal coherence. *Trends in Cognitive Sciences*, 9 (10), 474–480.

Fries, P. (2015). Rhythms for Cognition: Communication through Coherence. *Neuron*, 88 (1), 220–35.

Gibson, E. M., Purger, D., Mount, C. W., Goldstein, A. K., Lin, G. L., Wood, L. S., … Pamelyn J. Woo, Hannes Vogel, M. M. (2014). Neuronal Activity Promotes Oligodendrogenesis and Adaptive Myelination in the Mammalian Brain. *Science*, 344 (6183), 1252304.

Gonze, D., Bernard, S., Waltermann, C., Kramer, A., & Herzel, H. (2005). Spontaneous Synchronization of Coupled Circadian Oscillators. *Biophysical Journal*, 89, 120–129.

Hauptmann, C., Omel'chenko, O., Popovych, O. v., Maistrenko, Y., & Tass, P. A. (2007). Control of spatially patterned synchrony with multisite delayed feedback. *Physical Review E*, 76 (6), 066209.

Haken, H., (2002). *Brain dynamics : synchronization and activity patterns in pulse-coupled neural nets with delays and noise*. Springer.

Hipp, J. F., Engel, A. K., & Siegel, M. (2011). Article Cortical Networks Predicts Perception. *Neuron*, 69 (2), 387–396.

Markram, H., Lübke, L. H. R., Frotscher, M., & Sakmann, B., (1997). Regulation of Synaptic Efficacy by Coincidence of Postsynaptic APs and EPSPs. *Science*, 275 (5297), 213–215.

Ishibashi, T., Dakin, K. A., Stevens, B., Lee, P. R., Kozlov, S. v, Stewart, C. L., & Fields, R. D. (2006). Astrocytes promote myelination in response to electrical impulses. *Neuron*, 49 (6), 823–32.

Jensen, O., & Lisman, J. E. (2000). Position Reconstruction From an Ensemble of Hippocampal Place Cells: Contribution of Theta Phase Coding. *Journal of Neurophysiology*, 83 (5), 2602–2609.

Kasatkin, D. v., Yanchuk, S., Schöll, E., & Nekorkin, V. I. (2017). Self-organized emergence of multilayer structure and chimera states in dynamical networks with adaptive couplings. *Physical Review E*, 96 (6), 062211.

Kazanovich, Y., & Borisyuk, R. (2017). Reaction times in visual search can be explained by a simple model of neural synchronization. *Neural Networks*, 87, 1–7.

Kotwal, T., Jiang, X., & Abrams, D. M. (2017). Connecting the Kuramoto Model and the Chimera State. *Physical Review Letters*, 119 (26), 264101.

Krause, C. M., Pörn, B., Lang, A. H., & Laine, M. (1997). Relative alpha desynchronization and synchronization during perception of music. *Cognitive Brain Research*, 5 (4), 295–299.

Kumar, P., Verma, D. K., & P.Parmananda. (2017). Partially synchronized states in an ensemble of chemo-mechanical oscillators. *Physics Letters A*, 381 (29), 2337–2343.

Laing, C. R. (2009). Chimera states in heterogeneous networks. *Chaos: An Interdisciplinary Journal of Nonlinear Science*, 19 (1), 013113.

Lowet, E., Gips, B., Roberts, M. J., de Weerd, P., Jensen, O., & van der Eerden, J. (2018). Microsaccade-rhythmic modulation of neural synchronization and coding within and across cortical areas V1 and V2. *PLOS Biology*, 16 (5), e2004132.

Maistrenko, Y. L., Lysyansky, B., Hauptmann, C., Burylko, O., & Tass, P. A. (2007). Multistability in the Kuramoto model with synaptic plasticity. *Physical Review E*, 75 (6), 066207.

McKenzie, I. A., Ohayon, D., Li, H., de Faria, J. P., Emery, B., Tohyama, K., & Richardson, W. D. (2014). Motor skill learning requires active central myelination. *Science*, 346 (6207), 318–322.

Melloni, L., Molina, C., Pena, M., Torres, D., Singer, W., & Rodriguez, E. (2007). Synchronization of Neural Activity across Cortical Areas Correlates with Conscious Perception. *Journal of Neuroscience*, 27 (11), 2858–2865.

Montbrió, E., Pazó, D., & Schmidt, J. (2006). Time delay in the Kuramoto model with bimodal frequency distribution. *Physical Review E*, 74 (5), 056201.

Mörtl, A., Lorenz, T., & Hirche, S. (2014). Rhythm Patterns Interaction - Synchronization Behavior for Human-Robot Joint Action. *PLoS ONE*, 9 (4).

Nakamura, Y., Tominaga, F., & Munakata, T. (1994). Clustering behavior of time-delayed nearest-neighbor coupled oscillators. *Physical Review E*, 49 (6), 4849–4856.

Nickel, M., & Gu, C. (2018). Regulation of Central Nervous System Myelination in Higher Brain Functions. *Neural Plasticity*, 2018, 1–12.

Niebur, E., Schuster, H. G., & Kammen, D. M. (1991). Collective frequencies and metastability in networks of limit-cycle oscillators with time delay. *Physical Review Letters*, 67 (20), 2753–2756.

Niyogi, R. K., & English, L. Q. (2009). Learning-rate-dependent clustering and self-development in a network of coupled phase oscillators. *Physical Review E - Statistical, Nonlinear, and Soft Matter Physics*, 80 (6), 1–7.

Nowotny, T., Zhigulin, V. P., Selverston, A. I., Abarbanel, H. D. I., & Rabinovich, M. I. (2003). Enhancement of Synchronization in a Hybrid Neural Circuit by Spike-Timing Dependent Plasticity. *The Journal of Neuroscience*, 23 (30), 9776–9785.

Pajevic, S., Basser, P. J., & Fields, A. R. D. (2014). Role of Myelin Plasticity in Oscillations and Synchrony of Neuronal Activity. *Neuroscience*, 276, 135–147.

Pfister, J.-P., & Gerstner, W. (2006). Triplets of Spikes in a Model of Spike Timing-Dependent Plasticity. *Journal of Neuroscience*, 26 (38), 9673–9682.

Pikovsky, A., Rosenblum, M., Self, J. K.-, & 2001, undefined. (2003). A universal concept in nonlinear sciences. *Researchgate.Net*.

Popovych, O. v., Yanchuk, S., & Tass, P. A. (2013). Self-organized noise resistance of oscillatory neural networks with spike timing-dependent plasticity. *Scientific Reports*, 3 (1), 2926.

Purger, D., Gibson, E. M., & Monje, M. (2016). Myelin plasticity in the central nervous system. *Neuropharmacology*, 110, 563–573.

Quiroga, R. Q., Arnhold, J., & Grassberger, P. (2000). Learning driver-response relationships from synchronization patterns. *Physical Review E*, 61 (5), 5142–5148.

Fields, R. D., (2014). Myelin-More than Insulation. *SCIENCE*, 344 (6181), 264–266.

Sampaio-Baptista, C., Khrapitchev, A. A., Foxley, S., Schlagheck, T., Scholz, J., Jbabdi, S., … Johansen-Berg, H. (2013). Motor Skill Learning Induces Changes in White Matter Microstructure and Myelination. *Journal of Neuroscience*, 33 (50), 19499–19503.

Scholz, J., Klein, M. C., Behrens, T. E. J. J., & Johansen-Berg, H. (2009). Training induces changes in white-matter architecture. *Nature Neuroscience*, 12 (11), 1370–1371.

Schröder, M., Timme, M., & Witthaut, D. (2017). A universal order parameter for synchrony in networks of limit cycle oscillators. *Chaos*, 27 (7), 073119.

Schuster, H. G., & Wagner, P. (1989). Mutual Entrainment of Two Limit Cycle Oscillators with Time Delayed Coupling. *Progress of Theoretical Physics*, 81 (5).

Seliger, P., Young, S. C., & Tsimring, L. S. (2002). Plasticity and learning in a network of coupled phase oscillators. *Physical Review E - Statistical, Nonlinear, and Soft Matter Physics*, 65 (4), 1–7.

Singer, W. (1993). Synchronization of Cortical Activity and Its Putative Role in Information Processing and Learning. *Annu. Rev. Physiol*, 55, 349–74.

Siri, B., Quoy, M., Delord, B., Cessac, B., & Berry, H. (2007). Effects of Hebbian learning on the dynamics and structure of random networks with inhibitory and excitatory neurons. *Journal of Physiology Paris*, 101 (1–3), 136–148.

Song, S., Miller, K. D., & Abbott, L. F. (2000). Competitive Hebbian learning through spike-timing-dependent synapticplasticity. *Nature Neuroscience*, 3 (9), 919–926.

Timms, L., & English, L. Q. (2014). Synchronization in phase-coupled Kuramoto oscillator networks with axonal delay and synaptic plasticity. *Physical Review E - Statistical, Nonlinear, and Soft Matter Physics*, 89 (3).

Traubab, R. D., Spruston, N., Soltesz, I., Konnerth, A., Whittington, M. A., & Jefferys, J. G. R. (1998). Gamma-frequency oscillations: a neuronal population phenomenon, regulated by synaptic and intrinsic cellular processes, and inducing synaptic plasticity. *Progress in Neurobiology*, 55 (6), 563–575.

Wittenberg, G. M., & Wang, S. S.-H. (2006). Malleability of spike-timing-dependent plasticity at the CA3-CA1 synapse. *The Journal of Neuroscience : The Official Journal of the Society for Neuroscience*, 26 (24), 6610–7.

Womelsdorf, T., & Fries, P. (2007). The role of neuronal synchronization in selective attention. *Current Opinion in Neurobiology*, 17 (2), 154–160.

Yao, N., Huang, Z.-G., Lai, Y.-C., & Zheng, Z.-G. (2013). Robustness of chimera states in complex dynamical systems. *Scientific Reports*, 3 (1), 3522.

Yeung, M. K. S., & Strogatz, S. H. (1999). Time delay in the Kuramoto model of coupled oscillators. *Physical Review Letters*, 82 (3), 648–651.

Zanette, D. H. (2000). Propagating structures in globally coupled systems with time delays. *Physical Review E*, 62 (3), 3167–3172.

Zatorre, R. J., Fields, R. D., & Johansen-berg, H. (2012). Plasticity in gray and white: Neuroimaging changes in brain structure during learning. *Nature Neuroscience*, 15 (4), 528–536.

Zouridakis, G., Baluch, F., Stevenson, I., Diaz, J., & Subramanian, D. (2007). Long-Range Gamma-Band Synchronization During Learning of a Complex Visuomotor Task. In *3rd International IEEE EMBS Conference on Neural Engineering*. Kohala Coast, Hawaii, USA.

Karimian, M., Roberts, M., De Weerd, P., & Senden, M.
To be submitted

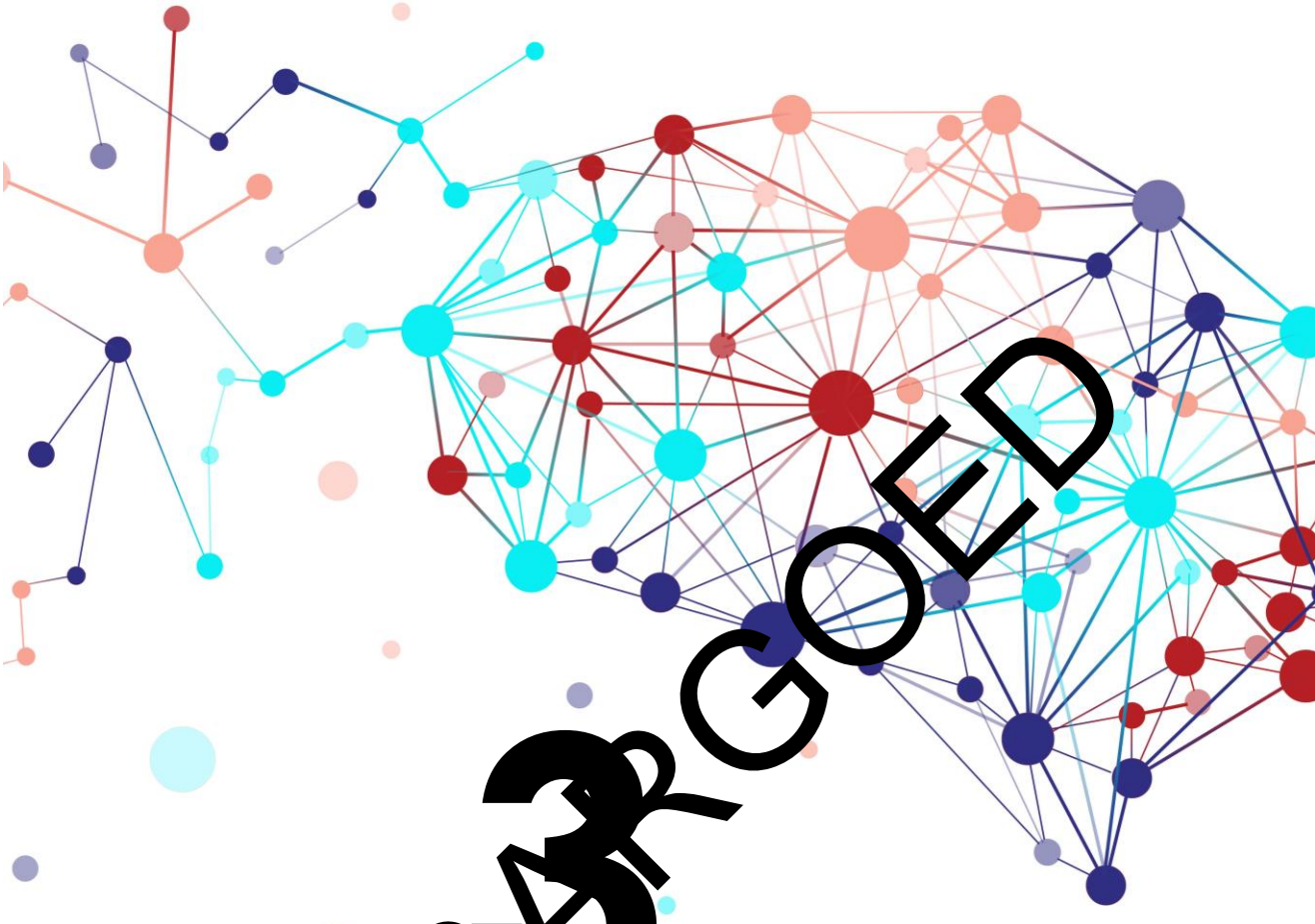

Chapter 3

Synchronization of Input-dependent Gamma Oscillations in V1: A Criterion to Predict Figure-ground Segregation in Texture Stimuli

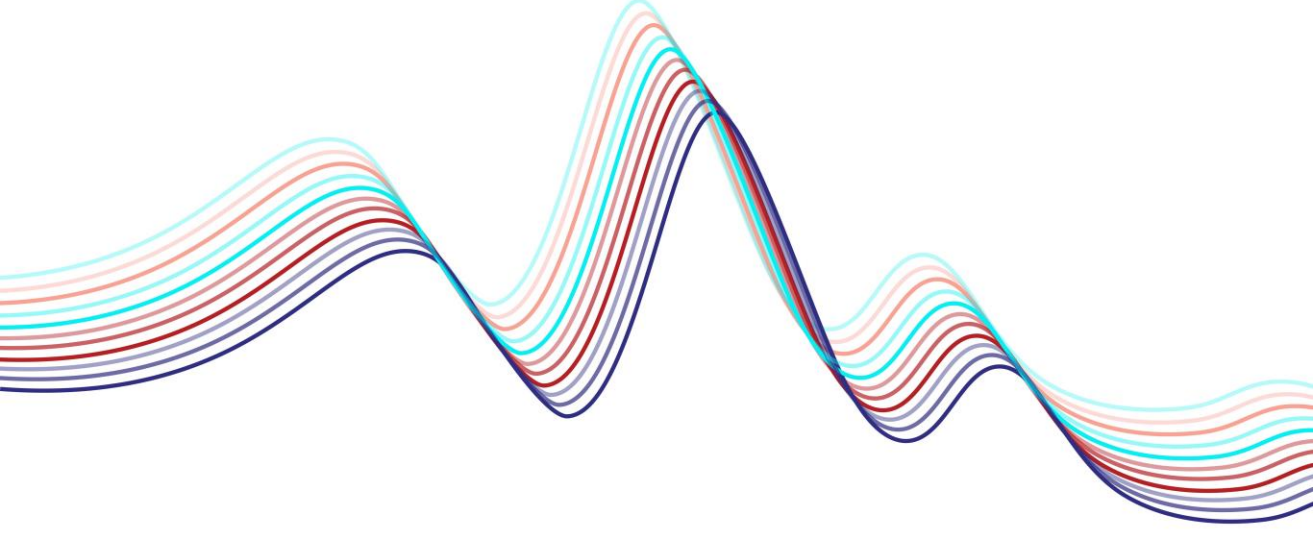

Karimian, M., Roberts, M., Senden, M., & De Weerd, P.

To be submitted

Chapter 4

Perceptual Learning of Figure-ground Segregation in Texture Stimuli and Synchronization of Gamma Oscillations in V1

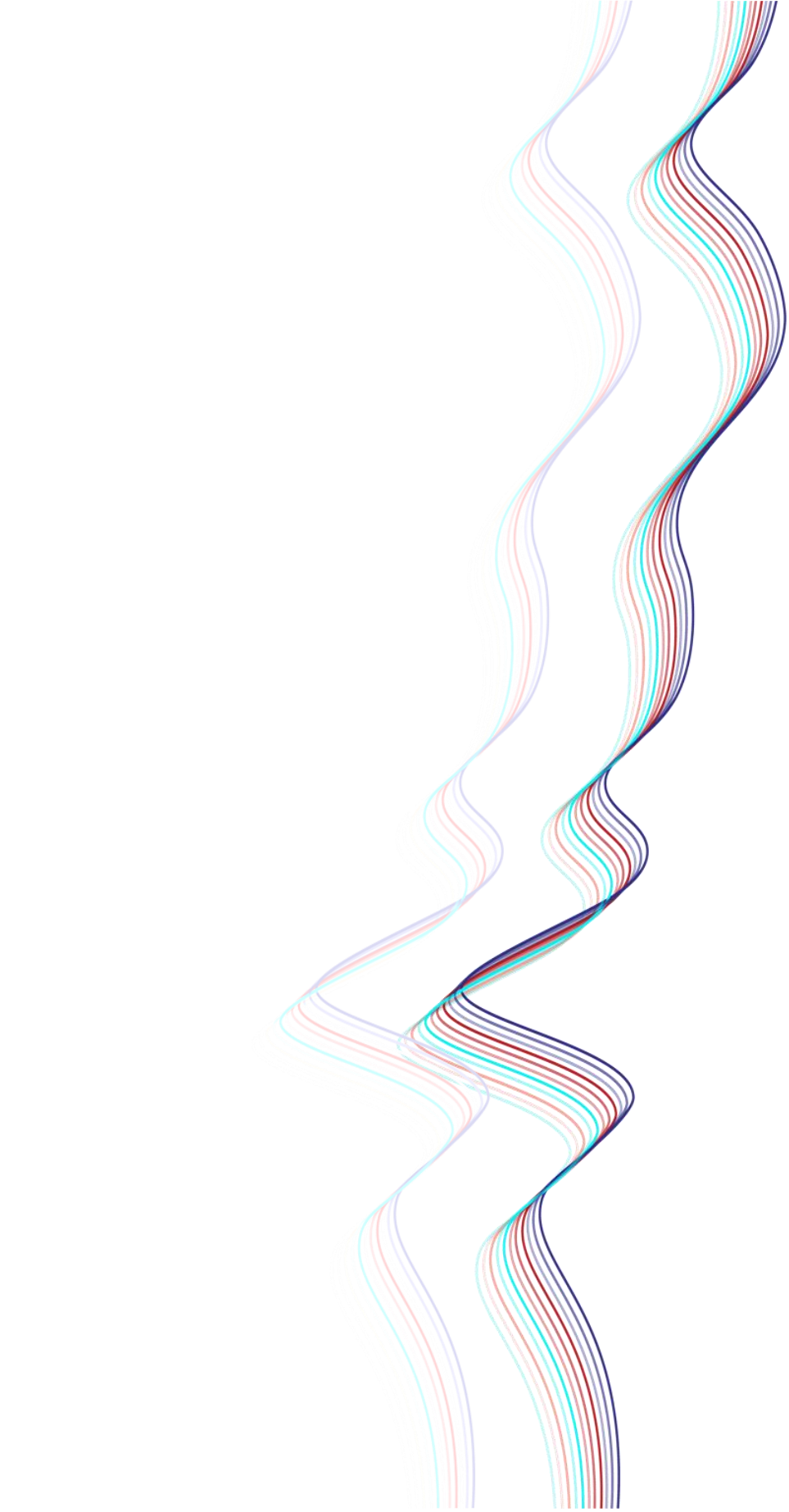

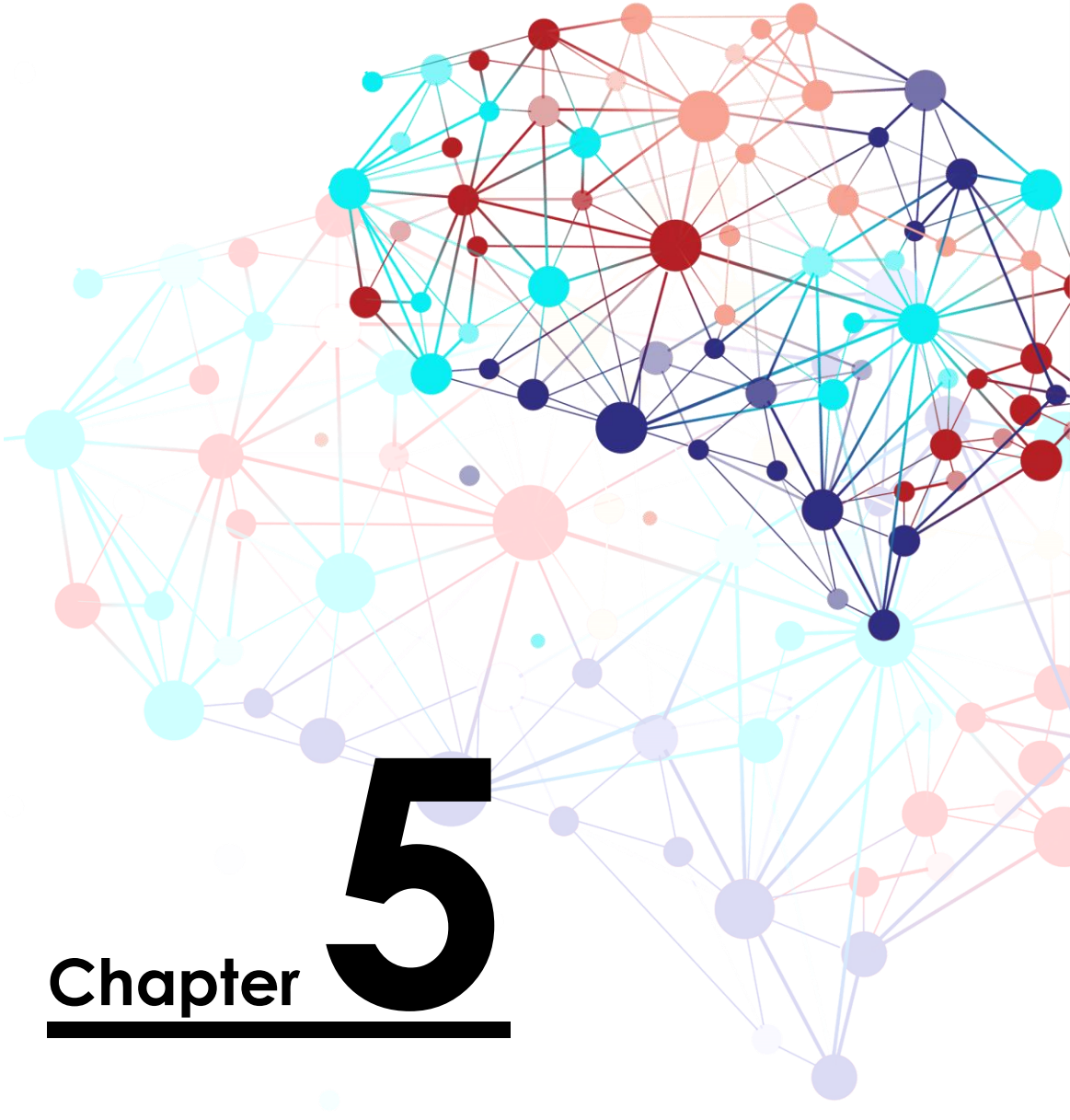

Chapter 5

General summary and Discussion

5-1. Aims of the thesis

Neural oscillators and their synchronization take centre stage in the present thesis with an emphasis on the role of gamma synchronization in cortical information processing. While stimulus-induced cortical oscillations in the gamma range are ubiquitous in the cortex (Bertrand & Tallon-Baudry, 2000; N. Brunet et al., 2015; Buzśaki & Wang, 2012), a number of studies have cast doubt on the notion that they play a functional role. In particular, critiques that long signal propagation delays (Ray & Maunsell, 2015) and high variance among frequencies in the gamma range (D. Hermes, Miller, Wandell, & Winawer, 2015; Jia, Xing, & Kohn, 2013; Ray & Maunsell, 2015) may interfere with synchrony-based neural information processing have been influential. Prior neurophysiological studies have shown however that neither propagation delays (Fries, Nikolić, & Singer, 2007; Nikolić, 2006) nor frequency variance (Fries et al., 2007; Lowet, Roberts, Peter, Gips, & de Weerd, 2017) are necessarily detrimental to the selective and flexible synchronization required for neural information processing. According to the theory of weakly coupled oscillators (TWCO), the distribution of intrinsic frequencies differences (frequency detuning) among oscillators as well as the strength of their interactions (coupling strength) determines the likelihood that oscillators synchronize (Pikovsky, Rosenblum, Self, & 2001, 2003). In other words, a frequency difference can still permit (partial) synchronization when there is sufficient coupling strength. The existence of long propagation delays and associated variability when communicating oscillators are at various distances from each other in a network can affect synchronization. Nevertheless, empirical evidence indicates that within a range, variable propagation delays do not render synchronization impossible (Fries et al., 2007; Nikolić, 2006). Thus, rather than considering the existence of variability in propagation delays among remote oscillators as an absolute argument against synchronization as a viable mechanism for information processing, it may be considered as a factor that can be used by the brain to control synchronization. Variability in propagation delays may exert their effect by affecting detuning (Buia & Tiesinga, 2006; Fries, 2005). Hence, TWCO posits that coupling strength and frequency detuning are crucial factors controlling synchronization behaviour among oscillators. Using this framework, and in order to investigate the usefulness of gamma synchronization in (visual) information processing, we aimed to address the following questions:

1) What are the effects of (plastic) coupling delays on the synchronization behaviour and synaptic plasticity within a phase oscillator network and how does this affect structural and functional features of the network (Chapter 2)?

2) To what extent is a phase oscillator network exposed to texture stimuli capable of predicting human figure-ground segregation performance (Chapter 3)?
3) To what extent are learning-induced structural changes in a phase oscillator network exposed to texture stimuli predictive of human performance improvement on a figure-ground segregation task (Chapter 4)?

5-2. Summary of Results

Before presenting a detailed summary of results per chapter addressing the above-formulated aims, the main results are briefly summarized here. The results in Chapter 2 demonstrate that signal propagation delays and experience-induced plasticity affect the (spatial) distribution of gamma frequencies in a network of oscillators (Buia & Tiesinga, 2006; Fries, 2005) as well as the strength of coupling among neural oscillators. Thus, propagation delays vary as a function of distance, but are at the same time subject to plastic regulatory mechanisms that use propagation delays as a tool to facilitate or prevent synchronization between different groups of oscillators. The results in Chapters 3 and 4 support the perceptual relevance of levels of synchronization as controlled by detuning and coupling strength in an oscillator network (Baldi & Meir, 1990; Buia & Tiesinga, 2006; Dubey & Ray, 2020; Feng, Havenith, Wang, Singer, & Nikolić, 2010; Gieselmann & Thiele, 2008; Gilbert & Wiesel, 1983; Gray, König, Engel, & Singer, 1989; Hadjipapas, Lowet, Roberts, Peter, & de Weerd, 2015; Hall et al., 2005; Henrie & Shapley, 2005; Logothetis, Pauls, Augath, Trinath, & Oeltermann, 2001; Lowet et al., 2015, 2017; Ray & Maunsell, 2010; Roberts et al., 2013; Shapira et al., 2017; Stettler, Das, Bennett, & Gilbert, 2002; Swettenham, Muthukumaraswamy, & Singh, 2009; Ts'o, Gilbert, & Wiesel, 1986; M. A. Whittington, Traub, Kopell, Ermentrout, & Buhl, 2000; Miles A. Whittington, Cunningham, LeBeau, Racca, & Traub, 2011). We found an excellent fit between model predictions of synchronization levels associated with manipulations of stimulus- and experience-dependent factors on the one hand, and behavioural measures of human figure-ground segregation on the other. Hence, the present thesis has contributed behavioural and computational modelling research that argues against the idea that (because of detuning and because of the long transmission delays in long-range communication) gamma oscillations would be useless epiphenomena of visual processing without a substantial contribution to visual perception and other forms of cognition.

5-2-1. Chapter 2: Effects of Plastic Coupling delays and Plastic Coupling Strengths on the Synchronization and Learning in Networks of Coupled Oscillators

Chapter 2 addressed the question how (plastic) coupling delays affect synchronization behaviour and synaptic plasticity in a phase oscillator network. In this chapter, synchronization was investigated in a ring network of coupled phase oscillators whose pairwise coupling strength and conduction velocities were plastic. What is presented in this chapter is a simple neural mass model developed to evaluate structural (pairwise connection strength and conduction velocity) and functional states (local and global synchronization behaviour) of a one-dimensional network of self-sustained oscillators that receives no external input. The network's states evolved based on the activity-dependent interplay between synaptic plasticity (connectivity strength) and myelin plasticity (conduction velocity). Synaptic plasticity was implemented in terms of activity-dependent modifications of pairwise connection strengths, whereas myelin plasticity was implemented indirectly through its effects on axonal conduction velocities and therefore signal transmission delays.

The contributions of synaptic plasticity to various forms of learning and memory have been extensively studied (Milner, Squire, & Kandel, 1998; Niyogi & English, 2009; Nowotny, Zhigulin, Selverston, Abarbanel, & Rabinovich, 2003; Seliger, Young, & Tsimring, 2002; Siri, Quoy, Delord, Cessac, & Berry, 2007; Song, Miller, & Abbott, 2000; Timms & English, 2014; Traubab et al., 1998), whereas the contribution of myelin plasticity to learning has become recognized only more recently as an important mechanism for learning and memory (Nickel & Gu, 2018; Sampaio-Baptista et al., 2013; Scholz, Klein, Behrens, & Johansen-Berg, 2009). Studies of the mechanisms of myelination (Fields, 2015; Fields & Bukalo, 2020; Giedd et al., 1996; Pajevic, Basser, & Fields, 2014; R. D. Fields, 2014) combined with diffusion neuroimaging studies of plastic changes in the integrity of white matter (Chang, Redmond, & Chan, 2016; Dutta et al., 2018; Fields, 2015; McKenzie et al., 2014; Pajevic et al., 2014; Purger, Gibson, & Monje, 2016; Scholz et al., 2009) indicate that myelination remains plastic throughout life (Giedd et al., 1996). Moreover, myelin plasticity depends, like synaptic plasticity, on the temporal relations of spiking activity between pre- and post-synaptic neural populations (Fields, 2015; Pajevic et al., 2014; R. D. Fields, 2014). Accordingly, synaptic and myelin plasticity in our model were both governed by Hebbian learning rules. The effects of both kinds of plasticity were assessed in terms of functional connectivity (synchronization behavior) in the model network and in terms of structural connectivity (myelination of axons and synaptic connectivity strength). The resulting

model revealed significant differences in both structural and functional connectivity when separately considering effects from pure synaptic plasticity, from pure myelin plasticity and from the interplay between the two. For example, with respect to synaptic plasticity, we found that for conditions in which the phase oscillator network developed two segregated structural clusters, also two corresponding, segregated, functional clusters emerged. In other words, parts of the network where the oscillators became more weakly connected also showed less synchronization. However, when in the same conditions that led to a segregation of the network into two separate clusters, myelin plasticity was allowed, this resulted in the formation of a single functional cluster. In other words, functional integration (synchronization) occurred across structurally segregated clusters. Because in this chapter we only studied the internal dynamics of the constructed network, without external input, an interpretation of these findings at the level of perception and cognition is difficult. Nevertheless, the fact that a larger network can be segregated into subnetworks is conceptually important for understanding perception and cognition. Note however that the model used in Chapter 2 does not relate to specific spatial and temporal scales. Instead, it provides a general framework to study neural oscillatory networks at any spatio-temporal scale.

5-2-2. Chapter 3: Role of the Synchronization among Stimulus-dependent Gamma Oscillations in Figure-ground Segregation

The third chapter asked the question whether gamma synchronization assists in figure-ground segregation. To address this question, we first designed a network of coupled phase oscillators exposed to texture stimuli. The oscillator network was designed to reflect elementary V1-like neural circuits. For this reason, dynamical and structural network parameters were based on electrophysiological recordings and organizational principles of V1 in macaques (Lowet et al., 2017) and humans (Balasubramanian & Schwartz, 2002; Polimeni et al., 2005; Schwartz, 1980). The scope of this chapter's main question was limited to an investigation of whether synchronization could constitute a pre-attentive process in early visual areas that supports figure-ground segregation in texture stimuli.

The texture stimuli comprised Gabor annuli arranged on a random grid. Each stimulus included a rectangular region, the figure, where annulus contrast was less heterogeneous than in the background. Based on prior observations in early visual cortex that local contrast drives gamma frequency (Hadjipapas et al., 2015; Henrie & Shapley, 2005; Lowet et al., 2015; Roberts et al., 2013; Shapira et al., 2017) and that coupling strength depends on cortical distance (Gilbert & Wiesel, 1983; Lowet

et al., 2015, 2017; Stettler et al., 2002; Ts'o et al., 1986), we assumed that contrast heterogeneity affects frequency detuning and physical proximity among annuli affects coupling strength among corresponding neural circuits. Hence, the starting point in this chapter is the realization that the mathematical factors that determine synchrony among weakly coupled oscillators can be linked to the stimulus features that guide figure-ground segregation.

If neural synchrony is indeed relevant for figure-ground segregation, one would expect that formalizing such a conceptual relation in a computational model would allow deriving quantitative predictions of figure-ground segregation performance from modelled synchronization behaviour. When the model was exposed to the texture stimuli, it revealed a triangular region of high synchronization in the space spanned by contrast heterogeneity (detuning) and grid coarseness (coupling strength). Remarkably, human participants who were asked to detect the figure from the ground in the same texture stimuli showed a quantitatively matched triangular region of supra-threshold figure-ground segregation performance for the same conditions. Interestingly, the model parameters chosen based on neurophysiological data in the macaque monkey were close to optimal to predict human figure-ground segregation performance. The consistency between model predictions and behavioural results suggests a mechanistic link between gamma synchronization in V1 and figure-ground segregation. This suggestion does not exclude that other mechanisms than the synchronization behaviour among neural groups in early visual cortex could contribute to figure-ground segregation. However, our data indicate at the very least that low-level neural synchrony is a viable mechanism for figure-ground segregation in the texture stimuli we used. Interestingly, participants' response times did not reveal an Arnold tongue as these were only affected significantly by contrast heterogeneity, but not by the physical distance between texture elements. This observation suggests that synchronization in V1 may not be a dominant factor in determining the speed of cortical information processing. Only after training-induced gains in synchrony and performance (see Chapter 4) did synchronization in our model become related to response times. This suggests a training-induced increase in the relevance of synchronization in the speed of cortical information processing. This finding will be discussed below. What can be inferred from the results of Chapter 3 is that the high stimulus dependency of gamma oscillations constitutes an essential aspect of the synchronization mechanism underlying figure-ground segregation. This dependency forms the basis of synchronization among figure elements (integration) and simultaneous de-synchronization between figure and ground elements (segregation). Therefore,

Chapter 3 shows that the high stimulus dependency of gamma oscillations may underlie, rather than preclude, a functional role in cortical information processing.

5-2-3. Chapter 4: Role of the Synchronization among Stimulus-dependent Gamma Oscillations in Perceptual Learning of Figure-ground Segregation

The fourth chapter addressed the question to what extent learning-induced changes in a phase oscillator model are predictive of human performance improvements in a figure-ground segregation task. In the third chapter, it was suggested that synchronization of gamma oscillations in V1 constitutes an important component of the neural mechanism that underlies figure-ground segregation. If this is indeed the case and if, as assumed in Chapter 2, synchronization behaviour is affected by experience-dependent changes in coupling strength, then any learning-induced gains in performance should be quantitatively related to learning-induced increases in neural synchrony. To evaluate this hypothesis, modelling was combined with psychophysics experimentation using the same stimulus conditions as in Chapter 3. Learning was incorporated into the model in the form of a three-factor learning rule that took phase coherence and the probability of correct responses on all trials of a session into account. Free parameters of the learning mechanism were estimated from the first two sessions, and subsequently used to predict learning effects in the remaining sessions. Results in Chapter 4 showed that synchrony and performance exhibit a close quantitative resemblance that was maintained across training sessions. In particular, the triangular region of supra-threshold accuracy data in a space defined by contrast heterogeneity and grid coarseness showed training-induced changes in shape that were closely matched by learning-induced changes in the Arnold tongue of the V1 oscillator model. Late in the training, an Arnold tongue emerged for response times as well. This further supports the idea that synchronization may be an important component of a neural figure-ground segregation mechanism and that learning-induced changes in figure-ground perception may at least in part be mediated by plasticity-induced changes in neural synchrony in a low-level visual area. The learning rule employed in Chapter 4 rested on the assumption that skill learning in early visual cortex is position specific (Merav Ahissar & Hochstein, 1996; Crist, Kapadia, Westheimer, & Gilbert, 1997; Karni & Sagi, 1991; A. A. Schoups, Vogels, & Orban, 1995). We verified this in a transfer session, in which figure-ground segregation was tested after moving the figure to the diametrically opposite visual field quadrant. Although figure-ground performance had increased significantly with training, it remained at baseline in the transfer

session. Overall, the psychophysical and modelling data in this chapter suggest that training-induced changes in synchrony in V1 may contribute to enhanced accuracy in figure-ground segregation in an expanded range of grid coarseness and contrast heterogeneity conditions. Moreover, towards the end of training, synchronization strength also becomes related to processing speed.

5-3. Theoretical Implications

The key conjecture of the present thesis is that oscillations are functionally relevant for neural information processing. In particular, the flexible synchronization behaviour of neural oscillators may underlie the flexible integration and segregation of stimulus-dependent and other types of information. This conjecture is central to two theories that feature prominently in neuroscience: the communication through coherence (CTC) theory (Fries, 2005) and the theory of weakly coupled oscillators (TWCO) (Ermentrout, Park, & Wilson, 2019; Pikovsky et al., 2003). CTC emphasizes long-range cortical interactions and proposes that synchronization within distributed neural networks facilitates selective communication (Fries, 2005). Specifically, it proposes that selective communication is achieved through coherence between oscillating activity in sending and receiving regions. However, CTC does not specify the mechanisms by which these regions synchronize in the first place. CTC simply states that two brain regions cannot communicate unless their activity patterns are in-phase (or more generally in a favourable phase-relation). Stated in this manner, CTC considers coherence as a prerequisite for communication. However, a crucial question is to understand how coherence is achieved in the first place, and therefore one may wonder if a form of communication needs to occur *prior* to the emergence of coherence. The latter idea is an essential aspect of the theoretical framework of TWCO, which stipulates that two brain regions may achieve synchrony through mutual interactions. In particular, TWCO formalizes and specifies the mutual interactions among oscillators under which specific phase relationships among two (or more) interacting oscillators can be achieved. As such, TWCO assumes that interaction precedes coherence. The opposition that is created here between CTC and TWCO may be overstated, and the two frameworks can be seen as compatible as long as one accepts that CTC is underspecified in terms of the mechanisms that enable the phase relations that in turn enable communication. Note that in joining the concepts of CTC and TWCO it is interesting to reflect on the meaning of the terms ‘interaction’ and ‘communication’. Interaction between two oscillators refers to the mutual influences that bring oscillators into a favourable phase-relationship that permits communication. If communication is defined as the

ability of action potentials from a sending population of neurons to trigger action potentials in a receiving population of neurons, then interaction may precede communication, because the interactions among connected oscillators will take place partly in time periods where communication as defined above is not (yet) possible. In this sense communication and interaction can be distinguished. However, at the same time, it is clear that the mutual interactions among neuronal pools occur through spiking, and that spikes from a sending population that arrive in an inhibitory period of a receiving population are still part of the interaction that leads to favourable phase relations required for action potentials from a sending population to trigger action potentials in a receiving population. From that perspective, the mechanisms of interaction and communication are closely related.

It is fascinating to note that TWCO is a general theory of synchronization phenomena, and that its concepts have been applied successfully and widely in chemistry, biology, and neuroscience (Ermentrout et al., 2019). As a general theory, TWCO is not concerned with whether or not oscillations and synchrony in the brain are relevant for neural information processing. However, a number of theoretical neuroscientists have over the years developed theories of neural information processing that are rooted in TWCO and that adhere to its fundamental principles. Noteworthy in this context is seminal work led by Izhikevich who suggested that synchrony allows for the flexible connection and disconnection of neural oscillators based on changing task demands (Hoppensteadt & Izhikevich, 1999; Izhikevich & Appl Math, 2006). At the macroscopic scale (involving long-range interactions), this concept is in line with dynamic routing of information to ensure that the output of local computations is sent to the appropriate brain regions for further processing. At the mesoscopic scale (i.e. within cortical areas), the flexibility of network synchronization may be utilized for local information integration and segregation such as required for associative memory (Hoppensteadt & Izhikevich, 1999) or figure-ground segregation. Depending on the spatio-temporal framework applied to the oscillator network and simulated data in Chapter 2, the findings in that chapter can be relevant in the context of a putative role of neural synchrony for long-range interactions[2]. Specifically, Chapter 2 revealed that dynamic conduction velocity

[2] In the context of fast oscillations such as gamma, typical cortical conduction velocities (on the order of 100 meters per second (Swadlow & Waxman, 2012)) may manifest as significant delays for long-range connections (between cortical areas) but not for short-range connections (within cortical areas). The reason is that a) delays typically manifest as phase-shifts and b) the impact of phase-shifts is relative to oscillation periods. As a rule of thumb (and exactly for pure sine interaction function as employed in the Kuramoto model), only

provides the possibility for synchronization even in the context of fast synaptic changes promoting structural network segregation. This indicates that adaptive myelination may have the capacity to compensate for synaptic effects that might otherwise desynchronize neural groups. Adaptive myelination may thus help to stabilize dynamic routing in the context of synaptic changes in long-range connectivity. Chapters 3 and 4 speak towards a putative role of neural synchrony at the mesoscopic scale. Depending on stimulus properties, and on the excitatory drive delivered locally to the various neuronal populations encoding the stimulus, these neuronal populations may synchronize and hence form an integrated neural group that is segregated from other groups in a manner that is relevant for visual perception (Lowet et al., 2015). The stimulus dependence of synchronization renders this process highly flexible and hence perceptually relevant. Furthermore, synchronized neuronal groups within cortical regions, rather than entire cortical regions, likely form higher-order oscillators that interact at the macroscopic scale. This interplay between local information processing and global routing may constitute a highly flexible mechanism for cortical information processing (Kirst, Timme, & Battaglia, 2016).

Though not the focus of the present thesis, results in Chapter 4 are also relevant for an ongoing debate whether (location) specificity is a defining characteristic of perceptual learning. Several studies have reported that experience-induced improvements in perceptual skills are specific to the retinotopic location (Merav Ahissar & Hochstein, 1996; Crist et al., 1997; Karni & Sagi, 1991; A. A. Schoups et al., 1995) and stimulus features (Merav Ahissar & Hochstein, 1996; Merav Ahissar, Laiwand, Kozminsky, & Hochstein, 1998; M. Ahissar & Hochstein, 1993; Crist et al., 1997; Fiorentini & Berardi, 1980; Karni & Sagi, 1991; A. Schoups, Vogels, Qian, & Orban, 2001) of the trained skill. However, other studies have reported that skills can generalize to novel locations and stimulus features (Aberg, Tartaglia, & Herzog, 2009; Jeter, Dosher, Petrov, & Lu, 2009; R. Wang, Cong, & Yu, 2013; R. Wang, Zhang, Klein, Levi, & Yu, 2012; Zhang et al., 2010). The modelling work in Chapter 4 assumes that perceptual learning is location-specific. We validated this assumption empirically by including an additional session wherein it was shown that improvements on a figure-ground segregation skill do not generalize across retinotopic locations.

---

phase-shifts between $\frac{1}{2}\pi$ and $\frac{3}{2}\pi$ will notably affect synchronization behaviour (Ermentrout & Ko, 2009). For gamma oscillations, such phase-shifts may occur for long-range but not short-range connections.

5-4. Implications for the Role of Local Gamma

While TWCO is agnostic with regard to the role of specific frequency bands, gamma range oscillations were of particular interest in the present thesis. Chapters 3 and 4 suggest that gamma oscillations contribute to visual processing. These studies show that local and global image statistics drive an oscillatory mechanism for image segmentation. This is in line with a number of studies (N. Brunet et al., 2015; Gray & Goodell, 2011) that have reported the presence of gamma oscillations in macaque visual cortical areas, specifically in V1, during free viewing of static images. Specifically, Lowet et al. (2015), who in a modelling study using an online image database (Martin, Fowlkes, Tal, & Malik, 2001) showed a meaningful link between border segmentation in natural images by human observers and gamma synchronization among nearby neuronal groups driven by image contrast within their receptive fields. Lowet et al.'s study (Lowet et al., 2015) suggested that surface perception is related both to the smaller contrast variations (thus lower detuning) within surfaces in comparison to the large contrast variations (thus higher detuning) across surfaces, at the surface borders. This led to the integration (synchronization) of neural activity induced within each figure surface, and to the segregation of activity across surface borders. Lowet et al.'s study (Lowet et al., 2015) together with our own data (Chapters 3 and 4) provide support for the idea that gamma synchronization provides a means for grouping elements into wholes that reflect objects in a scene. The utility of a synchronization-based algorithm for (natural) image segmentation has also been demonstrated previously (Lowet et al., 2015; Yogendra, Chamika, Fan, Shim, & Roy, 2017).

While previous findings along with those presented in this thesis provide converging evidence for a role of local gamma in visual scene analysis, some studies have failed to detect gamma oscillations in response to moving (Kayser, Salazar, & König, 2003) and even static (Dora Hermes, Miller, Wandell, & Winawer, 2015; Ray & Maunsell, 2015) natural images. This absence of gamma oscillations in response to static natural images is surprising and suggests that gamma oscillations may be sufficient but not necessary for visual processing. This conclusion, however, may be premature. A failure to detect gamma oscillations does not imply their absence. Indeed, failure to detect gamma can be due to inadequate spatial resolution of electrophysiological recording methods. Images with low degree of structure (i.e., with a high degree of heterogeneity, randomness and many small elements) are reflected by unstructured patterns of gamma oscillations on the cortical surface with variations in frequencies and phases that are too closely spaced to be detected with

typical electrodes (N. M. Brunet & Fries, 2019). Electrophysiological recordings with insufficient spatial resolution may capture several neuronal pools whose gamma rhythms may cancel each other out. Furthermore, signals from asynchronous neural oscillations may mask signals from synchronous oscillations. Insufficient data and the effect of noise for detecting low gamma power in response to images with low degree of structure could be another factor preventing the detection of gamma oscillations. Interestingly, even if the absence of gamma *oscillations* in response to natural images turns out to be a credible observation, this does not preclude that neuronal synchrony may be necessary for visual processing. Hermes et al. (2015) reported the presence of non-oscillatory broad-band signals (around 80-200 Hz) during the processing of natural images. Given that even non-oscillatory signals can become synchronized (Thivierge, 2008), predictions based on the synchronization (of non-oscillatory signals) among neural groups may still hold true for figure-ground segregation in natural images.

The present thesis provides support for a functional role of gamma oscillations and their synchronization. The absence of gamma oscillations in some conditions is a weak argument to make broad claims about its irrelevance. Likewise, observations of variations in gamma frequency or transmission delays are a weak argument against the functional contributions of gamma oscillations in the absence of a theoretical framework specifying factors that regulate synchronization. A step forward in assessing a potential role of gamma in perception is through the development of biologically constrained theoretical/computational models that formalize a putative perceptual role of gamma and generate testable predictions. Our work follows this approach and provides quantitative support for a role of gamma oscillations and synchronization in figure-ground segregation.

5-5. Reflections on the Modeling Approach Presented in this Thesis

We will not reiterate the limitations in terms of modelling choices and/or experimental setup that are already discussed in Chapters 2-4. Instead, the general modelling approach followed in this thesis will be evaluated. Throughout the thesis, a neural mass model has been utilized that reduces the dynamics of neural communities to the interaction between simple phase oscillators. This may be regarded as too abstract for a model to yield plausible mechanistic accounts of neural and behavioural phenomena. This concern shall be addressed in the following sections in the light of a deeper examination of scientific models in general.

5-5-1. Ontology, Epistemology and Semantics of Scientific Models

Models are highly relevant in many scientific contexts. However, the exact role models play within science is highly dependent on the context and the type of model employed. Analogical models, phenomenological models, theoretical models, mathematical models, computational models, explanatory models, idealized models, scale models, animal models, and didactic models are but some of the different types of models that can be identified in the literature (Roman & Hartmann, 2020). The diversity of models renders it difficult to provide an overarching definition of what a model is, and of its purpose. Instead, it can be elucidating to consider models from the perspective of their ontology, their epistemology and their semantics.

The ontological perspective on models focuses on the question what kind of objects scientists are dealing with when they work with models. It is important to realize that a model does not need to be a theoretical or mathematical entity. The class of models contains a heterogeneous collection of different objects that belong to different ontological kinds. Some models are physical objects such as animal models used in the life sciences or wooden scale models used in aeronautical engineering. Other models are fictional or abstract models such as imaginary atoms, populations, or economies. Nevertheless, in the natural sciences, most models are indeed equations and other forms of stylized descriptions of a target system.

Epistemology poses the question what can be learned from models. Models serve several epistemological functions as they allow scientists to learn something about the models themselves as well as to learn something about their target systems; aspects of the world that are of scientific interest. Both the construction of a model and its manipulation afford opportunities to learn about the model (Morgan, 1999) and once scientists have knowledge about the model, they can transfer this knowledge to the target system through the derivation and validation of testable hypotheses.

Finally, semantics poses the question which target systems are represented by models, and in which manner. Before elaborating on this motion, it is useful to note that models do not always represent a target system and may be an object of study in their own right. In particular, when models are highly abstract and lend themselves to the investigation of many diverse phenomena, scientists may be interested in the model per se rather than any specific target system they may represent. However, more frequently, models are used as stand-ins for a specific target system, which allows scientists to form hypotheses about the target; i.e., to convert truths found in the model into claims about the target system. According to Hughes (Hughes, 1997),

this involves three steps. First, elements of the target system are *denoted* by elements of the model. The precise conditions that need to be met for a model to denote (or represent) a target are still a matter of debate among philosophers of science (Roman & Hartmann, 2020) and depend on the type and intended use of a model. *Phenomenological (descriptive) models*, for instance, only represent observable properties of their target systems and refrain from postulating underlying mechanisms (Bokulich, 2009). A Gabor function may, for instance, be used as a phenomenological model of the receptive field of a neuron in V1 in that it captures the neuron's activation profile in response to different stimuli. *Mechanistic (explanatory) models*, on the other hand, represent both the components and the causal relations between these components that together constitute the mechanism underlying a target system (Kaplan, 2011). A model of the receptive field of a neuron in V1 would thus need to specify the components (such as retinal receptors, thalamic neurons, connection profiles etc.) and their (causally relevant) interactions in order to be considered mechanistic. Second, models exhibit internal properties and dynamics that allow researchers to *demonstrate* theoretical conclusions. This step takes place entirely within models and is thus removed from the target system. Finally, the results of these demonstrations are *interpreted* in terms of the target. The last step is necessary because demonstrations establish results only about the model itself, and only in interpreting these results can the model user draw inferences about the target, which can be used as hypotheses for experimental research.

5-5-2. Mechanisms and Idealizations

The central endeavour of science is to explain and understand natural phenomena. Though explanation and understanding are closely related, they are nevertheless distinct cognitive functions and this translates directly into how they affect scientific modelling. Models are considered to be explanatory of a target phenomenon if they meet the mechanism-model mapping (3M) criterion; i.e., if there is a mapping between elements in the model and elements in the mechanism that produces the target phenomenon (Kaplan, 2011). Explanatory models are thus mechanistic models. This implies that a) the variables in an explanatory model correspond to identifiable components and organizational features of the mechanism that produces, maintains or underlies the phenomenon and b) dependencies posited among variables in the model correspond to causal relations among the components of the target mechanism. Inclusion of model elements that take additional mechanism components into account as well as faithful representations of causal relations among mechanism components are generally considered to yield better

explanations of the target phenomenon (Boone & Piccinini, 2016; Kaplan, 2011). However, this does not necessarily improve understanding. In fact, due to humans' limited cognitive capacity, understanding may be hampered by excessive mechanistic fidelity and detail (Elgin, 2017). Indeed, understanding benefits from idealizations, such as deliberate distortions and omissions, and from abstractions (Humphreys, 1995; Strevens, 2004, 2008; Weisberg, 2007b).

Philosophers of science generally distinguish two major types of idealization, distortive idealization and minimalist idealization. Distortive idealizations involve simplifications that introduce deliberate distortions of the target such as point masses moving on frictionless planes or perfectly rational economic agents (Roman & Hartmann, 2020). Interestingly, distortive idealization is often not justified in terms of facilitating understanding and accommodating the limited capacity of our mental apparatus. Instead, distortive idealization may be justifiable in terms of computational tractability; i.e., the ability to analyze/simulate these models on existing hardware. Therefore, it is often argued that with advances in computational power and mathematical techniques, models should be de-idealized (McMullin, 1985). It is a matter of debate, however, whether this is possible without dismantling the models altogether (Batterman, 2002, 2010; Rice, 2015, 2019).

Minimalist idealization involves limiting models only to core causal factors; i.e., only those factors that make a difference in the occurrence of a target phenomenon (Strevens, 2003). In contrast to distortive idealization, minimalist idealization involves no commitment to de-idealization. The focus of the minimalist idealization approach on core causal factors roots its justification deeply in considerations of our restricted understanding due to limited cognitive capacity. Note that idealized models may still be considered mechanistic as long as they abide by the 3M criterion to the extent that there is a mapping between *at least one* element in the model and *at least one* element of the mechanism that produces the target phenomenon (Kaplan, 2011). Indeed, a common view is that abstracting away from irrelevant details may be as important to mechanistic explanation as including relevant details (Boone & Piccinini, 2016; Piccinini & Craver, 2011). Idealization thus serves an important role in science and the resulting models can arguably still be considered mechanistic. This does not mean that the practice of developing models that exhibit a high degree of mechanistic fidelity and detail is not important. Indeed, it is probably best practice to construct multiple models for any particular target phenomenon that exhibit varying degrees of mechanistic fidelity and detail. This allows scientists to seek an appropriate trade-off between explanation and understanding (Levins, 1966; Odenbaugh, 2003; Weisberg, 2007a, 2015).

5-5-3. Models in Computational Neuroscience

What holds true for scientific models in general, also applies to models in computational neuroscience. However, models in neuroscience, and biology in general, differ from models in disciplines such as physics and chemistry. In contrast to physics and chemistry, biology often deals with target systems that perform functions (Piccinini & Shagrir, 2014). In case of the brain, this function is arguably to perform information processing that allows animals (including humans) to interact with a dynamic environment in a meaningful way (i.e., such that the animal may survive and reproduce). This abstract function is typically decomposed into subordinate functions such as visual object recognition or the coordination of grasping movements that are performed by individual neural structures and processes that serve as targets for computational neuroscientists. This implies that the target systems studied by neuroscientists exhibit both, what may be termed, (*bio)physical* and *functional* phenomena and both need to be explained and understood. This requires computational neuroscientists to take a somewhat different perspective in constructing their models than, for example, a theoretical physicist. In addition to specify the physical, chemical and biological elements of neural structures and their causal interactions, computational neuroscientists also need to think about their computational and representational properties and functional purpose (Marr, 1982). When considering the neuronal membrane, for instance, computational neuroscientists need to specify physical and chemical properties such as voltage, conductance, capacitance, the presence of voltage- and/or chemically-gated ion channels, their dynamics and interactions in order to provide a mechanistic model of action potentials. In this aspect, the work of a computational neuroscientist is similar to (and may draw from) that of a theoretical physicist. However, computational neuroscientists also need to understand how information about external stimuli or intrinsic states is encoded and transmitted by action potentials and how this is functionally relevant. By contrast, a theoretical physicist who is interested, for example, in vortex shedding in fluids does not need to be concerned with any notions of representation or computations performed by the fluid. Within neuroscience, only the combination of the (bio)physical and functional perspective provides a complete account of neural target systems. An interesting advantage is that this enables scientists to draw testable *functional* conclusions from *biophysical* models and vice versa, thus raising the informative content of their models and hence their testability and falsifiability (Popper, 2014).

5-5-4. Models in the Present Thesis

It is now possible to evaluate the models used in the present thesis as well as the modelling approaches that were employed. All models in the present thesis utilized the Kuramoto equation, an abstract coupled oscillator model that can be used to study many kinds of synchronization phenomena (see Acebr et al., (2005) for a review). The ontology of the model is thus shared between chapters. However, Chapter 2 differs from Chapters 3 and 4 in terms of semantics and epistemology. Specifically, in the second chapter, the model should be considered to be inspired by properties of neural systems in general rather than to represent any specific neural target system. Hence, in Chapter 2, the model was the object of study in its own right. In this case, the question whether the model is appropriate, in the sense of whether the model can adequately represent a particular target system, is no longer pressing. What is relevant is whether the model can, in principle, represent some target systems. In the specific case of Chapter 2, we investigated the effects of adaptive coupling strength and of adaptive transmission delays on the collective behaviour of weakly coupled oscillators. This can be relevant to any synchronization phenomenon wherein coupling strength and transmission delays are adaptive. This is the case for neural oscillations and synchrony (Pajevic et al., 2014). The results in the second chapter were interpreted within this context. However, the conclusions that can be drawn from the second chapter are conclusions about the model and not conclusions about the brain. They only hint at new possibilities (such as a dissociation between structure and function) and future avenues for brain research, and any parallels we have drawn with specific brain processes in that chapter are to be considered with caution.

In contrast to the model in Chapter 2, the model presented in Chapter 3 and expanded in Chapter 4 does represent a specific target system; namely a network of oscillating neuronal populations in early visual cortex. However, individual neuronal populations were not modelled as circuits of excitatory and inhibitory neurons but instead by simple phase oscillators. Likewise, coupling between populations was not modelled in the form of synaptic interactions between neurons but instead by a simple (sinusoidal) coupling function. This raises the question in what sense the model represents neural processes in a sufficiently mechanistic manner. To answer this question, it is important to keep in mind the purpose of the model. The model was intended to represent *networks* of oscillating neuronal populations in early visual cortex. Therefore, it is possible to abstract away from the detailed neuronal and synaptic processes that give rise to interactions among individual populations that underlie the oscillations (Bartos, Vida, & Jonas, 2007; Hansel & Mato, 2003; X. J.

Wang & Buzsáki, 1996; Miles A. Whittington, Traub, & Jefferys, 1995; Wilson & Cowan, 1972), and focus instead on interactions among the oscillations at the population level. Whether the Kuramoto model is an appropriate choice for such an abstraction depends on whether it captures the synchronization behaviour of synaptically coupled neuronal circuits. Prior research has shown that this is indeed the case. It has, for instance, been shown that networks of quadratic integrate-and-fire, Izhikevich and Hodgkin-Huxley neurons as well as Winfree-type ensembles of oscillators exhibited synchronization behaviour comparable to that in networks of Kuramoto oscillators (Bhowmik & Shanahan, 2012; Lowet et al., 2015; Politi & Rosenblum, 2015). The chosen model can thus generally represent neural oscillator networks. To specifically represent neural oscillator networks in V1, elements of the model need to denote elements of this particular target system. These elements are the retinotopic organization of neuronal populations in V1, the distance-dependence of horizontal coupling and the relation between the contrast in an oscillator's population receptive field and their intrinsic frequencies in the gamma range. In Chapter 4, a learning algorithm was added to the model. The denotationally relevant elements of this are the eligibility of individual weights to change based on the co-occurrence of pre- and post-synaptic activity, and reward in response to synchronization behaviour. All of these are based on extensive pre-existing literature (Chubykin, Roach, Bear, & Shuler, 2013; Diekelmann & Born, 2010; Gerstner, Lehmann, Liakoni, Corneil, & Brea, 2018; He et al., 2015; Izhikevich, Jay, Drive, & Diego, 2007; Rasch & Born, 2013) as well as electrophysiological data (Lowet et al., 2017) in order to maximize their biological fidelity. The model thus specifies relevant components in early visual cortex and their interactions that are considered to be part of the mechanism that gives rise to neural synchrony in the gamma range. It further provides a mapping between elements in the model and elements in this mechanism. As such, the model may be considered mechanistic according to the 3M criterion. However, only the core causal factors were included in this specification, rendering the model a minimalist idealization.

Chapters 3 and 4 then proceeded to demonstrate how synchronization behaviour in the model depends on stimulus conditions and training-induced changes in coupling. This was interpreted to reflect synchronization behaviour among neuronal populations in the corresponding patch of V1. Importantly, from an epistemological perspective, the work conducted in these chapters was not intended to provide novel insights regarding the synchronization behaviour of neuronal populations in V1. This would have been the case, if the work was primarily intended to study *biophysical* phenomena, which could have been investigated, for example, with in vivo and in vitro recording methods (Jehee, Ling, Swisher, van Bergen, & Tong, 2012; Lowet et

al., 2017; A. Schoups et al., 2001; Shibata, Watanabe, Sasaki, & Kawato, 2011; Z. Wang et al., 2021; Yan et al., 2014), perhaps combined with optogenetic manipulations (Kirchberger et al., 2021). Instead, we intended to study *functional* phenomena and, specifically, to test the hypothesis that synchronization behaviour in our minimalist idealization of the target system could be predictive for perception. In order to do so, it is important to consider both the modelling and experimentation conducted within these two chapters and to view this approach from a falsification perspective. In essence, the work in Chapters 3 and 4 rests on two premises. First, *synchronization in the employed oscillator model reflects synchronization in V1*. Second, *synchronization in V1 has observable (i.e., testable) perceptual consequences*. This premise is the core hypothesis of Chapters 3 and 4. These premises together warrant the conclusion that *synchronization in the employed oscillator model has observable (i.e., testable) perceptual consequences* and rejection of the conclusion (i.e., failure to empirically verify model predictions) means that either the first, second or both premises are false. The first premise is supported not only by the care taken to ensure the model is an appropriate representation of the relevant components and processes in V1 but also by independent neurophysiological data (Lowet et al., 2017). Rejection of the conclusion must then entail rejection specifically of the second premise and hence falsification of the core hypothesis of the two chapters. Experiments in both chapters failed to falsify this hypothesis, thus rendering it tentatively acceptable. Therefore, we suggest that it is reasonable to conclude that synchronization mechanisms in V1 contribute to human perceptual performance.

The preceding overview of the scientific practice of modelling as well as analysis of the work presented in the core chapters of this thesis warrant the conclusion that, given the respective objectives of the three chapters and their accompanying requirements regarding modelling approaches, the employed models can indeed be considered adequate for their intended purposes.

5-6. Future Directions

The work presented in the present thesis may provide the impetus for several further research lines. First, the present focus on *function* may be supplemented by work focusing on *biophysics* in order to arrive at a more holistic understanding of gamma oscillations and synchrony in early visual cortex. This would involve both empirical and modelling work. The former might entail a replication of the studies presented in Chapters 3 and 4 using electrophysiological recordings in monkeys. The latter might entail translating the current model to a spiking neuron implementation

wherein local (columnar) oscillations are driven by external inputs in conjunction with recurrent interactions among intracolumnar excitatory and inhibitory neuronal populations, wherein synchrony may be the result of lateral interactions between columns. A combination of monkey electrophysiological and behavioural results with detailed biophysical modelling would permit a thorough validation of the proposed synchrony-based information integration mechanism at the biological and behavioural level. Introducing a biologically realistic laminar profile to the columnar model would additionally allow for studying the spatio-temporal profiles of feedforward, lateral and feedback (e.g., attention) signals and how they interact during visual scene analysis (Brosch, Tschechne, & Neumann, 2016).

The interaction between feedforward, lateral and feedback signals is also relevant from an extended functional perspective. While the present thesis provides evidence that local gamma may be relevant for figure-ground segregation, it is likely that it is merely one component of a larger mechanism that involves several cortical and subcortical structures. Another avenue for further research would therefore be the development of a large-scale model that leverages oscillations and synchrony to perform scene analysis in natural stimuli. Such a model should be able to segregate image regions corresponding to different objects and integrate those regions corresponding to the same object. This is a challenging task that requires a hierarchical neural architecture exhibiting feedforward, lateral and feedback connections. Notably, such a model should strive to unify the local synchronization mechanisms detailed in the present thesis with border reconstruction and filling-in mechanisms proposed by other groups (Poort, Self, van Vugt, Malkki, & Roelfsema, 2016; Roelfsema, Lamme, Spekreijse, & Bosch, 2002; Self, Kooijmans, Supèr, Lamme, & Roelfsema, 2012). An important validation for such a model, besides realistic perceptual performance, would be its ability to account for neurophysiological observations demonstrating the necessary contributions of feedback for figure-ground segregation, following an initial feedforward sweep (Kirchberger et al., 2019; Lamme, Supèr, & Spekreijse, 1998; Supèr & Lamme, 2007).

References

Aberg, K. C., Tartaglia, E. M., & Herzog, M. H. (2009). Perceptual learning with Chevrons requires a minimal number of trials, transfers to untrained directions, but does not require sleep. *Vision Research*, 49 (16), 2087–2094.

Acebr, J. A., Gradenigo, V., Matematica, D., Acebrón, J. A., Bonilla, L. L., Vicente, C. J. P., … Spigler, R. (2005). The Kuramoto model: A simple paradigm for synchronization phenomena. *Reviews of Modern Physics*, 77 (January), 137–185.

Ahissar, Merav, & Hochstein, S. (1996). Learning Pop-out Detection: Specificities to Stimulus Characteristics. *Vision Research*, 36 (21), 3487–3500.

Ahissar, Merav, Laiwand, R., Kozminsky, G., & Hochstein, S. (1998). Learning pop-out detection: building representations for conflicting target-distractor relationships. *Vision Research*, 38 (20), 3095–3107.

Ahissar, M., & Hochstein, S. (1993). Attentional control of early perceptual learning. *Proceedings of the National Academy of Sciences of the United States of America*, 90 (12), 5718–5722.

Balasubramanian, M., & Schwartz, E. L. (2002). The isomap algorithm and topological stability. *Science*, 295 (5552), 7.

Baldi, P., & Meir, R. (1990). Computing with Arrays of Coupled Oscillators: An Application to Preattentive Texture Discrimination. *Neural Computation*, 2 (4), 458–471.

Bartos, M., Vida, I., & Jonas, P. (2007). Synaptic mechanisms of synchronized gamma oscillations in inhibitory interneuron networks. *Nature Reviews Neuroscience 2007 8:1*, 8 (1), 45–56.

Batterman, R. W. (2002). *The Devil in the Details: Asymptotic Reasoning in Explanation, Reduction and Emergence*. Oxford University Press.

Batterman, R. W. (2010). Emergence, Singularities, and Symmetry Breaking. *Foundations of Physics*, 41 (6), 1031–1050.

Bertrand, O., & Tallon-Baudry, C. (2000). Oscillatory gamma activity in humans: a possible role for object representation. *International Journal of Psychophysiology*, 38 (3), 211–223.

Bhowmik, D., & Shanahan, M. (2012). How well do oscillator models capture the behaviour of biological neurons? *Proceedings of the International Joint Conference on Neural Networks*.

Bokulich, A. (2009). How scientific models can explain. *Synthese 2009 180:1*, 180 (1), 33–45.

Boone, W., & Piccinini, G. (2016). Mechanistic Abstraction. *Philosophy of Science*, 83 (5), 686–697.

Brosch, T., Tschechne, S., & Neumann, H. (2016). Visual Processing in Cortical Architecture from Neuroscience to Neuromorphic Computing. *Lecture Notes in Computer Science (Including Subseries Lecture Notes in Artificial Intelligence and Lecture Notes in Bioinformatics)*, 10087 LNCS, 86–100.

Brunet, N., Bosman, C. A., Roberts, M., Oostenveld, R., Womelsdorf, T., de Weerd, P., & Fries, P. (2015). Visual Cortical Gamma-Band Activity During Free Viewing of Natural Images. *Cerebral Cortex*, 25 (4), 918–926.

Brunet, N. M., & Fries, P. (2019). Human visual cortical gamma reflects natural image structure. *NeuroImage*, 200, 635–643.

Buia, C., & Tiesinga, P. (2006). Attentional modulation of firing rate and synchrony in a model cortical network. *Journal of Computational Neuroscience*, 20 (3), 247–264.

Buzśaki, G., & Wang, X. J. (2012). Mechanisms of Gamma Oscillations. *Annual Review of Neuroscience*, 35, 203–225.

Chang, K.-J., Redmond, S. A., & Chan, J. R. (2016). Remodeling myelination: implications for mechanisms of neural plasticity. *Nature Neuroscience*, 19 (2), 190–197.

Chubykin, A. A., Roach, E. B., Bear, M. F., & Shuler, M. G. H. (2013). A Cholinergic Mechanism for Reward Timing within Primary Visual Cortex. *Neuron*, 77 (4), 723–735.

Crist, R. E., Kapadia, M. K., Westheimer, G., & Gilbert, C. D. (1997). Perceptual learning of spatial localization: Specificity for orientation, position, and context. *Journal of Neurophysiology*, 78 (6), 2889–2894.

Diekelmann, S., & Born, J. (2010). The memory function of sleep. *Nature Reviews Neuroscience 2010 11:2*, 11 (2), 114–126.

Dubey, A., & Ray, S. (2020). Comparison of tuning properties of gamma and high-gamma power in local field potential (LFP) versus electrocorticogram (ECoG) in visual cortex. *Scientific Reports 2020 10:1*, 10 (1), 1–15.

Dutta, D. J., Ho Woo, D., Lee, P. R., Pajevic, S., Bukalo, O., Huffman, W. C., … Wake, H. (2018). Regulation of myelin structure and conduction velocity by perinodal astrocytes. *PNAS*, 115 (46), 11832–11837.

Elgin, C. Z. (2017). *True Enough*. MIT Press.

Ermentrout, B., & Ko, T. W. (2009). Delays and weakly coupled neuronal oscillators. *Philosophical Transactions of the Royal Society A: Mathematical, Physical and Engineering Sciences*, 367 (1891), 1097–1115.

Ermentrout, B., Park, Y., & Wilson, D. (2019). Recent advances in coupled oscillator theory. *Philosophical Transactions of the Royal Society A*, 377 (2160).

Feng, W., Havenith, M. N., Wang, P., Singer, W., & Nikolić, D. (2010). Frequencies of gamma/beta oscillations are stably tuned to stimulus properties. *NeuroReport*, 21 (10), 680–684.

Fields, R. D. (2015). A new mechanism of nervous system plasticity: activity-dependent myelination. *Nature Reviews Neuroscience*, 16 (12), 756–767.

Fields, R. D., & Bukalo, O. (2020). Myelin makes memories. *Nature Neuroscience*, 23 (4), 469–470.

Fiorentini, A., & Berardi, N. (1980). Perceptual learning specific for orientation and spatial frequency. *Nature 1980 287:5777*, 287 (5777), 43–44.

Fries, P. (2005). A mechanism for cognitive dynamics: neuronal communication through neuronal coherence. *Trends in Cognitive Sciences*, 9 (10), 474–480.

Fries, P., Nikolić, D., & Singer, W. (2007). The gamma cycle. *Trends in Neurosciences*, 30 (7), 309–316.

Gerstner, W., Lehmann, M., Liakoni, V., Corneil, D., & Brea, J. (2018). Eligibility Traces and Plasticity on Behavioral Time Scales: Experimental Support of NeoHebbian Three-Factor Learning Rules. *Frontiers in Neural Circuits*, 12, 53.

Giedd, J. N., Vaituzis, A. C., Hamburger, S. D., Lange, N., Rajapakse, J. C., Kaysen, D., … Rapoport, J. L. (1996). Quantitative MRI of the Temporal Lobe, Amygdala, and Hippocampus in Normal Human Development: Ages 4-18 Years. *THE JOURNAL OF COMPARATIVE NEUROLOGY*, 366, 223–230.

Gieselmann, M. A., & Thiele, A. (2008). Comparison of spatial integration and surround suppression characteristics in spiking activity and the local field potential in macaque V1. *European Journal of Neuroscience*, 28 (3), 447–459.

Gilbert, C. D., & Wiesel, T. N. (1983). Clustered intrinsic connections in cat visual cortex. *Journal of Neuroscience*, 3 (5), 1116–1133.

Gray, C. M., & Goodell, B. (2011). Spatiotemporal Dynamics of Synchronous Activity across Multiple Areas of the Visual Cortex in the Alert Monkey. In *The Dynamic Brain: An Exploration of Neuronal Variability and Its Functional Significance*.

Gray, C. M., König, P., Engel, A. K., & Singer, W. (1989). Oscillatory responses in cat visual cortex exhibit inter-columnar synchronization which reflects global stimulus properties. *Nature 1989 338:6213*, 338 (6213), 334–337.

Hadjipapas, A., Lowet, E., Roberts, M. J., Peter, A., & de Weerd, P. (2015). Parametric variation of gamma frequency and power with luminance contrast: A comparative study of human MEG and monkey LFP and spike responses. *NeuroImage*, 112, 327–340.

Hall, S. D., Holliday, I. E., Hillebrand, A., Singh, K. D., Furlong, P. L., Hadjipapas, A., & Barnes, G. R. (2005). The missing link: Analogous human and primate cortical gamma oscillations. *NeuroImage*, 26 (1), 13–17.

Hansel, D., & Mato, G. (2003). Asynchronous States and the Emergence of Synchrony in Large Networks of Interacting Excitatory and Inhibitory Neurons. *Neural Computation*, 15 (1), 1–56.

He, K., Huertas, M., Hong, S. Z., Tie, X. X., Hell, J. W., Shouval, H., & Kirkwood, A. (2015). Distinct Eligibility Traces for LTP and LTD in Cortical Synapses. *Neuron*, 88 (3), 528–538.

Henrie, J. A., & Shapley, R. (2005). LFP power spectra in V1 cortex: The graded effect of stimulus contrast. *Journal of Neurophysiology*, 94 (1), 479–490.

Hermes, D., Miller, K. J., Wandell, B. A., & Winawer, J. (2015). Stimulus dependence of gamma oscillations in human visual cortex. *Cerebral Cortex*, 25 (9), 2951–2959.

Hermes, Dora, Miller, K. J., Wandell, B. A., & Winawer, J. (2015). Gamma oscillations in visual cortex: The stimulus matters. *Trends in Cognitive Sciences*, 19 (2), 57.

Hoppensteadt, F. C., & Izhikevich, E. M. (1999). Oscillatory Neurocomputers with Dynamic Connectivity. *Physical Review Letters*, 82 (14), 2983.

Hughes, R. I. G. (1997). Models and Representation. *Philosophy of Science*, 64, S325–S336.

Humphreys, P. (1995). Abstract and Concrete. *Philosophy and Phenomenological Research*, 55 (1), 157–161.

Izhikevich, E. M., & Appl Math, S. J. (2006). Weakly Connected Quasi-periodic Oscillators, FM Interactions, and Multiplexing in the Brain. *Http://Dx.Doi.Org/10.1137/S0036139997330623*, 59 (6), 2193–2223.

Izhikevich, E. M., Jay, J., Drive, H., & Diego, S. (2007). Solving the Distal Reward Problem through Linkage of STDP and Dopamine Signaling. *Cerebral Cortex*, 17, 2443–2452.

Jehee, J. F. M., Ling, S., Swisher, J. D., van Bergen, R. S., & Tong, F. (2012). Perceptual Learning Selectively Refines Orientation Representations in Early Visual Cortex. *Journal of Neuroscience*, 32 (47), 16747–16753.

Jeter, P. E., Dosher, B. A., Petrov, A., & Lu, Z. L. (2009). Task precision at transfer determines specificity of perceptual learning. *Journal of Vision*, 9 (3), 1–1.

Jia, X., Xing, D., & Kohn, A. (2013). No Consistent Relationship between Gamma Power and Peak Frequency in Macaque Primary Visual Cortex. *Journal of Neuroscience*, 33 (1), 17–25.

Kaplan, D. M. (2011). Explanation and description in computational neuroscience. *Synthese 2011 183:3*, 183 (3), 339–373.

Karni, A., & Sagi, D. (1991). Where practice makes perfect in texture discrimination: evidence for primary visual cortex plasticity. *Proceedings of the National Academy of Sciences*, 88 (11), 4966–4970.

Kayser, C., Salazar, R. F., & König, P. (2003). Responses to natural scenes in cat VI. *Journal of Neurophysiology*, 90 (3), 1910–1920.

Kirchberger, L., Mukherjee, S., Schnabel, U. H., van Beest, E., Barsegyan, A., Levelt, C. N., … Roelfsema, P. (2019). The Essential Role of Feedback Processing for Figure-Ground Perception in Mice. *SSRN Electronic Journal*.

Kirchberger, L., Mukherjee, S., Schnabel, U. H., van Beest, E. H., Barsegyan, A., Levelt, C. N., … Roelfsema, P. R. (2021). The essential role of recurrent processing for figure-ground perception in mice. *Science Advances*, 7 (27).

Kirst, C., Timme, M., & Battaglia, D. (2016). Dynamic information routing in complex networks. *Nature Communications 2016 7:1*, 7 (1), 1–9.

Lamme, V. A. F., Supèr, H., & Spekreijse, H. (1998). Feedforward, horizontal, and feedback processing in the visual cortex. *Current Opinion in Neurobiology*, 8 (4), 529–535.

Levins, R. (1966). THE STRATEGY OF MODEL BUILDING IN POPULATION BIOLOGY. *American Scientist*, 54 (9), 421–431.

Logothetis, N. K., Pauls, J., Augath, M., Trinath, T., & Oeltermann, A. (2001). Neurophysiological investigation of the basis of the fMRI signal. *Nature*, 412 (6843), 150–157.

Lowet, E., Roberts, M., Hadjipapas, A., Peter, A., van der Eerden, J., & de Weerd, P. (2015). Input-Dependent Frequency Modulation of Cortical Gamma Oscillations Shapes Spatial Synchronization and Enables Phase Coding. *PLoS Computational Biology*.

Lowet, E., Roberts, M. J., Peter, A., Gips, B., & de Weerd, P. (2017). A quantitative theory of gamma synchronization in macaque V1. *ELife*, 6.

Marr, D. (1982). The Philosophy and the Approach. In Y. Steve (Ed.), *Visual Perception: Essential Readings* (pp. 104–123). PSYCHOLOGY PRESS.

Martin, D., Fowlkes, C., Tal, D., & Malik, J. (2001). A database of human segmented natural images and its application to evaluating segmentation algorithms and measuring ecological statistics. *Proceedings of the IEEE International Conference on Computer Vision*, 2, 416–423.

McKenzie, I. A., Ohayon, D., Li, H., de Faria, J. P., Emery, B., Tohyama, K., & Richardson, W. D. (2014). Motor skill learning requires active central myelination. *Science*, 346 (6207), 318–322.

McMullin, E. (1985). Galilean idealization. *Studies in History and Philosophy of Science Part A*, 16 (3), 247–273.

Milner, B., Squire, L. R., & Kandel, E. R. (1998). Cognitive Neuroscience Review and the Study of Memory. *Neuron*, 20, 445–468.

Morgan, M. S. (1999). Learning from models. In *Models as Mediators* (Vol. 52, pp. 347–388). Cambridge University Press.

Nickel, M., & Gu, C. (2018). Regulation of Central Nervous System Myelination in Higher Brain Functions. *Neural Plasticity*, 2018, 1–12.

Nikolić, D. (2006). Non-parametric detection of temporal order across pairwise measurements of time delays. *Journal of Computational Neuroscience*, 22 (1), 5–19.

Niyogi, R. K., & English, L. Q. (2009). Learning-rate-dependent clustering and self-development in a network of coupled phase oscillators. *Physical Review E - Statistical, Nonlinear, and Soft Matter Physics*, 80 (6), 1–7.

Nowotny, T., Zhigulin, V. P., Selverston, A. I., Abarbanel, H. D. I., & Rabinovich, M. I. (2003). Enhancement of Synchronization in a Hybrid Neural Circuit by Spike-Timing Dependent Plasticity. *The Journal of Neuroscience*, 23 (30), 9776–9785.

Odenbaugh, J. (2003). Complex systems, trade-offs and mathematical modeling: a response to Sober and Orzack. *Philosophy of Science*, 70 (5), 1496–1507.

Pajevic, S., Basser, P. J., & Fields, A. R. D. (2014). Role of Myelin Plasticity in Oscillations and Synchrony of Neuronal Activity. *Neuroscience*, 276, 135–147.

Piccinini, G., & Craver, C. (2011). Integrating psychology and neuroscience: functional analyses as mechanism sketches. *Synthese*, 183 (3), 283–311.

Piccinini, G., & Shagrir, O. (2014). Foundations of computational neuroscience. *Current Opinion in Neurobiology*, 25, 25–30.

Pikovsky, A., Rosenblum, M., Self, J. K.-, & 2001, undefined. (2003). A universal concept in nonlinear sciences. *Researchgate.Net*.

Polimeni, J. R., Hinds, O. P., Balasubramanian, M., Kouwe, A. J. W. van der, Wald, L. L., Dale, A. M., … Schwartz, E. L. (2005). Two-dimensional mathematical structure of the human visuotopic map complex in V1, V2, and V3 measured via fMRI at 3 and 7 Tesla. *Journal of Vision*, 5 (8), 898–898.

Politi, A., & Rosenblum, M. (2015). Equivalence of phase-oscillator and integrate-and-fire models. *Physical Review E - Statistical, Nonlinear, and Soft Matter Physics*, 91 (4), 042916.

Poort, J., Self, M. W., van Vugt, B., Malkki, H., & Roelfsema, P. R. (2016). Texture Segregation Causes Early Figure Enhancement and Later Ground Suppression in Areas V1 and V4 of Visual Cortex. *Cerebral Cortex*, 26 (10), 3964–3976.

Popper, K. (2014). *Conjectures and Refutations: The Growth of Scientific Knowledge*. Routledge.

Purger, D., Gibson, E. M., & Monje, M. (2016). Myelin plasticity in the central nervous system. *Neuropharmacology*, 110, 563–573.

Rasch, B., & Born, J. (2013). About sleep's role in memory. *Physiological Reviews*, 93 (2), 681–766.

Ray, S., & Maunsell, J. H. R. (2015). Do gamma oscillations play a role in cerebral cortex? *Trends in Cognitive Sciences*, 19 (2), 78–85.

Ray, S., & Maunsell, J. H. R. (2010). Differences in Gamma Frequencies across Visual Cortex Restrict Their Possible Use in Computation | Elsevier Enhanced Reader. *Neuron*, 67, 885–896.

R. D. Fields. (2014). Myelin-More than Insulation. *SCIENCE*, 344 (6181), 264–266.

Rice, C. (2015). Moving Beyond Causes: Optimality Models and Scientific Explanation. *Noûs*, 49 (3), 589–615.

Rice, C. (2019). Models don't decompose that way: A holistic view of idealized models. *The British Journal for the Philosophy of Science*, 70 (1), 179–208.

Roberts, M. J., Lowet, E., Brunet, N. M., TerWal, M., Tiesinga, P., Fries, P., & de Weerd, P. (2013). Robust gamma coherence between macaque V1 and V2 by dynamic frequency matching. *Neuron*.

Roelfsema, P. R., Lamme, V. A. F., Spekreijse, H., & Bosch, H. (2002). Figure - Ground segregation in a recurrent network architecture. *Journal of Cognitive Neuroscience*, 14 (4), 525–537.

Roman, F., & Hartmann, S. (2020). Models in Science.

Sampaio-Baptista, C., Khrapitchev, A. A., Foxley, S., Schlagheck, T., Scholz, J., Jbabdi, S., … Johansen-Berg, H. (2013). Motor Skill Learning Induces Changes in White Matter Microstructure and Myelination. *Journal of Neuroscience*, 33 (50), 19499–19503.

Scholz, J., Klein, M. C., Behrens, T. E. J. J., & Johansen-Berg, H. (2009). Training induces changes in white-matter architecture. *Nature Neuroscience*, 12 (11), 1370–1371.

Schoups, A. A., Vogels, R., & Orban, G. A. (1995). Human perceptual learning in identifying the oblique orientation: retinotopy, orientation specificity and monocularity. *The Journal of Physiology*, 483 (3), 797–810.

Schoups, A., Vogels, R., Qian, N., & Orban, G. (2001). Practising orientation identification improves orientation coding in V1 neurons. *Nature 2001 412:6846*, 412 (6846), 549–553.

Schwartz, E. L. (1980). Computational anatomy and functional architecture of striate cortex: A spatial mapping approach to perceptual coding. *Vision Research*, 20 (8), 645–669.

Self, M. W., Kooijmans, R. N., Supèr, H., Lamme, V. A., & Roelfsema, P. R. (2012). Different glutamate receptors convey feedforward and recurrent processing in macaque V1. *Proceedings of the National Academy of Sciences of the United States of America*, 109 (27), 11031–11036.

Seliger, P., Young, S. C., & Tsimring, L. S. (2002). Plasticity and learning in a network of coupled phase oscillators. *Physical Review E - Statistical, Nonlinear, and Soft Matter Physics*, 65 (4), 1–7.

Shapira, A., Sterkin, A., Fried, M., Yehezkel, O., Zalevsky, Z., & Polat, U. (2017). Increased gamma band activity for lateral interactions in humans. *PLoS ONE*, 12 (12), e0187520.

Shibata, K., Watanabe, T., Sasaki, Y., & Kawato, M. (2011). Perceptual learning incepted by decoded fMRI neurofeedback without stimulus presentation. *Science (New York, N.Y.)*, 334 (6061), 1413–1415.

Siri, B., Quoy, M., Delord, B., Cessac, B., & Berry, H. (2007). Effects of Hebbian learning on the dynamics and structure of random networks with inhibitory and excitatory neurons. *Journal of Physiology Paris*, 101 (1–3), 136–148.

Song, S., Miller, K. D., & Abbott, L. F. (2000). Competitive Hebbian learning through spike-timing-dependent synapticplasticity. *Nature Neuroscience*, 3 (9), 919–926.

Stettler, D. D., Das, A., Bennett, J., & Gilbert, C. D. (2002). Lateral connectivity and contextual interactions in macaque primary visual cortex. *Neuron*, 36 (4), 739–750.

Strevens, M. (2003). The Causal and Unification Accounts of Explanation unified—causally. *Noûs*.

Strevens, M. (2004). The Causal and Unification Approaches to Explanation Unified—Causally. *Noûs*, 38 (1), 154–176.

Strevens, M. (2008). Comments on Woodward, Making Things Happen. *Philosophy and Phenomenological Research*, 77 (1), 171–192.

Supèr, H., & Lamme, V. A. F. (2007). Altered figure-ground perception in monkeys with an extra-striate lesion. *Neuropsychologia*, 45 (14), 3329–3334.

Swadlow, H. A., & Waxman, S. G. (2012). Axonal conduction delays. *Scholarpedia*, 7 (6), 1451.

Swettenham, J. B., Muthukumaraswamy, S. D., & Singh, K. D. (2009). Spectral properties of induced and evoked gamma oscillations in human early visual cortex to moving and stationary stimuli. *Journal of Neurophysiology*, 102 (2), 1241–1253.

Thivierge, J.-P. (2008). Neural diversity creates a rich repertoire of brain activity. *Http://Www.Tandfonline.Com/Action/AuthorSubmission?JournalCode=kcib20&page=instructions*, 1 (2), 188–189.

Timms, L., & English, L. Q. (2014). Synchronization in phase-coupled Kuramoto oscillator networks with axonal delay and synaptic plasticity. *Physical Review E - Statistical, Nonlinear, and Soft Matter Physics*, 89 (3).

Traubab, R. D., Spruston, N., Soltesz, I., Konnerth, A., Whittington, M. A., & Jefferys, J. G. R. (1998). Gamma-frequency oscillations: a neuronal population phenomenon, regulated by synaptic and intrinsic cellular processes, and inducing synaptic plasticity. *Progress in Neurobiology*, 55 (6), 563–575.

Ts'o, D. Y., Gilbert, C. D., & Wiesel, T. N. (1986). Relationships between horizontal interactions and functional architecture in cat striate cortex as revealed by cross-correlation analysis. *Journal of Neuroscience*, 6 (4), 1160–1170.

Wang, R., Cong, L. J., & Yu, C. (2013). The classical TDT perceptual learning is mostly temporal learning. *Journal of Vision*, 13 (5), 9–9.

Wang, R., Zhang, J. Y., Klein, S. A., Levi, D. M., & Yu, C. (2012). Task relevancy and demand modulate double-training enabled transfer of perceptual learning. *Vision Research*, 61, 33–38.

Wang, X. J., & Buzsáki, G. (1996). Gamma Oscillation by Synaptic Inhibition in a Hippocampal Interneuronal Network Model. *Journal of Neuroscience*, 16 (20), 6402–6413.

Wang, Z., Tamaki, M., Frank, S. M., Shibata, K., Worden, M. S., Yamada, T., … Watanabe, T. (2021). Visual perceptual learning of a primitive feature in human V1/V2 as a result of unconscious processing, revealed by decoded functional MRI neurofeedback (DecNef). *Journal of Vision*, 21 (8), 1–15.

Weisberg, M. (2007a). Forty Years of 'The Strategy': Levins on Model Building and Idealization. *Biology and Philosophy*, 21 (5), 623–645.

Weisberg, M. (2007b). Three Kinds of Idealization. *The Journal of Philosophy*, 104 (12), 639–659.

Weisberg, M. (2015). Qualitative Theory and Chemical Explanation. *Philosophy of Science*, 71 (5), 1071–1081.

Whittington, M. A., Traub, R. D., Kopell, N., Ermentrout, B., & Buhl, E. H. (2000). Inhibition-based rhythms: experimental and mathematical observations on network dynamics. *International Journal of Psychophysiology*, 38 (3), 315–336.

Whittington, Miles A., Cunningham, M. O., LeBeau, F. E. N., Racca, C., & Traub, R. D. (2011). Multiple origins of the cortical gamma rhythm. *Developmental Neurobiology*, 71 (1), 92–106.

Whittington, Miles A., Traub, R. D., & Jefferys, J. G. R. (1995). Synchronized oscillations in interneuron networks driven by metabotropic glutamate receptor activation. *Nature 1995 373:6515*, 373 (6515), 612–615.

Wilson, H. R., & Cowan, J. D. (1972). Excitatory and Inhibitory Interactions in Localized Populations of Model Neurons. *Biophysical Journal*, 12 (1), 1–24.

Yan, Y., Rasch, M. J., Chen, M., Xiang, X., Huang, M., Wu, S., & Li, W. (2014). Perceptual training continuously refines neuronal population codes in primary visual cortex. *Nature Neuroscience 2014 17:10*, 17 (10), 1380–1387.

Yogendra, K., Chamika, L., Fan, D., Shim, Y., & Roy, K. (2017). Coupled Spin-Torque Nano-Oscillator-Based Computation. *ACM Journal on Emerging Technologies in Computing Systems (JETC)*, 13 (4).

Zhang, J. Y., Zhang, G. L., Xiao, L. Q., Klein, S. A., Levi, D. M., & Yu, C. (2010). Rule-Based Learning Explains Visual Perceptual Learning and Its Specificity and Transfer. *Journal of Neuroscience*, 30 (37), 12323–12328.

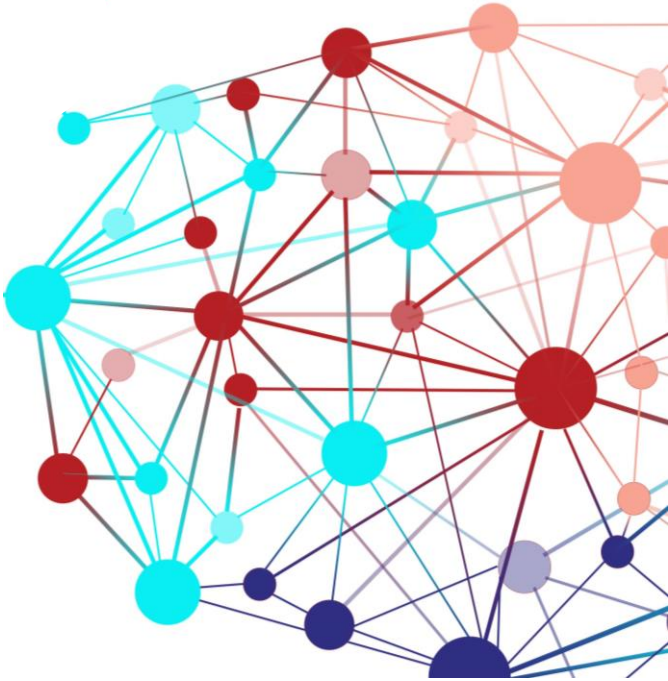

Impact Paragraph

Impacts of studies in the current thesis

Oscillations are a ubiquitous phenomenon in nature, society and technology. In nature, oscillations include predator-prey population cycles (Leconte, Masson, & Qi, 2022), sea surface temperature variations (Knudsen, Seidenkrantz, Jacobsen, & Kuijpers, 2011), and climate oscillations (Mann, Park, & Bradley, 1995). In addition, oscillations play a significant role in living organisms, specifically in human and animal organs. For example, heartbeats (Ryzhii & Ryzhii, 2014), insulin concentration changes in blood (Hellman, Gylfe, Grapengiesser, Dansk, & Salehi, 2007; Lang, Matthews, Peto, & Turner, 2010), and vocal cord vibrations (Titze, 1993) are all oscillatory. Many economic and societal phenomena exhibit oscillations as well. For example, when viewed over long periods of time, prosperity in society and related parameters like unemployment tend to be cyclical (Eeckhout & Lindenlaub, 2019; Mitchell, 1941). Similarly, the development of a circular economy is based on continual recycling between raw materials and derived finished products (Mitchell, 1941). Finally, oscillations are relevant for technology, as many devices and instruments work based on rhythmicity. For example, electrical devices use alternating currents that reverse direction and change their amplitude periodically (Bhargava & Kulshreshtha, 1983). String instruments, like a guitar, produce sound as the result of the vibration in their strings (Perov, Johnson, & Perova-Mello, 2015). Quartz wristwatches, digital clocks, computers and cellphones have electronic oscillator circuits known as crystal oscillators, which keep track of time and stabilize clock signals or frequencies (Matthys, n.d.).

In addition to isolated oscillations, it is also possible to observe systems of coupled oscillators. Whenever a group of oscillators interacts, synchronization can arise (Pikovsky, Rosenblum, Self, & 2001, 2003). This insight occurred to Christiaan Huygens (1629-1695) in the 17th century when he observed that two pendulum clocks suspended from the same beam synchronize (Huygens & Oscillatorium, 1986). Huygens' observations are in line with the more recently formulated theory of weakly coupled oscillators (TWCO). TWCO describes the rules according to which two or more oscillators interact with each other.

In the present thesis, we used a simple, yet well-defined formulation of TWCO known as the Kuramoto model (Ermentrout, Park, & Wilson, 2019) to study how synchronization arises in neural networks. In particular, we used the Kuramoto model to investigate the factors that determine the size and number of clusters of synchronized (integrated) and unsynchronized (segregated) neuronal groups. We showed that structural characteristics of neural networks (like synaptic strength and conductivity) can interact with the functional segregation of networks and

demonstrated how external influences (visual stimuli) affect integration and segregation in behavioural experiments. We found that TWCO was a powerful framework to understand and predict our observations. According to the principles of TWCO, depending on how the oscillations evolve, different functionally segregated networks can form very quickly. Because of this flexibility, oscillations are thought to play a major role in cognition. One's ability to switch quickly from one thought to another may be intimately related to oscillatory mechanisms, and to the ability to quickly change functional networks through synchronization mechanisms. At the same time, specific aspects of the hardware design of the network can influence how likely it is that a large neural network will segregate into smaller ones, all showing their own local synchronization around their own synchronization frequency.

The relationship between oscillations and cognition suggests that aberrations in neural oscillations may be linked to psychiatric disease. Neuroscientific studies have indeed revealed that many mental diseases and disorders, such as major and bipolar depression (Canali et al., 2015; Fitzgerald & Watson, 2018; Linkenkaer-Hansen et al., 2005), obsessive-compulsive disorder (Min, Kim, Park, & Park, 2011), schizophrenia (Canali et al., 2015; Chung, Geramita, & Lewis, 2022; Shin, O'Donnell, Youn, & Kwon, 2011), spatial attentional deficits (Banerjee, Snyder, Molholm, & Foxe, 2011), post-traumatic stress disorder (Popescu et al., 2019; Reuveni et al., 2022) and epilepsy (Lehnertz et al., 2009; Traub & Wong, 1982) are related to abnormalities in ongoing interactions within and between oscillating networks in the brain, which either impede desired synchrony or give rise to undesirable synchronization patterns. The insights afforded by the present thesis may thus not only provide a better understanding of information processing in healthy brains but may also be exploited for clinical applications. In Chapter 2 of the present thesis, we showed that plastic delays can significantly alter the spread of synchrony across a network of oscillators. This might be relevant for computational models of epilepsy that are being used to identify epileptogenic zones of drug-resistant epilepsy patients in order to provide targets for surgery (Jirsa et al., 2017; Olmi, Petkoski, Guye, Bartolomei, & Jirsa, 2019; Proix, Bartolomei, Guye, & Jirsa, 2017; Proix, Jirsa, Bartolomei, Guye, & Truccolo, 2018). The effects of delays on synchrony as well as synchrony-induced changes of delays described in the second chapter provide additional insights that might improve the fidelity of epilepsy models and hence render them more accurate in identifying epileptogenic zones. This might render them safer and thus useful to a larger patient population. Beyond physically removing a source of pathological synchronization, synchronization states can also be modulated by external interventions. Transcranial alternating current stimulation

(tACS) (Elyamany, Leicht, Herrmann, & Mulert, 2020) or high-frequency repetitive transcranial magnetic stimulation (rTMS) (Zrenner et al., 2020) can help to treat or control some of the mentioned mental diseases (e.g. major depression, obsessive-compulsive disorder, schizophrenia, spatial attentional deficits). In such treatments, the repetitive synchronization of neural oscillations in selected functional systems with electrical pulses modulates these selected neural networks, which results in plastic changes, of which positive therapeutic outcomes have been documented (Elyamany et al., 2020; Zrenner et al., 2020). Insights gleaned from Chapter 2 may provide a better understanding of plastic changes and their implications.

The previous paragraphs already showed that external influences (e.g. TMS pulses) and ensuing changes in neural network structure modulate neural oscillations and synchrony in the brain to a significant degree. In the present thesis, we focused on a related finding, which is that neural oscillations in the visual cortex depend on visual stimuli in the outside world. Remarkably, stronger stimuli (e.g. moving faster, or having greater contrast) produce faster oscillations in visual neurons. This is an important finding, as it suggests that local contrasts in an image will help in determining which parts in an image belong together and which parts do not. TWCO hence is useful to understand how a figure is perceptually segregated from the background, but, conversely, it can also be used to understand situations in which figure-ground segregation is unsuccessful.

In Chapters 3 and 4, we have experimentally investigated the effects of the stimulus-dependence of oscillations on visual perception. We used a computational model rooted in TWCO to predict which areas in a stimulus would be perceived as separate from others in figure-ground segregation experiments. The computational model consisted of a network of connected oscillators, in which each oscillator corresponds to a small pool of neurons receiving input from a given receptive field (RF). In this computational model, we used additional knowledge about V1, specifying that more distant neurons have weaker connections, and specifying that RF stimuli would produce higher-frequency oscillations the higher the local contrast of the stimuli. Second, we used the TWCO principles specifying that neuronal populations (oscillators) that can influence each other more effectively (coupled by stronger connections) and neuronal populations (oscillators) that are stimulated with stimuli generating more similar oscillation frequencies, would be more likely to reach synchronization. This computational network, which incorporated V1 architectural knowledge and TWCO principles, was able to predict whether human observers would be able to see one specific texture as different from another texture in experimental stimuli. Specifically, whenever the V1 neural network model converged to two different synchronization states in response to different areas in a

large texture stimulus, human observers would also *perceive* these texture differences.

This view on figure-ground segregation, aside from providing insight into a set of mechanisms giving rise to the distinct perception of objects in the visual field, provides an interesting perspective on visual tricks in nature, such as camouflage. Camouflage in prey or predator animals is a functional form of unsuccessful figure-ground segregation that can be understood in the TWCO framework. Many animals use camouflage to merge with their background and to hide from their predators and/or prey[39,40]. Our findings suggest that animals can blend in with their surroundings because neuronal groups whose receptive fields fall on the animal will synchronize with those neuronal groups whose receptive fields fall on the surroundings because they receive highly similar low-level features. A deeper understanding of the contribution of oscillations and synchrony to successful and unsuccessful figure-ground segregation may thus prove relevant not only to vision neuroscientists but also to evolutionary ecologists interested in the competing evolutionary drives for better camouflage and the ability to see through this camouflage.

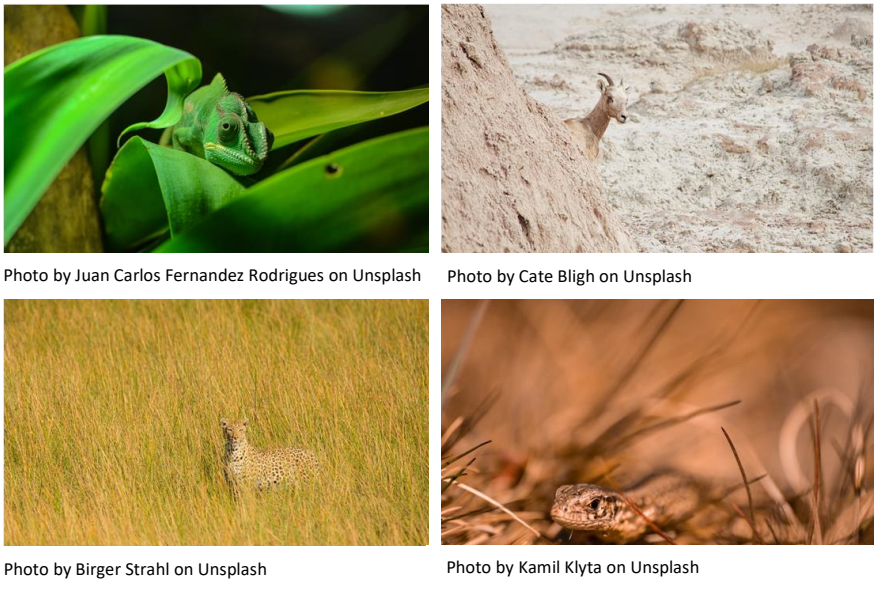

Photo by Juan Carlos Fernandez Rodrigues on Unsplash

Photo by Cate Bligh on Unsplash

Photo by Birger Strahl on Unsplash

Photo by Kamil Klyta on Unsplash

Animal camouflage

Insights from the third and fourth chapters on how oscillations and synchrony contribute to figure-ground segregation (a form of image segmentation) are not only

relevant for biological but also for computer vision. There is a growing interest in neuromorphic, and in particular, oscillation-based computing (Csaba & Porod, 2020). In particular, spin-torque nano-oscillators (STNOs) are a developing technology for oscillation-based computing that is very energy efficient, noise tolerant and has promising applications in technologies that heavily rely on computer vision, such as in self-driving cars. The reliability of self-driving cars depends on the accuracy and time-efficiency of decision-making processes, which, in turn, depend on the precision of information received by sensors of the surrounding environment. Visual signals comprise a large proportion of this information. Hence, self-driving cars need to perform fast and efficient analysis of visual signals while minimizing battery use. In particular, self-driving cars need to continuously perform segmentation on the stream of incoming images (Sellat et al., 2022). The results of Chapters 3 and 4 provide insights into how image segmentation may be achieved by networks of oscillators that may prove relevant for the development of networks of coupled STNOs specifically dedicated to this task. Importantly, the present thesis also provides insights on how a form of (tri-factor) biological reinforcement learning can be utilized to improve figure-ground segregation and, by extension, image segmentation. These insights might be exploited for the development of systems that are capable of continuously adjusting their performance based on past experience.

To summarize, oscillations and synchronization are essential to normal cognition and perception and understanding the precise role of these phenomena may pave the way for new technological developments. Furthermore, tracking as well as manipulation of oscillations and synchronization in the brain may help in alleviating pathology in brain function and mental disease. Novel insights gained from the results presented in the present thesis have the potential to contribute to further improvement of both brain-inspired technology and healthcare.

References

Banerjee, S., Snyder, A. C., Molholm, S., & Foxe, J. J. (2011). Oscillatory Alpha-Band Mechanisms and the Deployment of Spatial Attention to Anticipated Auditory and Visual Target Locations: Supramodal or Sensory-Specific Control Mechanisms? *Journal of Neuroscience*, 31 (27), 9923–9932.

Bhargava, N., & Kulshreshtha, N. (1983). *Basic Electronics and Linear Circuits*. Tata McGraw-Hill Education.

Canali, P., Sarasso, S., Rosanova, M., Casarotto, S., Sferrazza-Papa, G., Gosseries, O., … Benedetti, F. (2015). Shared reduction of oscillatory natural frequencies in bipolar disorder, major depressive disorder and schizophrenia.

Chung, D. W., Geramita, M. A., & Lewis, D. A. (2022). Synaptic Variability and Cortical Gamma Oscillation Power in Schizophrenia. *Https://Doi.Org/10.1176/Appi.Ajp.2021.21080798*, 179 (4), 277–287.

Csaba, G., & Porod, W. (2020). Coupled oscillators for computing: A review and perspective. *Applied Physics Reviews*, 7 (1), 011302.

Eeckhout, J., & Lindenlaub, I. (2019). Unemployment Cycles. *American Economic Journal: Macroeconomics*, 11 (4), 175–234.

Elyamany, O., Leicht, G., Herrmann, C. S., & Mulert, C. (2020). Transcranial alternating current stimulation (tACS): from basic mechanisms towards first applications in psychiatry. *European Archives of Psychiatry and Clinical Neuroscience 2020 271:1*, 271 (1), 135–156.

Ermentrout, B., Park, Y., & Wilson, D. (2019). Recent advances in coupled oscillator theory. *Philosophical Transactions of the Royal Society A*, 377 (2160).

Fitzgerald, P. J., & Watson, B. O. (2018). Gamma oscillations as a biomarker for major depression: an emerging topic. *Translational Psychiatry 2018 8:1*, 8 (1), 1–7.

Hellman, B., Gylfe, E., Grapengiesser, E., Dansk, H., & Salehi, A. (2007). Insulin oscillations--clinically important rhythm. Antidiabetics should increase the pulsative component of the insulin release. *Lakartidningen*, 104 (32–33), 2236–2239.

Huygens, C., & Oscillatorium, H. (1986). *The pendulum clock*. Trans RJ Blackwell, The Iowa State University Press.

Jirsa, V. K., Proix, T., Perdikis, D., Woodman, M. M., Wang, H., Bernard, C., … Chauvel, P. (2017). The Virtual Epileptic Patient: Individualized whole-brain models of epilepsy spread. *NeuroImage*, 145 (Pt B), 377–388.

Knudsen, M. F., Seidenkrantz, M. S., Jacobsen, B. H., & Kuijpers, A. (2011). Tracking the Atlantic Multidecadal Oscillation through the last 8,000 years. *Nature Communications 2011 2:1*, 2 (1), 1–8.

Lang, D. A., Matthews, D. R., Peto, J., & Turner, R. C. (2010). Cyclic Oscillations of Basal Plasma Glucose and Insulin Concentrations in Human Beings. *New England Journal of Medicine*, 301 (19), 1023–1027.

Leconte, M., Masson, P., & Qi, L. (2022). Limit cycle oscillations, response time, and the time-dependent solution to the Lotka–Volterra predator–prey model. *Physics of Plasmas*, 29 (2), 022302.

Lehnertz, K., Bialonski, S., Horstmann, M. T., Krug, D., Rothkegel, A., Staniek, M., & Wagner, T. (2009). Synchronization phenomena in human epileptic brain networks. *Journal of Neuroscience Methods*, 183 (1), 42–48.

Linkenkaer-Hansen, K., Monto, S., Rytsälä, H., Suominen, K., Isometsä, E., & Kähkönen, S. (2005). Breakdown of Long-Range Temporal Correlations in Theta Oscillations in Patients with Major Depressive Disorder. *Journal of Neuroscience*, 25 (44), 10131–10137.

Mann, M. E., Park, J., & Bradley, R. S. (1995). Global interdecadal and century-scale climate oscillations during the past five centuries. *Nature 1995 378:6554*, 378 (6554), 266–270.

Matthys, R. J. (Ed.). (n.d.). *Crystal oscillator circuits*. New York: Wiley-Interscience.

Min, B. K., Kim, S. J., Park, J. Y., & Park, H. J. (2011). Prestimulus top-down reflection of obsessive-compulsive disorder in EEG frontal theta and occipital alpha oscillations. *Neuroscience Letters*, 496 (3), 181–185.

Mitchell, W. C. (1941). *Business Cycles and Their Causes*. *Business Cycles and Their Causes*. University of California Press.

Olmi, S., Petkoski, S., Guye, M., Bartolomei, F., & Jirsa, V. (2019). Controlling seizure propagation in large-scale brain networks. *PLOS Computational Biology*, 15 (2), e1006805.

Perov, P., Johnson, W., & Perova-Mello, N. (2015). The physics of guitar string vibrations. *American Journal of Physics*, 84 (1), 38.

Pikovsky, A., Rosenblum, M., Self, J. K.-, & 2001, undefined. (2003). A universal concept in nonlinear sciences. *Researchgate.Net*.

Popescu, M., Popescu, E. A., DeGraba, T. J., Fernandez-Fidalgo, D. J., Riedy, G., & Hughes, J. D. (2019). Post-traumatic stress disorder is associated with altered modulation of prefrontal alpha band oscillations during working memory. *Clinical Neurophysiology*, 130 (10), 1869–1881.

Proix, T., Bartolomei, F., Guye, M., & Jirsa, V. K. (2017). Individual brain structure and modelling predict seizure propagation. *Brain : A Journal of Neurology*, 140 (3), 641–654.

Proix, T., Jirsa, V. K., Bartolomei, F., Guye, M., & Truccolo, W. (2018). Predicting the spatiotemporal diversity of seizure propagation and termination in human focal epilepsy. *Nature Communications*, 9 (1), 1–15.

Reuveni, I., Herz, N., Peri, T., Schreiber, S., Harpaz, Y., Geisser, R., … Goldstein, A. (2022). Neural oscillations while remembering traumatic memories in post-traumatic stress disorder. *Clinical Neurophysiology*.

Ryzhii, E., & Ryzhii, M. (2014). Modeling of Heartbeat Dynamics with a System of Coupled Nonlinear Oscillators. *Communications in Computer and Information Science*, 404 CCIS, 67–75.

Sellat, Q., Bisoy, S., Priyadarshini, R., Vidyarthi, A., Kautish, S., & Barik, R. K. (2022). Intelligent Semantic Segmentation for Self-Driving Vehicles Using Deep Learning. *Computational Intelligence and Neuroscience*, 2022.

Shin, Y. W., O'Donnell, B. F., Youn, S., & Kwon, J. S. (2011). Gamma Oscillation in Schizophrenia. *Psychiatry Investigation*, 8 (4), 288.

Titze, I. R. (1993). Current topics in voice production mechanisms. *Acta Oto-Laryngologica*, 113 (3), 421–427.

Traub, R. D., & Wong, R. K. S. (1982). Cellular Mechanism of Neuronal Synchronization in Epilepsy. *Science*, 216 (4547), 745–747.

Zrenner, B., Zrenner, C., Gordon, P. C., Belardinelli, P., McDermott, E. J., Soekadar, S. R., … Müller-Dahlhaus, F. (2020). Brain oscillation-synchronized stimulation of the left dorsolateral prefrontal cortex in depression using real-time EEG-triggered TMS. *Brain Stimulation*, 13 (1), 197–205.

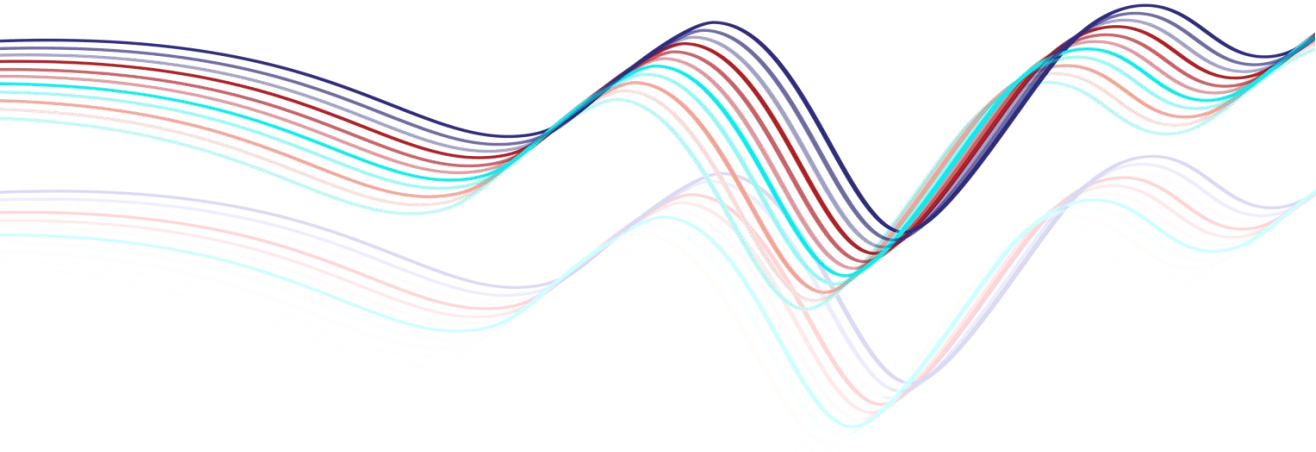

Acknowledgements

What a great feeling when you look back at the way and remember every day of this PhD journey, each as step, building up the road and bring you where you are now. During this journey, I had the great chance to learn and experience not only research, but also independence, crisis management, emotion control, constructive communication and many other valuable things that made my life more productive. Definitely, all these were not possible without the support, accompany and criticism of all the people to whom I want to express my greatest gratitude.

***

First and foremost, my deep and heartfelt appreciation goes to my supervisory team, **Prof. Peter de Weerd**, **Dr. Mario Senden** and **Dr. Ronald Westra**.

Peter, you are an insightful, experienced and supportive supervisor, whom I always counted on and was always proud of. You went beyond your role as a

supervisor. Even though you were heavily busy with teachings, supervision and administrative work of the faculty, from time to time, you made room in your schedule for a friendly conversation, a walk, or a coffee break. You are a good listener and always provide well-thought suggestions. Repetitive ups and downs, unexpected obstacles, and occasional disappointments are inevitable aspects of the research work. When I was stuck in such situations, you were always there to help me regain my self-confidence and overcome problems. I am very grateful to you for all your constant support and encouragement during my research study, and I hope to get the chance to work with you again in future.

Mario, without your contribution I would not be writing this thesis at all. You were both a mentor and a friend, patiently helping me find my way when I was lost and confused. You were always available, with your astonishing ability to immediately find a solution for every problem and your honest feedback which helped me grow as a scientist. You did all of these while your weekdays were compact with supervision, teachings, student projects and grant writings. Moreover, you created a friendly atmosphere in your group. We had exciting group meetings, journal clubs and boot camps where we got acquainted with state-of-the-art literature. In such gatherings, all opinions were heard, we were constantly learning new things and we had the chance to broaden our intellectual horizons. Specifically, you taught us the principles of argumentation and critical thinking which are not only the prerequisites for writing the thesis and articles but also are used many times in daily life. I wish the very best for you and your lovely family.

Ronald, I first met you in my interview session. Your friendly and welcoming manner in this interview made me comfortable and eager. Then, you offered me the opportunity to pursue my PhD in Maastricht University. Short after I moved to Maastricht, you took a whole day to show me around the faculty building and the beautiful city corners. I learned a lot from you and gained valuable experiences while working with you. I wish you a life full of happiness with your family.

Secondly, I would like to gratefully thank my assessment committee members, **Prof. Alexander Sack**, **Prof. Gustavo deco**, **Prof. Pascal Fries**, **Dr. Vincent van de Ven**, **Prof. Rainer Goebel**, **Prof Federico De Martino** and **Dr. Judith Peters** for taking the time to read and evaluate my thesis and my presentation.

A special thanks to **Tonio** and **Kris**, my dear paranymphs. You are such generous and kind colleagues that accepted this responsibility right after I asked you. **Kris**, I had no doubt that you are the right person to do me this favour because I had already seen your companionship and support in our small reading club. **Tonio**,

I was also very confident about you. I say this because I know you with your friendly attitude and eagerness to help.

Next, I would like to extend my thanks to those from whom I was able to learn the skills I needed to develop my codes or write my manuscripts. **Dr. Mark Roberts**, you generously passed me your knowledge in the design of Psychophysics experiments. **Dr. Michelle Moerel** and **Dr. Domenica Dibenedetto**, I benefitted from your experiences and mentorship during the first years of my PhD. Thank you all. In addition, thank to **Robin**, my assistant, who helped me performing my behavioural experiments.

I spent four years of my PhD with my MaCSBio colleagues. **Isma**, **Chaitra** and **Samar**, during these four years, we were each other's caring neighbours. Thanks for being there for me. **Bart**, **Balázs**, **David** and **Charlie**, you were the source of energy in the office. I enjoyed seeing your deep and sincere friendship. Take good care of it. **Bob** and **Shauna**, it was my pleasure to spend time with you. Good luck wherever you are.

I also would like to thank the lovely CN family, especially my friends in CCN (**Alex**, **Salil**, **Vaish**, **Raphael**, **Ibrahim**, **Andrea**, **Rick**, **Danny**, **Tonio** and **Kris**). I enjoyed every single moment I spent with you, whether in group meetings, scientific and philosophical discussions (not about consciousness though ☺) or in social events, online and board games, coffee breaks and lunchtime with other lovely colleagues. Don't let your research drag you away from keeping the work environment lively and friendly.

Thank to **Prof. Elia Formisano** and **Prof. Ilja Arts**, for the powerful management of NeuGenNet and MaCSBio.

Christl, **Eva** and **Claudia**, without your efforts, everything would be super-complicated and messed up. Thank you all for keeping the trains of CN and MaCSBio on track.

Last but not least, my deepest love and gratitude to **my parents**, **my sisters** and **my brother**, who encouraged and supported me from childhood. Thank you for bearing the hardship of separation so that I can invest wherever I want for my goals. Thanks for having my back.

And …

Zahed, words fail to describe how you make my life meaningful. You are my husband, my friend, my counselor when I am confused, my therapist when I am frustrated and my company in happiness and sadness. You and I went through the

ups and downs of the PhD journey together and that made you the one who supported and understood me the most. You prioritized my wishes over yours and did everything for me to achieve my goals. Thanks for being in my life.

***

Also, I am grateful to all those whose names I have not mentioned, but who have helped me grow, directly or indirectly, through encouragement and support or through criticism.

About the Author

Maryam Karimian was born on January 1990, in Esfahan, Iran. After finishing her high school in 2008, she started her bachelor's degree in Physics at Esfahan University of Technology (IUT). In 2012, Maryam graduated with distinction and because of that, she had the honour to start her master's degree without the Iranian University Entrance Exam (Konkour). In January 2015, Maryam got her master's degree in Condensed Matter Physics from IUT. Her thesis was focused on the collective behaviour of oscillatory complex networks, under the supervision of Dr. Farhad Shahbazi. In the same year, Maryam started working as a PhD candidate at the Maastricht Center for System's Biology (MaCSBio). The PhD project was funded by the Dutch province of Limburg as part of the "NeuGenNet" project. In MaCSBio, Maryam's research work involved computational modelling of plasticity in neural networks of the brain under the supervision of Prof. Peter De Weerd, Dr. Mario Senden and Dr. Ronald Westra. In 2018, Maryam joined the department of Cognitive Neuroscience (CN), and expanded her research to investigate perception and perceptual learning of visual figure-ground segregation under the supervision of Prof. Peter De Weerd and Dr. Mario Senden.

She will soon start her postdoctoral research on an interdisciplinary project "behavioural contagion in human and artificial multi-agent system" at the Institute of "Science of Intelligence" (SCIoI), Humbuldt University, Berlin.

List of Publications

Karimian, M., Dibenedetto, D., Moerel, M., Burwick, T., Westra, R. L., De Weerd, P., & Senden, M. (2019). Effects of Synaptic and Myelin Plasticity on Learning in a Network of Kuramoto Phase Oscillators. *Chaos: An Interdisciplinary Journal Of Nonlinear Science* 29. 8, 083122.

Ameli, S., **Karimian, M.** and Shahbazi, F. (2021). Time-delayed Kuramoto Model in the Watta-Strogatz Small-world Networks. *Chaos: An Interdisciplinary Journal Of Nonlinear Science* 31. 11, 113125.

Karimian, M., Roberts, M., De Weerd, P., & Senden, M. (To be submitted), Synchronization of Input-dependent Gamma Oscillations in V1: A Criterion to Predict Figure-ground Segregation in Texture Stimuli.

Karimian, M., Roberts, M., De Weerd, P., & Senden, M. (To be submitted), Perceptual Learning of Figure-ground Segregation in Texture Stimuli, and Synchronization of Gamma Oscillations in V1.